# NASA Technical Memorandum 81811



## FRICTION EVALUATION OF UNPAVED, GYPSUM-SURFACE RUNWAYS AT NORTHRUP STRIP, WHITE SANDS MISSILE RANGE, IN SUPPORT OF SPACE SHUTTLE ORBITER LANDING AND RETRIEVAL OPERATIONS

THOMAS J. YAGER and WALTER B. HORNE

JUNE 1980

National Aeronautics and Space Administration

**Langley Research Center**
Hampton, Virginia 23665

CONTENTS

## SUMMARY

In preparation for possible Space Shuttle Orbiter landing and retrieval operations on the unpaved gypsum surface runways at Northrup Strip, White Sands Missile Range, a NASA Langley test team and equipment were sent, at the request of NASA JSC, to Northrup Strip in April 1979 to obtain a runway friction evaluation. Test runs were conducted with an instrumented tire test vehicle equipped with an aircraft tire inflated to the planned Orbiter main gear tire pressure to determine the rolling resistance and braking and cornering friction capability on the gypsum surface for both dry and artificially wetted conditions. Additional friction measurements were acquired with a diagonal-braked vehicle which was also used in similar tests performed in 1976 on the two Shuttle runways (lakebed and concrete) at Dryden Flight Research Center and on the grooved concrete runway at Kennedy Space Center.

The results from these ground friction measuring vehicle tests conducted at 41 different runway locations at Northrup Strip are presented together with comments and photographs describing the extent of tire surface rutting which occurred during the test runs in different tire operational modes. Based on the friction measurements, estimates of Shuttle Orbiter and B-747 aircraft tire friction performance are presented and discussed. Similar friction data obtained on paved and other unpaved runway surfaces is shown for comparison and to aid in arriving at these estimates. Also included in this report are general observations concerning the gypsum surface characteristics and recommendations are made for improving and maintaining adequate surface friction capabilities prior to the first Shuttle Orbiter landing.


## INTRODUCTION

During the time period of April 13-26, 1979, a Langley test team obtained friction measurements on the gypsum surface runways at Northrup Strip, White Sands Missile Range, N.M., using an instrumented tire test vehicle and a diagonal-braked vehicle. These tests were performed in support of a NASA Johnson Space Center request to evaluate the friction capability of two unpaved runways recently prepared to serve as backup landing and retrieval sites to the primary sites located at Dryden Flight Research Center for the Space Shuttle Orbiter during test flights STS-1 through STS-4. Similar tests were performed with the diagonal-braked vehicle in 1976 on the two Shuttle runways (lakebed and concrete) at Dryden and on the grooved concrete runway at Kennedy Space Center.

The purpose of this report is twofold: (1) Document the scope of the tests performed, the range and type of friction data obtained, and the extent of any anomalies found in the runway surface friction capability which might compromise the safety of Shuttle landing and retrieval operations; and (2) Provide estimates, based on the ground vehicle acquired friction data, of tire friction coefficients available for decelerating and steering the Space Shuttle Orbiter vehicle and the B-747 transport aircraft during ground operations on the runways at Northrup Strip. A detailed description of the gypsum soil

properties is beyond the scope of this paper which only addresses the available friction as measured at the time of test. Reference 1 provides pertinent data on gypsum soil properties obtained by an Air Force test team.

## TEST SITE

The Northrup Strip airfield runway layout at White Sands Missile Range is shown schematically in figure 1. The original Northrup Strip runway 17/35 was recently extended to 10 668 m (35 000 ft) from 6096 m (20 000 ft) and the cross-runway 5/23 was constructed to the same length. Both runways are 91.4 m (300 ft) wide, and they do not have a conventional runway crown. Standing at the runway intersection, some longitudinal gradient on both runways was observed and noted as a positive (uphill) gradient for runway headings of 350 and 230. Figure 1 also indicates some of the Tyndall Air Force Engineering and Services Center's runway survey stations (see ref 1) which were used to identify the runway sections selected for ground vehicle friction tests. Based on these runways station markers, which were placed at 76.2 m (250 ft) intervals on the runway centerline, the point of runway intersection occurs at Sta. 177+52 (54 411 m (17 752 ft)) for runway 17 and at Sta. 195+56 (5961 m (19 556 ft)) for runway 05. Although both runway surfaces were rolled and compacted after completion of grading work, various amounts of loose, unconsolidated, gypsum material were found covering the entire surface of both runways due to the effects of weathering, wind, ground vehicle and aircraft traffic, and possibly, missile impacts in the vicinity of the airfield from Army test firings. In general, runway surface roughness was also observed to vary considerably based on visual surface inspections and the ride quality experienced by the test vehicle operators. The roughest areas were found in portions of both ends (overrun areas) of runway 17/35, the east end of runway 5/23 near the gypsum sand dunes, and the runway intersection. One additional surface characteristic observed from inspections following ground vehicle tests at all 41 different locations on the two runways should be noted. At less than 2.5 cm (1 in.) below the loose, cover material, the surface coloration changed from white to light brown and some definite moisture content could be felt in handling samples of this underlying material. During this test period, no rainfall occurred in nearly two weeks and relative humidity readings were low (<20%). This discoloration and moisture content could be observed directly on the upper surface in many areas of the west end of runway 5/23 where the loose covering material was sparse and shallow.

## GROUND FRICTION MEASURING VEHICLES

### Instrumented Tire Test Vehicle

The main features of the NASA Langley instrumented tire test vehicle used in this investigation and in previous tire friction studies are identified in the photographs presented in figure 2. To enhance the quality of test tire data acquisition, four adjustable screw jacks were mounted between the steel truck bed and frame to provide a level, stable platform. Vertical load was applied to the test tire by means of two pneumatic cylinders and this load, together with the drag and side loads developed on the tire during test runs, were measured by strain gage beams centered about the wheel and mounted

above the wheel-axle support structure. Continuous time histories of the output from these strain gages were recorded on an oscillograph mounted in the vehicle cab compartment. A hydraulic system to lower or raise the test tire from the surface was installed with vehicle operator control in the cab compartment. Simulated tire braking at fixed slip ratios was obtained by driving the test wheel with an adjustable steel shaft (see fig. 2(b)) connected through a universal coupling to interchangeable sprocket gears, which in turn, were chain driven by a sprocket replacing one left rear driving wheel of the vehicle. Changing the slip ratio involved replacement of the sprocket gear positioned at the driving end of the universal coupling. For unbraked, yawed tire tests, the universal coupling was completely removed or positioned and locked so that the sprocket gear did not engage the chain driven wheel. To obtain the desired tire yaw, the test fixture was manually unlocked, rotated to the preselected angle, and locked in place. The instrumented trailing wheel identified in figure 2 was used to provide an accurate measurement of vehicle speed and distance traveled. This data, together with data from the test wheel, was displayed on digital readout meters to the vehicle operator and recorded on an oscillograph.

### Diagonal-Braked Vehicle

The NASA diagonal-braked vehicle (DBV) used in this investigation is shown in figure 3(a). It was developed in the late 1960's to evaluate pavement surface slipperiness conditions (see ref. 2 through 6). The same DBV used in these friction tests at Northrup Strip was used in 1976 to obtain a similar friction evaluation on the two runway surfaces (lakebed and concrete) at Dryden prior to the Shuttle Approach and Landing Tests and also on the grooved concrete runway surface at KSC. The diagonal-braking system installed in the vehicle (see schematic, fig. 3(b)) permits the operator to select and brake to a locked-wheel skid one diagonal wheel pair, equipped with ASTM smooth tires, while the opposite diagonal wheel pair, equipped with conventional tread tires, remains unbraked and freely rolling. The two freely-rolling wheels enable sufficient steering or side forces to be developed for maintaining vehicle stability through the test speed range. The use of smooth tires on the braking wheels of the vehicle eliminates tread wear and tread design effects. An instrumented trailing wheel, similar to the one installed on the test truck, was used to provide accurate speed and distance readings to the operator; however, the distance readout meter on the DBV was activated by a microswitch installed on the vehicle brake pedal to provide stopping distance values from brake application. A positive indication of diagonal wheel lockup during a test run was obtained from magnetic pickups mounted on the inside wheel rims. The output from this instrumentation, together with the deceleration level measured by a longitudinal, ±1g, accelerometer mounted near the vehicle center of gravity, was recorded on an oscillograph to acquire continuous data time histories for each test run.

## TEST PROCEDURE

### Instrumented Tire Test Vehicle

For all test runs, a worn 22x5.5, type VII, 12-ply rated, 3-groove air-

craft tire was mounted on the instrumented tire fixture. Although this tire is smaller in size than the Shuttle main gear tire (44.5x16.21) a tire inflation pressure of 2172 kPa (315 lb/in$^2$) was selected for these tests to correspond to the planned Shuttle Orbiter main gear tire inflation pressure value. The air loading cylinders were adjusted and set to provide a nearly constant vertical load on the tire of 13.8 kN (3100 lb). Static test tire footprint bearing pressure measurements taken at Langley confirmed that this minimum tire loading produced an average footprint bearing pressure nearly equal to the inflation pressure. A complete instrument calibration and several test runs on a dry concrete surface were performed prior to shipping the test vehicle to Northrup Strip. After an additional check of the strain gage load calibration proved satisfactory at Northrup Strip, testing commenced.

In the conduct of a typical test run, the tire was first lowered to the surface and loaded to 13.8 kN (3100 lb) while the vehicle remained stationary. The vehicle was then accelerated to the desired test speed prior to entering the test section marked off with traffic cones. The vehicle operator maintained the desired speed through the test section and upon exiting, raised the tire fixture from the surface and positioned the vehicle for the next test run.

The general test sequence conducted on both dry surface runways at Northrup Strip included vehicle constant speed runs at selected intervals from 1 knot (2 mph) up to 34.7 knots (40 mph) for each free-rolling, yawed, or braked tire test mode. Free-rolling, unyawed tire test runs were first conducted over the entire length of both runways at a vehicle speed of 21.7 knots (25 mph) to determine variations in rolling resistance coefficient values on each runway. Based on this data, a 152.4 m (500 ft) area near the centerline of runway 17/35 between Sta. 70+00 and 75+00 was selected for additional rolling resistance and yawed, unbraked tire tests through the vehicle speed range. The yaw angles selected to determine the cornering or side friction coefficient values were 3, 6, 9, 12 and 15 degrees. The unyawed, braked tire tests over a range of constant slip ratios and vehicle speeds was also performed near the centerline of runway 17/35 between Sta. 45+00 and 65+00. The constant slip ratio values selected for evaluating the braking or drag friction capability of the dry gypsum surface were 7, 12, 20, 35, and 45 percent where 0 percent equals free rolling and 100 percent equals locked wheel. To obtain an assessment of the surface friction variation with runway location, additional test runs were conducted at a vehicle speed of 21.7 knots (25 mph) in different portions of both runways with the unbraked tire yawed 12$^o$ and then with the unyawed tire braked at a constant slip ratio of 12 percent.

An attempt to determine the effect of surface moisture on the tire friction coefficients was made using a water tanker truck equipped with a spray nozzle to wet artificially a 35 m (115 ft) strip close to the shoulder of runway 5/23 near Sta. 50+00. Two passes were made with the water truck, and approximately .14 m$^3$ (30 gallons) of water was spread 1 m (3 ft) wide during each pass. Rolling resistance, 6$^o$ yaw, and 12 percent braking slip runs were conducted on this artificially wetted surface at vehicle speeds of 8.7, 17.4, and 26 knots (10, 20, and 30 mph). After each three-run test series at one tire operating mode, the test section was displaced laterally and rewetted (two passes) prior to the next three-run test series.

Before concluding the test program at Northrup Strip, an attempt to obtain locked-wheel (100 percent slip ratio), skidding friction coefficient data at low speed (≈ 1 knot) was made on both the dry and artificially wet gypsum surface. The universal coupling was restricted from turning in the forward direction by attaching one end of a chain hoist to the universal with the other end secured and pulled tight to the tire fixture mounting structure. Once forward motion of the vehicle commenced, the test tire promptly started skidding along and down through the gypsum surface top covering material. After return of the test vehicle to Langley, however, laboratory tests indicated that this arrangement for locking the tire did not permit constant tire loading. As a result, accurate and reliable skidding tire friction coefficient data could not be obtained from the time history records.

To provide additional insight into the variations in tire frictional behavior, surface material chracteristics were recorded at each test location, and coarse measurements of tire rut depth were taken after most test runs using a straight edge and ruler. A limited series of rolling resistance, $6^{o}$ yaw, and 12 percent slip braking tests was performed on runway 5/23 to obtain an assessment of the effect of inflation pressure on the tire friction data. The deposit of tire tread rubber on the surface which occurred during some of the tire braking and cornering tests was also noted.

## Diagonal-Braked Vehicle

The general procedure followed for each test run with the DBV involved accelerating the vehicle to slightly above the desired test speed, placing the transmission in neutral, and then applying and maintaining full locked-wheel diagonal braking in the runway test section down to a complete stop. For these test runs, the smooth ASTM tires were inflated to 165 kPa (24 lb/in$^2$). At most runway test locations, two runs were conducted at a brake application speed of 52.1 knots (60 mph), and average values of the locked-wheel skidding friction coefficient variation with speed were obtained. Test runs at a brake application speed of 69.4 knots (80 mph) were also conducted at three different runway locations but further braking runs at higher speeds were not attempted because of the effects of surface roughness. Tire rut depth and surface material characteristics were also noted at each runway test location evaluated by the DBV. An attempt to obtain braking data at a higher tire bearing pressure using modified ASTM test tires with a 2.5 cm (1 in.) wide center rib (similar to the tires used during the lakebed runway tests at Dryden) proved unsuccessful because the loose, unconsolidated material on top of the hard surface was deeper than the tread rib thickness of these test tires.

In using the water tanker truck to obtain an artificially wetted surface for DBV tests, a wider and longer strip than that used for the instrumented tire test vehicle was sprayed with water (two passes) from the truck nozzle. Approximately .45 m$^3$ (100 gallons) of water was spread 4 m (12 ft) wide during each pass. Although the surface area wetted was closer to the runway centerline than the instrumented tire test vehicle area, the DBV test runs were conducted in the same station location on runway 5/23. The surface wetness condition obtained for the DBV test was similar to that achieved in the surface test areas evaluated by the instrumented tire test vehicle.

To document further the test conditions, surface characteristics, and tire rut depths encountered during both DBV and instrumented tire test vehicle runs, support was obtained from the U.S. Army photographic branch at White Sands Missile Range. All the photographs used in this report were provided by the Army photographic coverage.

## DATA REDUCTION

### Instrumented Tire Test Vehicle

The continuous tire force time history records obtained with the instrumented tire test vehicle oscillograph were faired to derive average force or load values developed on the tire during each run. Oscillations, which occurred in the recorded force traces due to effects of surface roughness and tire rutting, necessitated reading several segments of each test run record to obtain accurate and reliable values. In calculating the various types of friction coefficient developed between the test tire and the surface, both the unyawed, rolling resistance and the drag or braking friction coefficient values were computed by dividing the measured drag load by the applied vertical load. During the yawed, unbraked tire tests, the measured side load and drag load were perpendicular and parallel to the wheel plane, respectively. Consequently, a trigonometric transformation was made to obtain the side or cornering friction coefficient perpendicular to the vehicle direction of motion.

Test wheel revolution count data were used to compute the slip ratio values developed from each different sprocket gear. These data were recorded for both the unyawed free-rolling and driven modes over the same distance on the runway surface. The percent slip ratio values referred to in this report were computed by dividing the difference between the unbraked (free-rolling) and braked test wheel revolution count (for the same distance) by the unbraked revolution count and then multiplying by 100. Slip ratio values of zero and 100 percent correspond to a free-rolling tire and a locked-wheel, skidding tire, respectively.

### Diagonal-Braked Vehicle

Locked-wheel, skidding friction coefficient values at different speed increments were derived from the recorded accelerometer trace by simply doubling the measured "g" level since only half the braking capacity is acting on the total DBV mass. The small contribution of air drag and tire rolling resistance on the DBV-measured deceleration throughout the braking speed range was subtracted from the faired deceleration levels.

## RESULTS AND DISCUSSION

### Instrumented Tire Test Vehicle

Rolling resistance friction coefficient. - The data contained in table I and figure 4 indicate the typical variation found in tire rolling resistance coefficient, $\mu_r$, values developed between the unyawed tire and the dry gypsum surface runway in various locations at a vehicle speed of 21.7 knots (25 mph).

At this test speed, the maximum value measured was 0.059 at Sta. 11+00 (335 m (1100 ft)) on runway 17/35 and the minimum value was 0.012 measured at several locations on both runways. These variations in rolling resistance appear to be dependent upon the amount or depth of the loose, unconsolidated material covering the hard gypsum undersurface with higher $\mu_r$ values occurring at runway locations having the most uncompacted surface material. Tire penetration into the surface was also greatest in the locations with higher $\mu_r$ values compared to other portions of the runways. For comparison, the solid line in each plot of figure 4 indicates the level of $\mu_r$ measured on a concrete surface at the same test speed.

The effect of vehicle test speed on tire rolling resistance is illustrated by the data shown in figure 5. Unyawed, free-rolling, tire test runs were conducted through a speed range to 34.7 knots (40 mph) at several different dry surface runway locations. The very low speed, breakaway tests were conducted near the centerline of runway 5/23 at Sta. 90+00. Despite differences in the depth of the loose material on the surface, which contributed to the data scatter shown in figure 5, the general data trend indicates that with increasing speed, the $\mu_r$ values tend to decrease from the maximum breakaway value of 0.052. This trend is opposite to results of previous tire rolling resistance tests on paved surfaces (see ref. 7) which generally show the $\mu_r$ to increase with increasing speed. This phenomenon may be explained by tire surface rutting which tended to decrease with increased speed on the dry gypsum surface and the relatively low speed range of these tests. The data trends shown in reference 7 also indicate that a decrease in the tire rolling resistance occurs on an unpaved surface at speeds above 40 knots.

Drag friction coefficient. - The variation of unyawed tire drag, or braking, force friction coefficient $\mu_{drag}$ with ground speed at the five different slip ratios investigated is shown in figure 6. These data were obtained from tests conducted near the centerline of runway 17/35 between Sta. 45+00 and 65+00. The data of this figure indicate that $\mu_{drag}$ increases with increasing speed over the test speed range. The effect of braking slip on $\mu_{drag}$ is better illustrated in figure 7 where the test data at four different speed increments are replotted. At each speed $\mu_{drag}$ is shown to increase with increasing braking slip. An indication of the typical variation in $\mu_{drag}$ at various runway surface locations is included in table I. The $\mu_{drag}$ values shown in this table were obtained during 21.7 knots (25 mph) constant speed tests conducted at a fixed 12 percent slip.

Side friction coefficient. - Figure 8 presents the cornering, or side, force friction coefficient (perpendicular to the vehicle direction of motion) $\mu_{side}$ as a function of speed at each of the five test yaw angles. These data were obtained from yawed, unbraked tire tests conducted near the centerline of runway 17/35 between Sta. 70+00 and 75+00. The figure shows that at each yaw angle studied, $\mu_{side}$ developed on dry gypsum tends to increase with speed up to approximately 10-15 knots and remain constant or decrease slightly at higher

speeds. The variation of $\mu_{side}$ with yaw angle at selected speeds is shown in figure 9. Data of this figure suggest that the maximum side friction coefficient value occurs near the highest test yaw angle. Data are also included in table I to show the variation in $\mu_{side}$ with runway location. These data were obtained at $12^0$ yaw angle and again at 21.7 knots (25 mph).

Effect of surface wetness. - Figure 10 shows the variation in tire friction coefficients with speed for both the artificially wetted and dry gypsum test surfaces located near the shoulder area of runway 5/23 at Sta. 50+00. For these tests a braking slip of 12 percent and a yaw angle of $6^o$ were used to evaluate the drag and side friction capability. In general, the rolling resistance friction coefficients were approximately the same for the wet and dry surface conditions whereas the $\mu_{drag}$ and $\mu_{side}$ values measured on the wet surface were slightly lower than that obtained on the dry surface.

## Diagonal-Braked Vehicle

Table II lists values of the DBV locked-wheel, skidding friction coefficient $\mu_{skid}$ as measured at various locations on both runways at five selected speeds. Variations in $\mu_{skid}$ values at a given speed may be attributed to differences in surface characteristics and the extent of tire rutting. The faired average $\mu_{skid}$ variation with speed for each runway surface at Northrup Strip is shown by the solid curves in figure 11. On both surfaces, the skidding friction coefficient increases with decreasing speed, reaches a maximum at between 10 and 20 knots, and then decreases as the speed is reduced to zero. The decrease may be attributed at least in part to tire heating, characteristics of the surface, and tire rutting behavior. Also included in the figure are the results from the DBV test on the artificially wetted surface (runway 5/23). This faired $\mu_{skid}$ curve indicates a significant loss in available skidding friction coefficient when the surface is wetted.

## Tire Surface Rutting Characteristics

Tire penetration into the gypsum surface during the ground friction measuring vehicle tests varied with tire operating mode, speed, and the amount (depth) of loose, unconsolidated material on top of the hard undersurface. An indication of the effect of these factors on tire rutting is given in the photographs shown in figures 12 through 18. Similar Shuttle tire surface rutting variations can be expected during operations on this dry gypsum surface. The ruler and straightedge shown in these photographs do not necessarily indicate the actual tire rut depth which was determined later from an average of several measurements taken from the level of undisturbed surface down to the bottom of the tire rut. The effect of braking slip on unyawed tire dry surface rutting at low speed is illustrated in figure 12. For the free-rolling case (zero percent slip), conducted to determine rolling resistance, the surface rut developed by the tire (see fig. 12 (a)) was 0.32 cm (0.125 in.) deep. At a braking slip of 45 percent, the rut depth (see fig. 12 (b)) increased to 1.59 cm (0.625 in.), and for the locked-wheel

case (100 percent slip), the surface rut depth (see fig. 12 (c)) was 2.22 cm (0.875 in.). These photographs were obtained from instrumented tire test vehicle runs conducted near the centerline of runway 17/35 at Sta. 50+00. For the locked-wheel case (fig. 12 (c)), the tire penetrated the loose, upper layer of the gypsum surface and tread rubber was deposited on the hard undersurface. Rubber deposits were also observed during other low speed, braking runs at several different test surface locations. The effect of vehicle speed on surface rutting during tire braking tests at 45 percent slip is shown in figure 13. The photograph in figure 13(a) shows that the rut depth produced at a speed of approximately 1 knot was 1.59 cm (0.625 in.) whereas at 21.7 knots (25 mph) the depth (see fig. 13(b)) decreased to 0.64 cm (0.25 in.).

Rutting of the dry gypsum was also observed to increase with increasing yaw angle during the tire cornering tests as shown by the photographs of figure 14. These tests were conducted near the centerline of runway 5/23 at Sta. 320+00. At a vehicle speed of approximately 1 knot, the unbraked tire operating at a yaw angle of $3^{0}$ developed a rut (see fig. 14(a)) of 0.64 cm (0.25 in.). Increasing the angle to $12^{0}$ resulted in a surface rut depth (see fig. 14(b)) of 1.59 cm (0.625 in.). The photographs in figure 15 show that, as in the case of the braked unyawed tire, the rutting decreased with increased test speed.

During the braking and cornering tests on the artificially wetted gypsum of runway 5/23, rut depths were also observed to decrease with increasing speed as indicated by the photographs of figure 16. Severe surface rutting (see figure 17) was observed during one series of tire braking runs conducted near the shoulder of runway 5/23 in an area which, compared to other wetted areas, had considerably more loose, unconsolidated material on the surface. Once the uncompacted material on this area was wetted with the water truck, it became soft and sticky. The closeup view, shown in figure 17(b), of the rut produced from a 26 knot braking tire run at 12 percent slip indicates that the tire penetrated the surface to a depth of 6.35 cm (2.5 in.).

The extent of surface rutting which occurred during diagonal-braked vehicle test runs on both the dry and artificially wetted gypsum surface is shown in figure 18. In both photographs, the rut produced by the test tires just prior to DBV stop from a brake application speed of 52 knots (60 mph) is shown. In addition to similarities observed in the tread rubber deposits on both the dry and wetted surfaces, the tire rut depth of approximately 0.64 cm (0.25 in.) was essentially the same on both. Except for one DBV test location near the shoulder of runway 17/35 at Sta. 50+00 where the surface rut depth measured 3.81 cm (1.5 in.) when the DBV came to rest, all other test location rut depths produced by the DBV tires did not exceed 1.27 cm (0.5 in.). The less severe rutting associated with the locked-wheel skidding tires of the DBV relative to that that incurred by the instrumented tire test vehicle is attributed to the much lower tire pressure (165 versus 2172 kPa) used in the smooth ASTM test tires of the DBV.

From all the measurements of dry surface rut depth taken during friction tests on both runways with the instrumented tire test vehicle, figure 19 indicates the average variation of tire surface rut depth with speed for each mode

of tire operation. As expected, the most severe surface rutting occurred during low speed, locked-wheel, skidding tests and the smallest rut depths were produced during unyawed, free-rolling tests. The data also indicate that the rate of decrease in surface rutting with increasing speed up to 35 knots was similar during the rolling resistance, braking, and cornering friction tests.

## Comparison to Other Surfaces

With a tire loading similar to that employed during the Northrup Strip friction tests, rolling resistance and cornering runs were conducted on a dry Portland Cement Concrete surface at Langley with the instrumented tire test vehicle. Figure 20 compares these concrete friction data with those obtained on the unpaved, dry gypsum surface. The rolling resistance friction coefficient developed between the tire and the concrete surface was lower than that obtained on the gypsum surface but as noted earlier the effect of speed is quite different. The side force friction coefficients developed between the tire and the dry concrete at a speed of 17.4 knots are shown to be higher than those obtained on the gypsum surface at corresponding yaw angles. For both surfaces however, $\mu_{side}$ appears to peak at approximately the same tire yaw angle but this result is mainly attributed to the low test speed. It is expected that at higher speeds, $\mu_{side}$ on each surface would be less in magnitude and peak at different tire yaw angles.

Figure 21 is presented here in an effort to put the slow-speed rolling resistance data obtained at White Sands, using a small test tire in this investigation and the large tire on the load cart (see ref. 1), into perspective with the landing conditions associated with the Shuttle Orbiter vehicle. This figure contains rolling resistance friction coefficients obtained over a speed range during two separate aircraft test programs conducted at several locations on the Harpers dry lakebed at Edwards AFB. Figure 21(a) shows the variation in $\mu_r$ with speed as obtained during a B-707 aircraft flight test program (see ref. 8) on lakebed surfaces with CBR values ranging from 2 to 6, and figure 21(b) shows similar data as obtained during C-5A aircraft flight tests (see ref. 9) conducted at a different lakebed surface location where CBR values ranged from 13 to 21. The figure shows that the variation of $\mu_r$ with speed is highly dependent upon the load-supporting capability of the unprepared surface. It is reasonable to assume that surface rutting is a major factor in determining the magnitude of the rolling resistance since that resistance is shown to increase with surface penetrability. However, it is significant to note that although $\mu_r$ varies considerably with CBR values at ground speeds in excess of approximately 50 knots, there is little to differentiate between the rolling resistance for all CBR values at lower speeds. Thus, with data available to only 40 knots, it would be impossible to predict the rolling resistance at some higher speed without advance knowledge of the surface hardness. Note that the gypsum surface data (to 40 knots) agree with the Harpers dry lake data. Since it is known that portions of the runways at White Sands offer different resistance to penetration (see ref. 1), the rolling resistance of tires on that surface over the landing speed range of the Space Shuttle cannot be estimated with any degree of confidence, particu-

larly on areas of the runway where the tires penetrate the surface. However, on the basis of the data presented in figure 21, it would appear that the rolling resistance friction coefficient on runway areas where rutting is minimal, as is apparently the case along most of the centerline of both gypsum runways, would never exceed 0.06. Since tire rolling resistance at low speed can produce a significant load factor in planned towing operations with the Shuttle Orbiter vehicle after landing, continued use of the load cart at White Sands is recommended as a means of identifying runway areas requiring additional compaction.

Figure 22 presents comparative skidding friction coefficient data as obtained from diagonal-braked vehicle tests on the White Sands gypsum runways and both the Shuttle ALT lakebed runway and the paved runway at Dryden Flight Research Center. The White Sands data presented in this figure represent the faired average of that obtained from both runway 5/23 and 17/35. The figure shows that $\mu_{skid}$ developed at White Sands is significantly higher than that measured on the lakebed ALT runway and is nearly equal to the $\mu_{skid}$ level measured on the paved concrete runway at DFRC. On the basis of this limited comparison it would appear that the friction capability provided by the dry White Sands surfaces is adequate for Shuttle landing and retrieval operations similar to those conducted on the Dryden lakebed during the Shuttle approach and landing tests.

## SHUTTLE ORBITER AND B-747 AIRCRAFT TIRE FRICTION ESTIMATES

### General Method and Assumptions

The friction coefficient data obtained with the instrumented tire test vehicle were used as the basis for deriving tire friction estimates for ground operation of the Shuttle Orbiter and the B-747 aircraft on the dry gypsum runways at White Sands Missile Range. Tire friction performance of the Shuttle Orbiter and B-747 aircraft were estimated for the various tire sizes, loads, inflation pressures, and speeds associated with these two aircraft from measurements made on a single tire size operating over a relatively low speed range on the ground vehicle. To make these estimates, the following general tire frictional behavior characteristics and empirical equations, obtained from Langley Landing Loads Track and flight test data, were used:

(a) The characteristic dry friction coefficient $\mu_{cd}$ defined as the maximum friction coefficient obtainable on a dry pavement under braked rolling, yawed rolling, or locked-wheel sliding conditions at low speed (<2 knots), can be calculated from the following equation (see refs. 6 and 10):

For S.I. units:

$$\mu_{cd} = 0.93 - 1.6 \times 10^{-4} p \qquad (1a)$$

For U.S. Customary units:

$$\mu_{cd} = 0.93 - 1.1 \times 10^{-3} p \qquad (1b)$$

where p is the tire inflation pressure, kPa ($lb/in^2$).

(b) Tire cornering power values at low speed (<3 knots) can be determined from the empirically derived equations in reference 10.

(c) The maximum braked-rolling friction coefficient $\mu_{max}$ developed by aircraft tires on dry pavements can be estimated from the empirical equation:

$$\mu_{max} = \mu_{cd} \cdot K_{T,R} \tag{2}$$

where $K_{T.R}$ is the tire frictional heating factor for braked-rolling operations and is determined from the empirical expression

$$K_{T,R} = 1 - 0.0013\ V_G \tag{3}$$

where $V_G$ is the ground speed in knots.

(d) The locked-wheel, sliding friction coefficient $\mu_{skid}$ developed by aircraft tires on dry pavements can be estimated from the empirical equation:

$$\mu_{skid} = \mu_{cd} \cdot K_{T,S} \tag{4}$$

where $K_{T,S}$ is the tire frictional heating factor for locked-wheel operations and is determined from the empirical expressions

$$K_{T,S} = 1 - 0.0208\ V_G + 0.00017\ V_G^2;\ \text{for } V_G \leq 58 \text{ knots} \tag{5a}$$

$$K_{T,S} = 0.432 - 0.00113\ V_G;\ \text{for } V_G > 58 \text{ knots} \tag{5b}$$

(e) The cornering or side friction coefficient $\mu_s$ developed by aircraft tires on dry pavements can be estimated from the empirical equations:

For speeds $\leq$ 3 knots-

$$\mu_s = \mu_{cd} \cdot \cos\Psi \left[ N_{\Psi,P} - \frac{4}{27} \left( N_{\Psi,P} \right)^3 \right];\ \text{for } N_{\Psi,P} \leq 1.5 \tag{6a}$$

$$\mu_s = \mu_{cd} \cdot \cos\Psi;\ \text{for } N_{\Psi,P} > 1.5 \tag{6b}$$

For speeds > 3 knots-

$$\mu_s = \mu_{cd} \cdot \cos\Psi \cdot K_{T,\Psi} \left[ N_{\Psi,P} - \frac{4}{27} \left( N_{\Psi,P} \right)^3 \right];\ \text{for } N_{\Psi,P} \leq 1.5 \tag{7a}$$

$$\mu_s = \mu_{cd} \cdot \cos\Psi \cdot K_{T,\Psi};\ \text{for } N_{\Psi,P} > 1.5 \tag{7b}$$

where $\Psi$ is the yaw angle in deg, and $N_{\Psi,P}$ is the cornering power parameter as determined from the expression:

$$N_{\Psi,P} = \frac{N \cdot \Psi}{\mu_{cd} \cdot F_z} \quad (8)$$

where $F_z$ is the tire vertical load, kN (lb) and N is the tire cornering power, kN/deg (lb/deg).

$K_{T,\Psi}$ is considered the tire frictional heating factor for yawed rolling operations and is determined from the expression:

$$K_{T,\Psi} = 1 - 0.0104 (V_G \cdot \sin\Psi) + 0.000085 (V_G \cdot \sin\Psi)^2; \text{ for}$$

$$V_G \cdot \sin\Psi \leq 58 \text{ knots} \quad (9a)$$

$$K_{T,\Psi} = 0.75 - 0.00113 (V_G \cdot \sin\Psi); \text{ for } V_G \cdot \sin\Psi > 58 \text{ knots} \quad (9b)$$

The following assumptions are made in applying the equations to estimate Shuttle Orbiter and B-747 aircraft tire friction performance on both dry paved surfaces and the unpaved, gypsum-surface runways at White Sands:

(a) The maximum tire cornering or side friction coefficient is equal to the maximum braking or drag friction coefficient.

(b) Tire frictional heating developed during operations on the dry gypsum surface does not significantly affect the tire braking or yawing friction coefficient values, and thus can be ignored.

(c) Valid tire friction data at higher speeds can be derived from extrapolation of Landing Loads Track data. (The maximum speed for this data is 110 knots.)

(d) Antiskid controlled braking for the Shuttle Orbiter and B-747 aircraft on the dry gypsum runways at White Sands is expected to operate at approximately 12 percent braking slip based on dry pavement Langley Track tests with this type of antiskid brake system (see ref. 11).

(e) The effects of tire surface rutting on the value of side (yawed rolling) friction coefficient is neglected for yaw angles $\leq 20^o$.

(f) The segment of dry gypsum surface exposed to the free rolling, yawed rolling, or unyawed braking tire is homogeneous.

## Data Analysis

Before deriving estimates of the Shuttle Orbiter and B-747 aircraft tire friction performance, the 22 x 5.5 aircraft tire friction coefficients obtained experimentally with the instrumented tire test vehicle were compared to the calculated values derived from the appropriate equations. Table III gives the pertinent 22 x 5.5 tire parameter values used in this analysis which first considered the yawed rolling tire friction coefficient values.

The tire cornering or side force friction coefficient data obtained ex-

perimentally at a speed of 17.4 knots (20 mph) and shown in figure 20 for both dry concrete and gypsum surfaces are replotted in figure 23 together with the corresponding calculated coefficients. The calculated $\mu_s$ for the dry concrete surface was based on a characteristic dry friction coefficient of 0.58 (from eq. 1) and good agreement is evident between the experimental and calculated data. Since no such characteristic dry friction coefficient was available for gypsum, the maximum experimental side force friction coefficient value of 0.38 was selected as the characteristic dry friction coefficient for that surface. It should be noted that friction coefficients higher than 0.38 were measured when the tire was operated in the braking mode, however these braking coefficients include drag due to surface rutting. Ignoring tire heating effects, the variation of tire side friction coefficient with yaw angle on the gypsum surface was calculated. As indicated by the dashed curve in figure 23, these calculated values reach a maximum at a smaller yaw angle than the experimental and, as a result, the calculated data tend to overestimate the experimental tire side friction coefficient values.

Since the characteristic dry friction coefficient is dependent exclusively upon the tire inflation pressure (see eq. 1), further tests were necessary on the dry gypsum surface to aid in the selection of the appropriate values of that coefficient to accommodate the wide range of tire inflation pressures associated with the Shuttle and the B-747. To this end, drag force friction tests were conducted at 12-percent braking slip with tire inflation pressures ranging from 690 to 2172 kPa (100 to 315 psi) on runway 5/23. Figure 24 presents the results from these tests together with the expression which fairs the data. This expression:

$$\mu = 0.73 - 1.6 \times 10^{-4} p \text{ for S.I. units} \qquad (10)$$

is equation 1 with a simple modification and was used to compute the characteristic dry surface friction coefficient values at any tire inflation pressure.

## Shuttle Orbiter Tire Friction Estimates

The tire parameter values given in table IV were used to estimate Shuttle Orbiter tire braking and cornering friction coefficients developed on a dry concrete surface and on the dry gypsum surface at White Sands. Two different main gear tires, distinguished by ply rating as "light weight" and "heavy weight", are currently being considered for use on the Shuttle Orbiter, and data for both tires are included. Tire braking friction coefficients, which are not significantly affected by vertical loading, are given in figure 25 for both the light-weight and heavy-weight tires under consideration. Tire cornering or side friction coefficient estimates given in figures 26 and 27 are for both the static and the dynamic loading case since vertical loading affects the tire cornering power (see eq. 8).

Braking friction coefficient. The variation of Shuttle Oribter main gear tire braking friction coefficient with landing speed is presented in figure 25. Curves for the maximum braked-rolling friction coefficient $\mu_{max}$ on concrete were derived using equations 1, 2, and 3; and curves for the locked-wheel skidding friction coefficient $\mu_{skid}$ were obtained using equations 1, 4,

and 5 together with the appropriate tire parameter values listed in table IV. As noted in the figure, friction coefficient estimates above 110 knots are an extrapolation since the basic equations were derived primarily from NASA Track data limited to 110 knots. In general, tire braking friction coefficient values developed on a dry paved surface decrease with increasing inflation pressure as well as speed (see ref. 10); hence, estimated values for the light weight tire are correspondingly higher than values for the heavy weight tire.

An estimated value of the maximum friction coefficient developed on the dry gypsum surface at 12 percent braking slip is shown in figure 25 for both tires (12-percent was chosen because that is the anticipated braking slip for the Shuttle Orbiter antiskid system). Only a single data point at near zero velocity is given because of the uncertain contribution to the drag due to rutting with speed on this unpaved surface. Since the component of braking friction coefficient due to rutting is added to the braked rolling friction coefficient developed between the tire and the gypsum surface, somewhat higher actual $\mu_{max}$ values can be expected from those indicated in the figure. Available data at this time does not permit such an assessment. Aircraft tires using tires similar in size and inflation pressure to those planned for the Shuttle Orbiter would be required to obtain such data.

Cornering friction coefficient. - The variation of the estimated unbraked cornering or side force friction coefficient $\mu_s$ with yaw angle up to 20 degrees at ground speeds to 100 knots is given in figures 26 and 27 for the Shuttle Orbiter nose gear tire and both the light-weight and heavy-weight main gear tires operating on dry concrete and gypsum surfaces. Estimated tire cornering friction coefficients developed for the static loading case are presented in figure 26, and those coefficients based on the more severe, dynamic loading case are presented in figure 27. Equations 1 and 6 through 9 were used to calculate $\mu_s$ on the dry concrete surface, whereas only equations 6 and 10 were used to derive estimates of $\mu_s$ on the dry gypsum surface since tire frictional heating developed during yawed rolling on gypsum is assumed to be insignificant. Thus, a single curve describes the tire cornering behavior up to 100 knots on the dry gypsum.

The general data trends shown in figures 26 and 27 indicate that unbraked tire cornering friction coefficient developed on a dry paved surface decreases with increasing speed and tire inflation pressure. In the static loading case, higher $\mu_s$ values are developed over most of the tire yaw angle range on the paved surface than on the gypsum, however, in the dynamic loading case, the difference in estimated $\mu_s$ variation with yaw angle between these two surfaces is negligible. The peak friction in both cases occurs at smaller tire yaw angles on the gypsum surface than on the concrete surface. Compared to the static case, the increased vertical loading associated with the dynamic case resulted in reduced tire cornering power (see table IV), lower $\mu_s$ values throughout the yaw angle and speed ranges considered, and much higher yaw angles at which maximum cornering capability is developed. The large reduction shown in estimated Shuttle tire cornering friction between the static and the dynamic loading conditions, combined with the large yaw angles required to develop significant side forces, suggest that directional control inputs be minimized particularly during the high-speed portion of the Shuttle Orbiter landing operation.

## B-747-100 Aircraft Tire Friction Estimates

Estimates of tire braking and cornering friction coefficients for B-747-100 aircraft operations on a dry concrete surface and the dry gypsum surface were derived using the tire parameter values given in table V. The methods and equations used to obtain these tire friction performance data were similar to those used for the Shuttle Orbiter tire. These data are presented in figures 28 and 29. Tire loading for this exercise was based on a 3282.8 kN (738000 lb) static gross weight for the mated Shuttle Orbiter/aircraft configuration with the loading on the nose tire computed at the most forward CG and the main tire loading at the most aft CG location.

Braking friction coefficient. - Figure 28 presents the estimated aircraft main gear tire braking friction coefficient as a function of ground speed on a dry concrete surface together with a single data point at near zero velocity for the estimated $\mu_{max}$ value developed at 12 percent braking slip on the dry gypsum surface. The previous discussion on the effects of rutting and the lack of available data to determine the $\mu_{max}$ variation with ground speed on the gypsum surface also applies to these data. It should be pointed out that the component of the braking friction coefficient attributed to rutting enhances deceleration during landings but degrades takeoff performance. It is anticipated that the B-747-100 would develop better braking capability than that estimated for the Shuttle Orbiter on the dry gypsum surface because of the lower inflation pressure of its main gear tires.

Cornering friction coefficient. - The variation of the estimated B-747-100 aircraft nose and main gear tire unbraked cornering friction coefficient with yaw angle and ground speed is given in figure 29 for both dry concrete and dry gypsum surfaces. The trends indicated in the figure are similar to those for the Shuttle Orbiter tires. Up to a tire yaw angle of 10 degrees, the estimated $\mu_s$ for the dry gypsum surface is comparable to that indicated for the dry concrete surface. At yaw angles above 10 degrees, the estimated $\mu_s$ for the dry gypsum surface is less than that estimated for the dry concrete at 100 knots ground speed.

## CONCLUDING REMARKS AND RECOMMENDATIONS

In preparation for possible Space Shuttle Orbiter landing and retrieval operations on the unpaved gypsum surface runways at Northrup Strip, White Sands Missile Range, a NASA Langley test team performed friction measurements on these runways in April 1979. Tests runs were conducted with an instrumented tire test vehicle equipped with an aircraft tire inflated to the planned Orbiter main gear tire pressure to determine rolling resistance and braking and cornering friction capability on the gypsum surface for both dry and artificially wetted conditions. Additional friction measurements were acquired with a diagonal-braked vehicle which was also used in similar tests performed in 1976 on the two Shuttle runways (lakebed and concrete) at Dryden Flight Research Center and the grooved concrete runway at Kennedy Space Center.

Results from these ground vehicle friction tests conducted at 41 different

runway locations at Northrup Strip indicate that the dry gypsum surface friction capability is comparable to paved and other unpaved surfaces and appears suitable for landing and retrieval operations with the Shuttle Orbiter and the B-747 aircraft. The ground vehicle friction measurements, an assessment of surface characteristics, and estimates of Shuttle Orbiter and B-747 aircraft tire friction performance, suggest the following observations:

## Ground Vehicle Friction Evaluation

1. The ground vehicle friction measurements obtained in similar test modes were found to vary with runway location and surface characteristics.

2. The skidding friction developed by the diagonal-braked vehicle tires on the dry gypsum surface was nearly equal to that measured on the paved runway at Dryden and was higher than that measured on the Dryden lakebed runway.

3. Significantly lower diagonal-braked vehicle skidding friction was developed on the gypsum surface following artificially wetting.

4. Rolling resistance friction measured by the instrumented tire test vehicle:

   (a) Decreased with increasing speed up to 40 knots

   (b) Was not significantly effected by surface wetness

   (c) Was higher on dry gypsum surface than on dry paved surface

5. Braking or drag friction measured by the instrumented tire test vehicle:

   (a) Increased with increasing speed (up to 30 knots) and braking slip (up to 45 percent)

   (b) Was reduced slightly on the artificially wetted surface from that measured on the dry surface

   (c) Increased with decreasing tire inflation pressure.

6. Cornering or side friction measured by the instrumented tire test vehicle:

   (a) Increased with increasing speed (up to 30 knots) and yaw angle (up to 14$^{o}$)

   (b) Was reduced slightly on the artificially wetted surface from that measured on the dry surface

   (c) Was lower on the dry gypsum surface compared to a dry paved surface but the peak value on both surfaces occurred at approximately 14$^{o}$ yaw angle.

## Assessment of Surface Characteristics

1. Depths of loose, unconsolidated material covering the hard, compacted gypsum surface (mantle) varied from nearly zero to approximately 5 cm (2 in.). In general, the greater amounts were found in the overrun areas of both runways.

2. Tire surface rutting varied with tire operating mode, inflation pressure, speed, and the depth of loose, unconsolidated material covering the hard surface. In general, rutting decreased with increasing speed and increased with greater braking slip values.

3. Tire surface rutting was found to significantly affect the friction coefficient values developed during unyawed free rolling and braking.

4. Surface rutting was found to decrease with decreasing tire inflation pressure.

5. Based on comparisons to aircraft data through a greater speed range on different soil surfaces, the validity of extending the dry gypsum surface tire rolling resistance data at limited speed to the full ground speed range of the Shuttle Orbiter is questionable.

6. Tire tread rubber was deposited on the hard gypsum undersurface during heavy braking and large angle cornering tests once the tire penetrated through the loose material on the surface. Insignificant tread penetration of this hard surface was observed.

7. Artificial wetting of the loose, gypsum material produced a soft, sticky mix and degraded friction. Inability to adequately measure surface moisture content precluded an assessment of friction variation throughout a range of surface wetness conditions.

8. Surface roughness in the overrun areas and the runway intersection was considered too severe based on the ride quality experienced in the ground test vehicles. Inspection of the surface in these rough areas indicated that wind and water erosion effects, combined with surface ruts from previous ground vehicle and aircraft operations, contributed to the roughness.

9. Repair of missile impact crater near the shoulder of runway 17/35 at Sta. 10+00 appeared successful on the basis of ground vehicle friction measurements but surface roughness was observed.

10. Some corrosive effects of gypsum material were found on metal components of ground test vehicles within two months of test completion.

11. Variation in gypsum surface characteristics should be expected from effects of weathering, wind, precipitation, and traffic.

## Shuttle Orbiter and B-747 Aircraft Tire Friction Estimates

1. Uncertainties surrounding the effects of ground speed on tire surface

rutting and its contribution to vehicle drag do not permit an estimation of tire braking friction coefficient over the full ground speed range of both vehicles on the dry gypsum surface.

2. The component of braking friction coefficient developed between the tire and the dry gypsum surface due to surface rutting (see Appendix) should contribute to the deceleration level of both vehicles during landings.

3. On the dry gypsum surface, tire braking friction decreases with increasing inflation pressure, hence, the light-weight tire should develop better braking capability than the higher pressure heavy-weight tire on the Shuttle Orbiter.

4. The unbraked tire cornering friction coefficient developed on both the dry paved and unpaved surfaces decreases with increasing inflation pressure and loading, thus better cornering capability would be anticipated from the light-weight tire.

5. Increasing the tire vertical loading results in reduced tire cornering power, lower cornering friction coefficients through the yaw angle and speed ranges considered, and a higher yaw angle at which peak cornering friction is developed. Thus, from an operational standpoint, the most critical condition, in terms of developing tire braking and cornering friction on the dry gypsum surface, is that associated with the dynamic loading case on the Shuttle Orbiter.

## Recommendations

1. Continued maintenance of runway surface is needed because of weathering, wind, precipitation and traffic.

2. Accumulation of loose, unconsolidated material on the surface should be minimized and controlled.

3. Additional compaction and grading work should be performed in runway overrun areas and at the runway intersection to reduce roughness and tire rutting.

4. Precautionary measures should be planned to minimize the corrosive effects of the gypsum material on Shuttle Orbiter and B-747 aircraft hardware.

5. Ground vehicle and aircraft traffic should be restricted from using the runways when wet to minimize development of surface irregularities and rutting tracks.

6. Shuttle Orbiter landing and retrieval operations should not be attempted if runway surfaces are wet. If an adequate measuring device for surface moisture content can be obtained, additional load cart and ground friction measuring vehicle tests should be conducted to define exact surface wetness condition which can be used as criteria for restricting use of runway.

7. Additional ground vehicle friction tests should be performed if load and roughness test results necessitate extensive compaction and grading work on the runway surfaces and/or a prolonged time period elapses between these friction tests and the first Shuttle Orbiter landing.

8. Consideration should be given to conducting comparable aircraft braking tests prior to the first Shuttle Orbiter landing at White Sands to obtain a better assessment of the gypsum surface braking capability.

9. Braking and nose wheel steering inputs should be minimized as much as possible when high tire loads are present (after pitch down) during Shuttle Orbiter landing rollout to alleviate possibility of tire failures.

10. The large reduction in estimated Shuttle tire cornering friction between static and dynamic loading conditions, combined with the large yaw angles required to develop significant side forces for directional control, provides justification for considering the following:

(a) The estimated tire cornering data in this analysis should be correlated with actual tire dynamometer data

(b) Shuttle simulator landings, using the estimated tire cornering data in this analysis, should be conducted to assist in determining a runway crosswind limitation for actual Shuttle landing operations

(c) A runway crosswind limitation should be established and used in selecting a Shuttle runway landing site because large steering control requirements may result in excessive tire deflection(s) and possible tire failure(s).

## REFERENCES


1. Major Clark, James I.: Project Touchdown - A Comprehensive Evaluation of the Northrup Strip Airfield, White Sands Missile Range, as a Landing Site for the Space Shuttle Orbiter. Tyndall AFB Engineering and Services Center, July 1979.

2. Pavement Grooving and Traction Studies. NASA SP-5073, 1969.

3. Yager, Thomas J.; Phillips, W. Pelham; Horne, Walter B.; and Sparks, Howard C. (appendix D by R. W. Sugg): A Comparison of Aircraft and Ground Vehicle Stopping Performance on Dry, Wet, Flooded, Slush-, Snow-, and Ice-Covered Runways. NASA TN D-6098, 1970.

4. Horne, Walter B.; Yager, Thomas J.; Sleeper, Robert K.; and Merritt, Leslie R.: Part I - Traction Measurements of Several Runways under Wet and Dry Conditions with a Boeing 727, a Diagonal-Braked Vehicle, and a Mu-Meter. NASA TMX-73909, 1971.

5. Horne, Walter B.; Yager, Thomas J.; Sleeper, Robert K.; Smith, Eunice G.; and Merritt, Leslie R.: Part II - Traction Measurements of Several Runways Under Wet, Snow Covered, and Dry Conditions with a Douglas DC-9, a Diagonal-Braked Vehicle, and a Mu-Meter. NASA TM X-73910, 1972.

6. Horne, Walter B.: Status of Runway Slipperiness Research. NASA SP-416, 1976, pp. 191-245.

7. Leland, Trafford J. W.; and Smith, Eunice G.: Aircraft Tire Behavior During High-Speed Operations in Soil. NASA TN D-6813, 1972.

8. Richmond, L. D.; Breuske, N. W.; and Debord, K. J.: Aircraft Dynamic Loads from Substandard Landing Sites. Part II Development of Tire-Soil Mathematical Model. Technical Report AFFDL-TR-67-145, Sept. 1968.

9. Anon.: C-5A Category I/II Engineering Flight Test Performance Test Results. LG1T19-1-5, Vol 1, Dec 1, 1970 (revised Oct 1, 1972).

10. Smiley, Robert F.; and Horne, Walter B.: Mechanical Properties of Pneumatic Tires with Special Reference to Modern Aircraft Tires. NASA TR R-64, 1960 (Supersedes NACA TN 4110).

11. Stubbs, Sandy M.; Tanner, John A.; and Smith, Eunice G.: Behavior of Aircraft Antiskid Braking Systems on Dry and Wet Runway Surfaces - A Slip-Velocity-Controlled, Pressure-Bias-Modulated System. NASA TP-1051, 1979.

Table I. - Typical instrumented tire test vehicle friction coefficient values obtained at selected dry gypsum surface runway locations. Speed, 21.7 kt (25 mph)

| Location | | | $\mu_r$ | $\mu_{drag}$ (12% slip) | $\mu_{side}$ (12° yaw) |
|---|---|---|---|---|---|
| R/W | Longitudinal Station | Lateral Position | | | |
| 17 | 10+00 | Lt Shoulder | - | - | .379 |
| | 30+00 | Left of ℄ | .024 | - | .419 |
| | 47+50 | Right of ℄ | .021 | .405 | - |
| | 70+00 | Left of ℄ | .033 | - | .365 |
| | 105+00 | Rt Shoulder | - | - | .379 |
| | 120+00 | Right of ℄ | .023 | .431 | - |
| | 180+00 | Rt Shoulder | - | - | .390 |
| | 215+00 | Right of ℄ | .032 | .455 | - |
| | 255+00 | Rt Shoulder | - | - | .375 |
| | 270+00 | Right of ℄ | .050 | .480 | - |
| | 325+00 | Right of ℄ | .024 | .437 | - |
| | 335+00 | Rt Shoulder | - | - | .397 |
| ▼ | 335+00 | Left of ℄ | .051 | - | .414 |
| 05 | 45+00 | Right of ℄ | .027 | .412 | - |
| | 45+00 | Left of ℄ | .045 | .436 | - |
| | 50+00 | Lt Shoulder | .042 | .472 | - |
| | 50+00 | Rt Shoulder | .030 | .460 | - |
| | 60+00 | Left of ℄ | .042 | - | .366 |
| | 135+00 | Left of ℄ | .023 | .422 | - |
| | 170+00 | Left of ℄ | .025 | .499 | - |
| | 175+00 | Lt Shoulder | - | - | .393 |
| | 225+00 | Lt Shoulder | - | .469 | - |
| | 240+00 | Lt Shoulder | - | - | .359 |
| | 265+00 | Lt Shoulder | - | - | .371 |
| | 320+00 | Right of ℄ | .034 | .454 | .364 |

Table II. - Typical diagonal-braked vehicle skidding friction coefficient values at selected speeds and dry gypsum surface runway locations.

| Location | | | Skidding friction coefficient | | | | |
|---|---|---|---|---|---|---|---|
| R/W | Longitudinal Station | Lateral Position | 43.4 kt. (50 mph) | 34.7 kt. (40 mph) | 26 kt. (30 mph) | 17.4 kt. (20 mph) | 8.7 kt (10 mph) |
| 17 | 10+00 | Lt Shoulder | .72 | .70 | .68 | .79 | .81 |
| ↓ | 52+50 | Left of ℄ | .58 | .66 | .76 | .92 | .89 |
| | 52+50 | Lt shoulder | .66 | .71 | .78 | .92 | .91 |
| | 75+00 | Left of ℄ | .72 | .71 | .73 | .72 | .66 |
| | 75+00 | Right of ℄ | .76 | .76 | .80 | .82 | .86 |
| | 185+00 | Right of ℄ | .74 | .74 | .74 | .74 | .74 |
| | 185+00 | Left of ℄ | .82 | .82 | .82 | .82 | .82 |
| | 195+00 | Right of ℄ | .83 | .83 | .82 | .81 | .81 |
| | 195+00 | Left of ℄ | .78 | .81 | .81 | .80 | .76 |
| | 345+00 | Right of ℄ | .54 | .60 | .57 | .63 | .71 |
| ↓ | 345+00 | Left of ℄ | .66 | .71 | .78 | .80 | .82 |
| 05 | 50+00 | Right of ℄ | .76 | .82 | .82 | .82 | .72 |
| ↑ | 100+00 | Left of ℄ | .76 | .81 | .82 | .86 | .85 |
| | 100+00 | Right of ℄ | .63 | .66 | .71 | .76 | .76 |
| | 170+00 | Left of ℄ | .71 | .81 | .86 | .92 | .91 |
| | 170+00 | Right of ℄ | .84 | .89 | .92 | .95 | .94 |
| | 210+00 | Left of ℄ | .83 | .84 | .85 | .86 | .87 |
| | 210+00 | Right of ℄ | .84 | .85 | .85 | .85 | .85 |
| | 255+00 | Left of ℄ | .73 | .76 | .76 | .80 | .76 |
| ↓ | 255+00 | Right of ℄ | .80 | .82 | .89 | .86 | .86 |

Table III. - Compilation of instrumented vehicle test tire parameters.

| PARAMETER | VALUE |
|---|---|
| Size and type | 22 x 5.5, Type VII |
| Ply rating | 12 |
| Loading, kN (lb) | 13.8 (3100) |
| Inflation pressure, kPa (psi) | 2172 (315) |
| Rated inflation pressure, kPa (psi) | 1620 (235) |
| Unloaded diameter, cm (in) | 55.5 (21.85) |
| Unloaded width, cm (in) | 14.0 (5.525) |
| Loaded deflection*, cm (in) | .84 (.33) |
| Cornering power**, kN/deg (lb/deg) | .92 (205.80) |
| Low speed $\mu_{cd}$ ** | .58 |

*Actual measurement.

**Values calculated from equations in reference 10.

Table IV. - Compilation of Shuttle Orbiter tire parameters for 894.1 kN (201000 lb) gross weight.

| LOADING CASE / PARAMETER | STATIC LOADING | | | DYNAMIC LOADING | | |
|---|---|---|---|---|---|---|
| Tire designation | NOSE | LIGHT WEIGHT MAIN | HEAVY WEIGHT MAIN | NOSE | LIGHT WEIGHT MAIN | HEAVY WEIGHT MAIN |
| Size | 32 x 8.8 | 44.5 x 16.21 | | 32 x 8.8 | 44.5 x 16.21 | |
| Ply rating | 20 | 28 | 34 | 20 | 28 | 34 |
| Loading, kN (lb) | 96.6 (21708) | 199.4 (44823) | 199.4 (44823) | 158.1 (35550) | 455.9 (102500) | 455.9 (102500) |
| Inflation pressure, kPa (psi) | 2068 (300) | 1793 (260) | 2172 (315) | 2068 (300) | 1793 (260) | 2172 (315) |
| Unloaded diameter* cm (in) | 79.5 (31.30) | 112.7 (44.36) | 113.1 (44.53) | 79.5 (31.30) | 112.7 (44.36) | 113.1 (44.53) |
| Unloaded width* cm (in) | 23.0 (9.05) | 39.3 (15.47) | 40.6 (16.0) | 23.0 (9.05) | 39.3 (15.47) | 40.6 (16.0) |
| Loaded deflection* cm (in) | 5.3 (2.08) | 8.6 (3.40) | 7.1 (2.80) | 7.9 (3.10) | 16.9 (6.65) | 14.2 (5.60) |
| Cornering power** kN/deg (lb/deg) | 6.4 (1446.5) | 16.1 (3609.6) | 21.0 (4721.9) | 5.3 (1193.8) | 6.6 (1472.5) | 12.7 (2859.8) |
| Low speed $\mu_{cd}$ ** | .60 | .64 | .58 | .60 | .64 | .58 |

*Values obtained from tire manufacturer's load/deflection curves.

**Values calculated from equations in reference 10.

Table V. - Compilation of B-747-100 aircraft tire parameters for 3282.8 kN (738 000 lb) mated maximum gross weight.

| PARAMETER | LANDING GEAR | |
|---|---|---|
| | NOSE | MAIN |
| Size and type | 46 x 16, Type VII | 46 x 16, Type VII |
| Ply rating | 30 | 30 |
| Loading*, kN (lb) | 170.8 (38400) | 189.6 (42625) |
| Inflation pressure, kPa (psi) | 1310 (190) | 1448 (210) |
| Rated infl. pressure, kPa (psi) | 1551 (225) | 1551 (225) |
| Unloaded diameter**, cm (in) | 113.8 (44.80) | 113.8 (44.80) |
| Unloaded width**, cm (in) | 39.4 (15.51) | 39.4 (15.51) |
| Loaded deflection**, cm (in) | 8.13 (3.20) | 8.26 (3.25) |
| Cornering power***, kN/deg (lb/deg) | 12.6 (2837.8) | 13.5 (3029.1) |
| Low speed $\mu_{cd}$*** | .72 | .69 |

*Maximum static load for nose at most forward CG; for main at most aft CG.

**Values obtained from tire manufacturers' load/deflection curves.

***Values calculated from equations in reference 10.

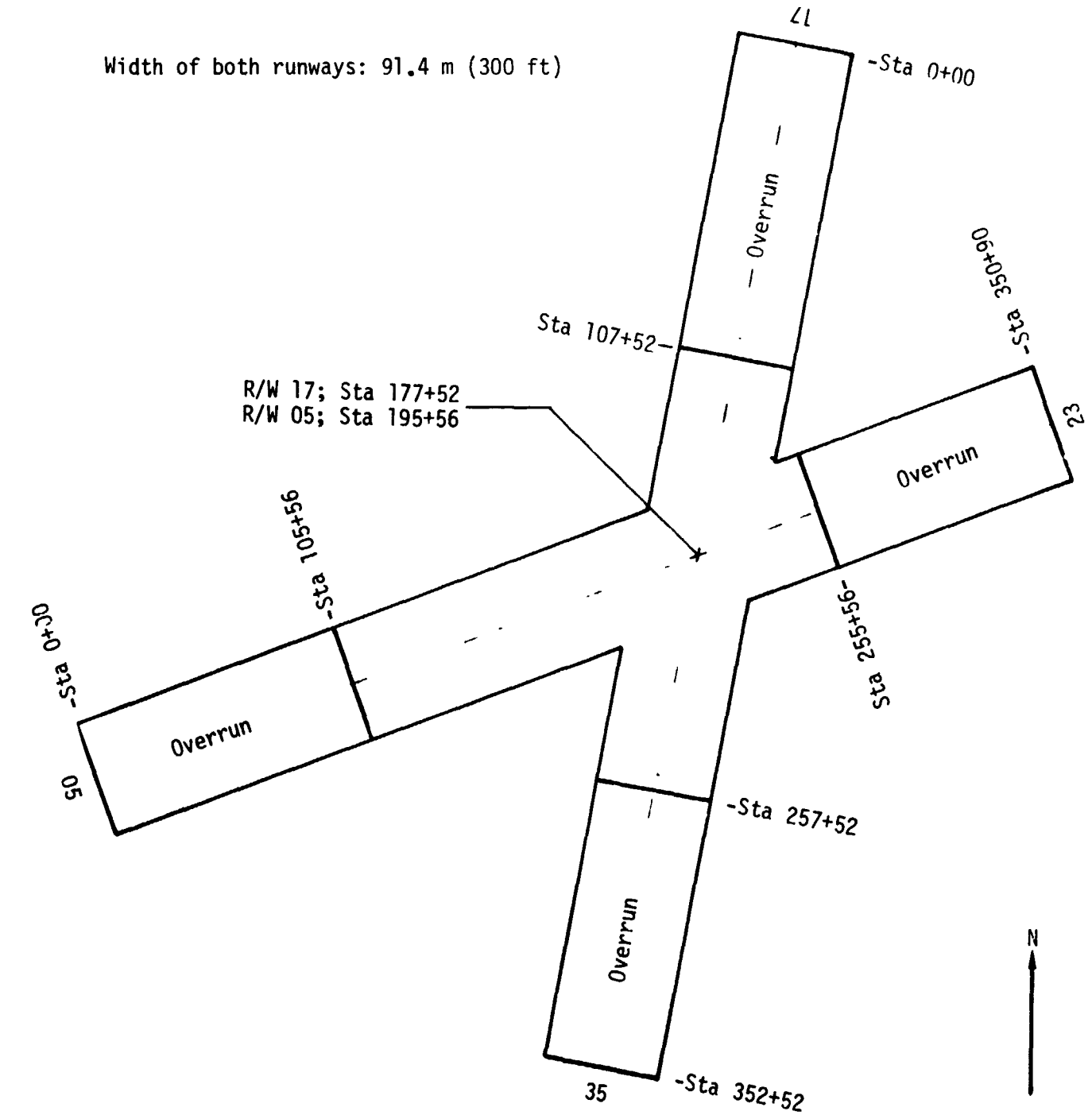


Figure 1. - Runway layout at Northrup Strip airfield, White Sands Missile Range.

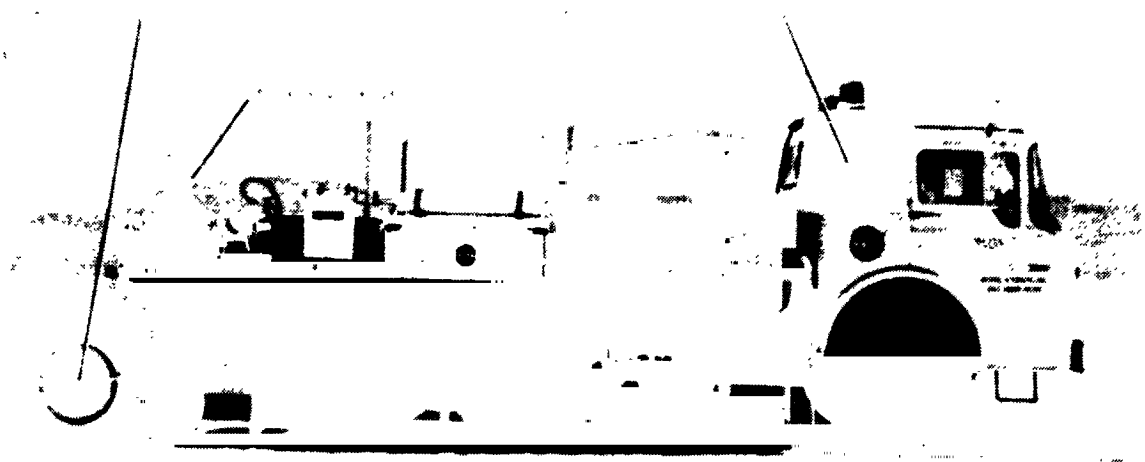

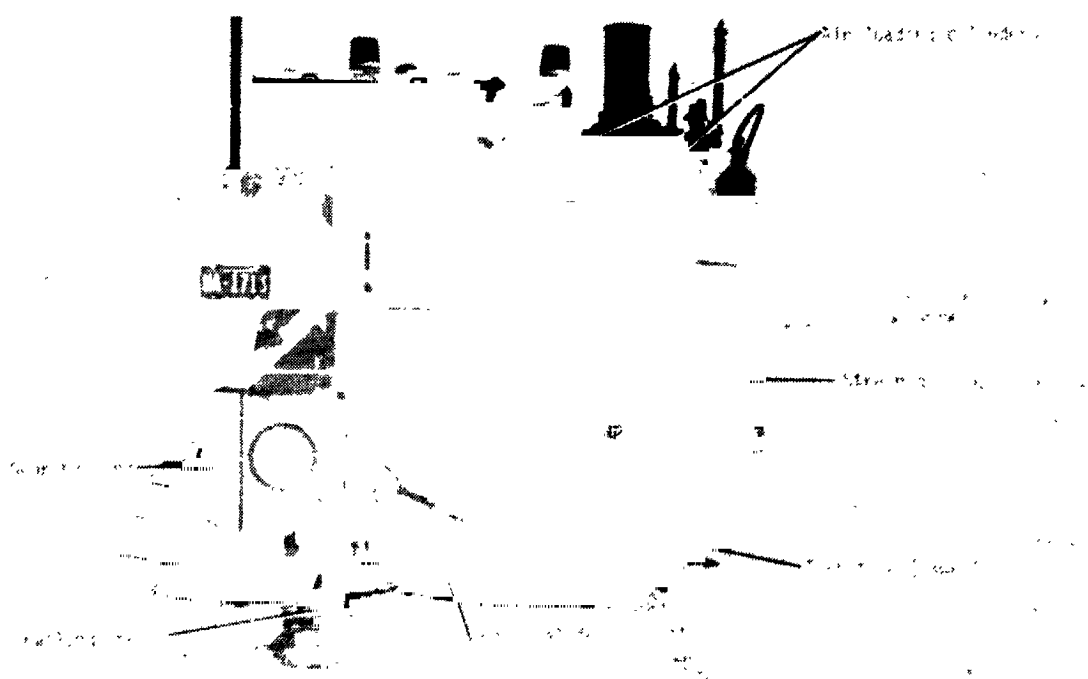

(a) NASA DIAGONAL-BRAKED VEHICLE

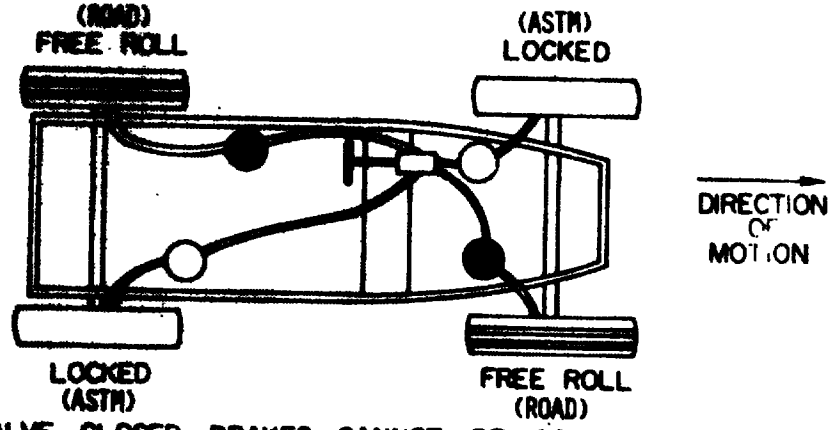


● VALVE CLOSED; BRAKES CANNOT BE ACTUATED

○ VALVE OPEN; BRAKES CAN BE ACTUATED

(b) SCHEMATIC OF DIAGONAL-BRAKING SYSTEM

**Figure 3.-** Diagonal-braked ground friction measuring vehicle.

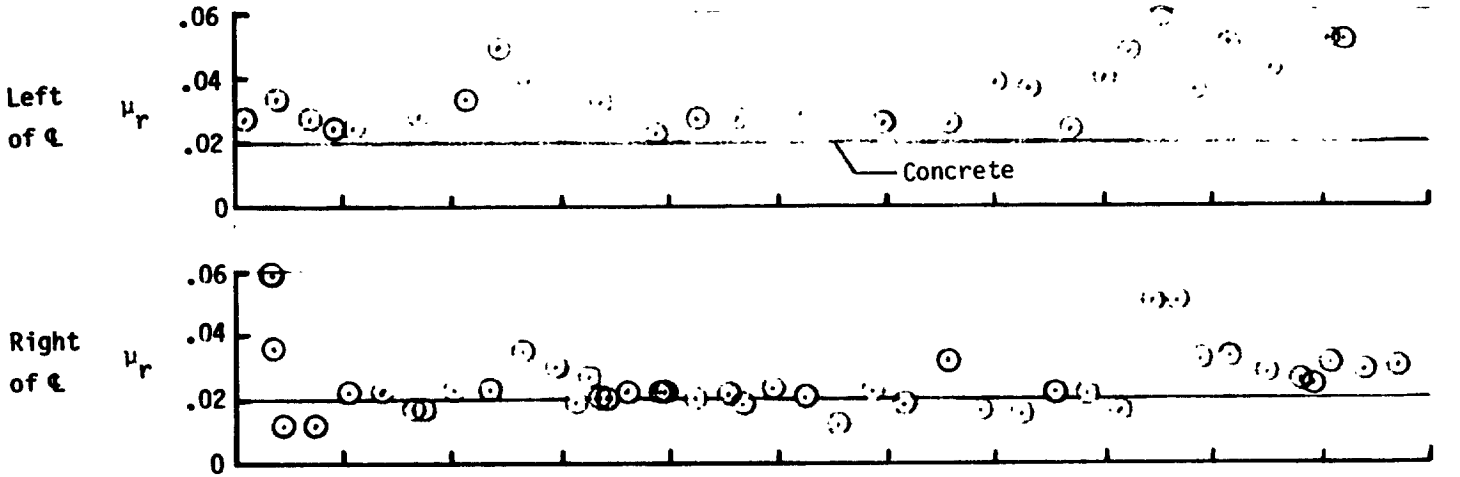


(a) Runway 17/35.

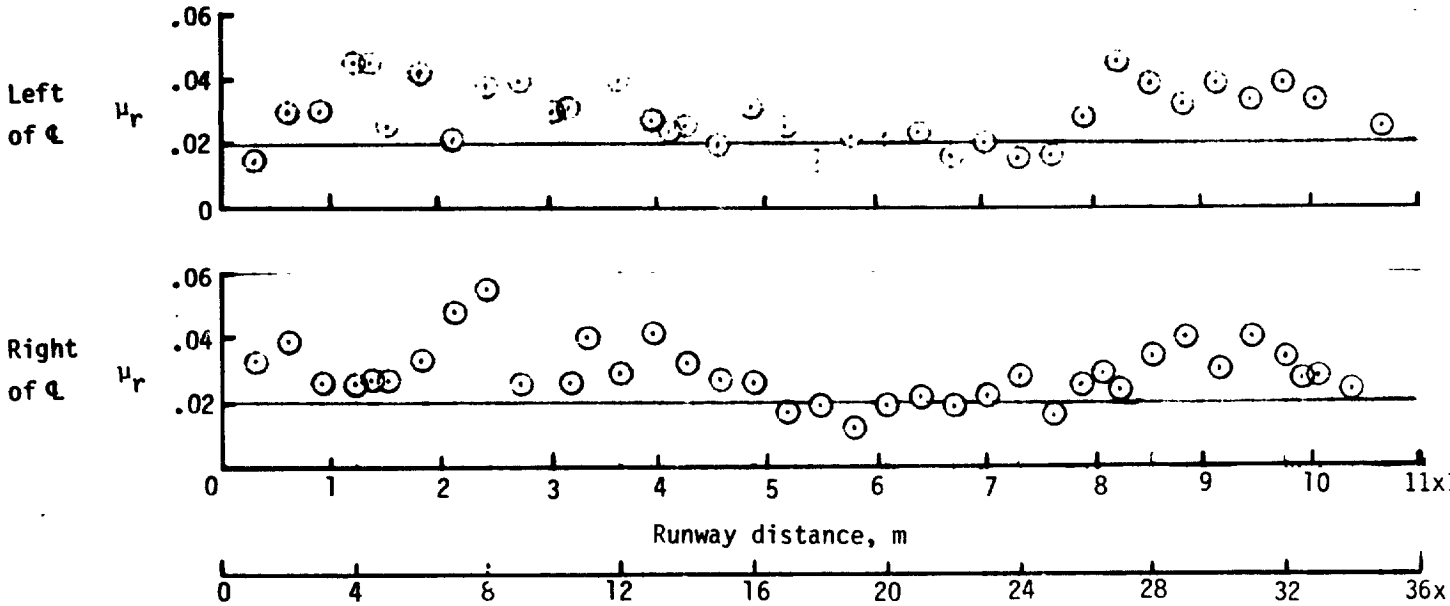


(b) Runway 05/23.

Figure 4. - Variation in tire rolling resistance coefficient values on both dry gypsum surface runways. Instrumented tire test vehicle; 22 x 5.5 tire; Ground speed, 21.7 knots (25 mph); yaw angle, 0 deg.

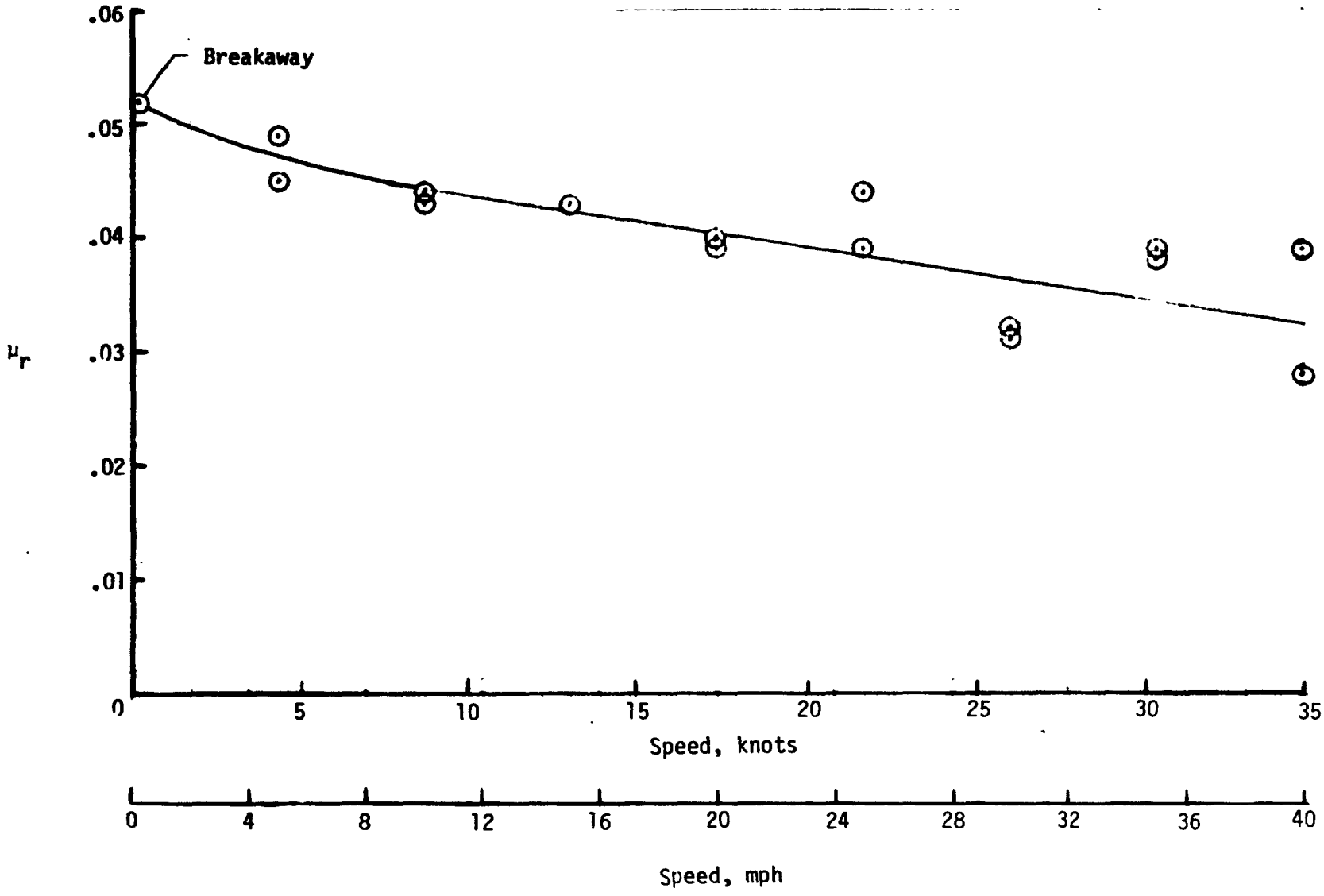


Figure 5. - Effect of speed on tire rolling resistance coefficient values obtained on dry gypsum surface runways. Instrumented tire test vehicle; 22 x 5.5 tire.

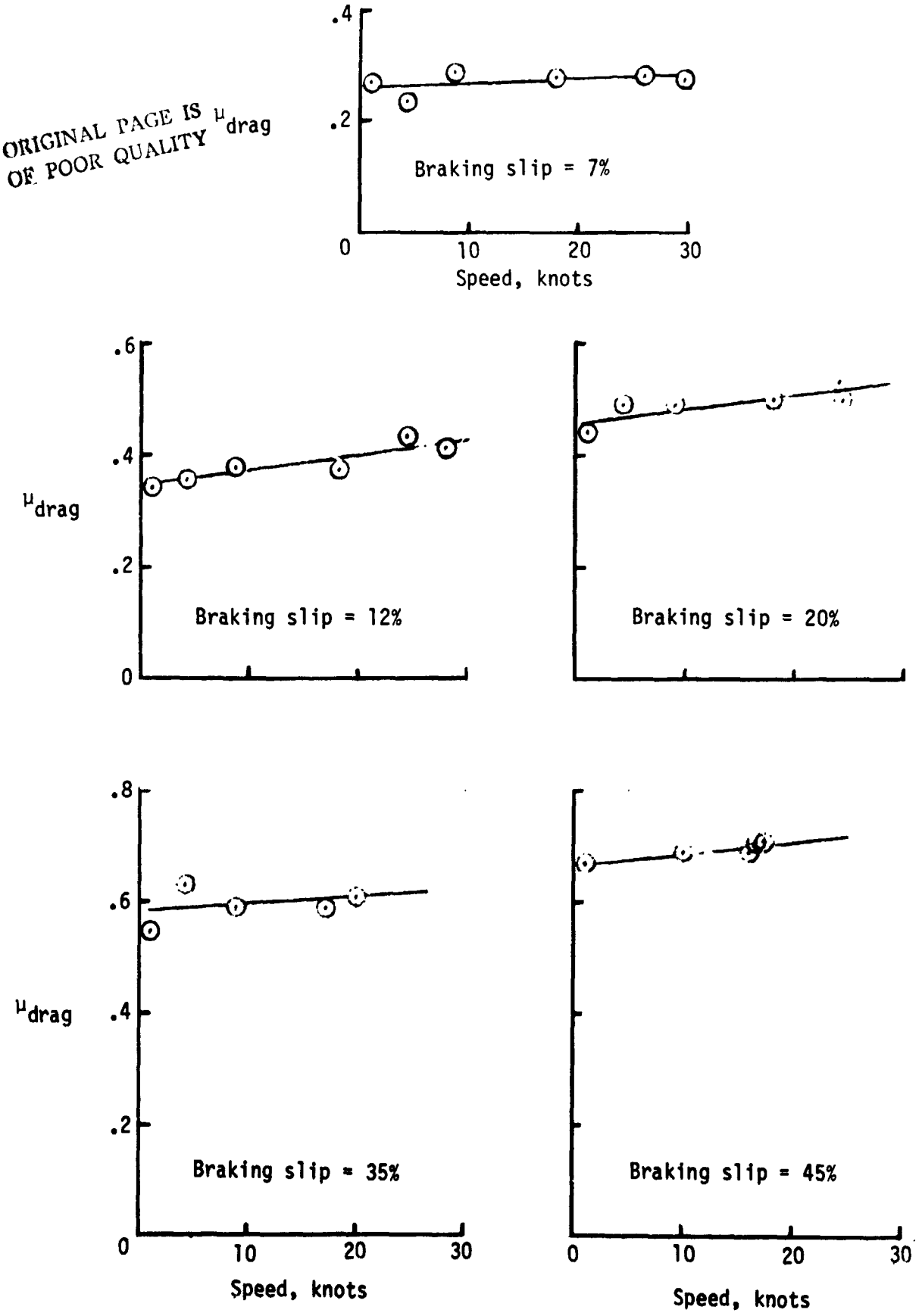


Figure 6. - Effect of speed on tire drag friction coefficient values obtained at different percent braking slips on dry gypsum surface runways.

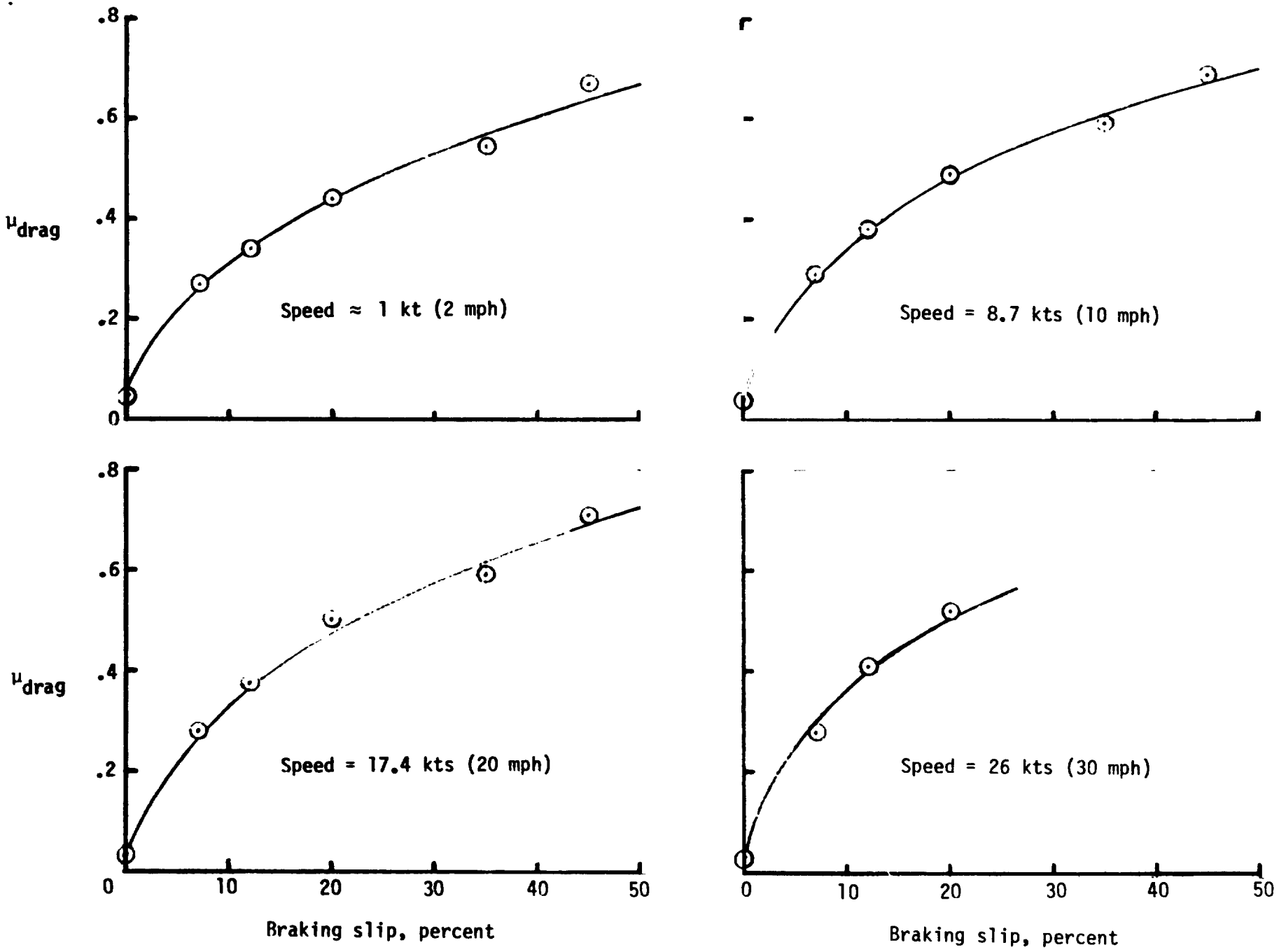


Figure 7. - Effect of braking slip and speed on tire drag friction coefficient values obtained on dry gypsum surface runways.

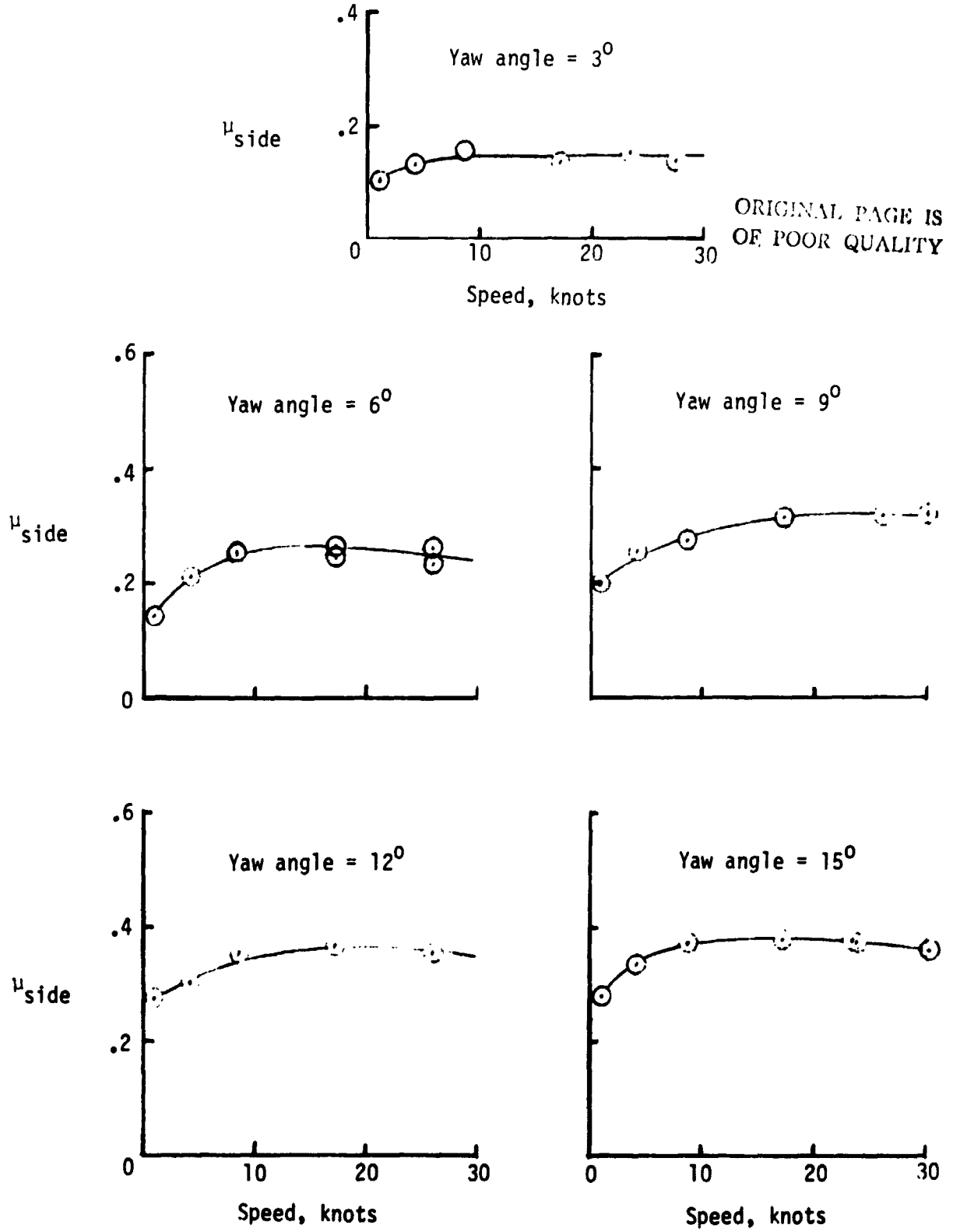


Figure 8. - Effect of speed on tire side friction coefficient values obtained at different yaw angles on dry gypsum surface runways.

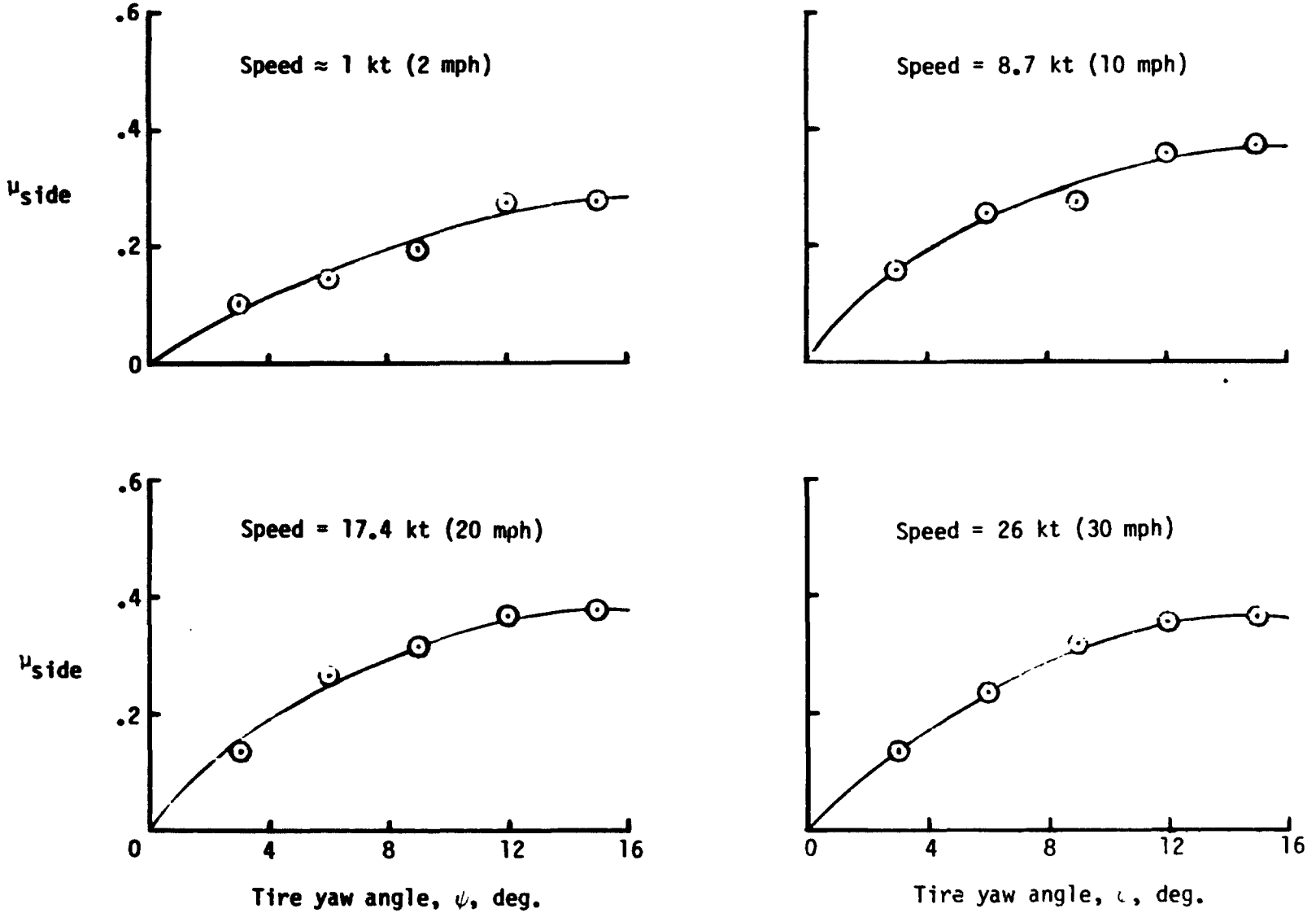


Figure 9. - Effect of yaw angle and speed on tire side friction coefficient values obtained on dry gypsum surface runways.

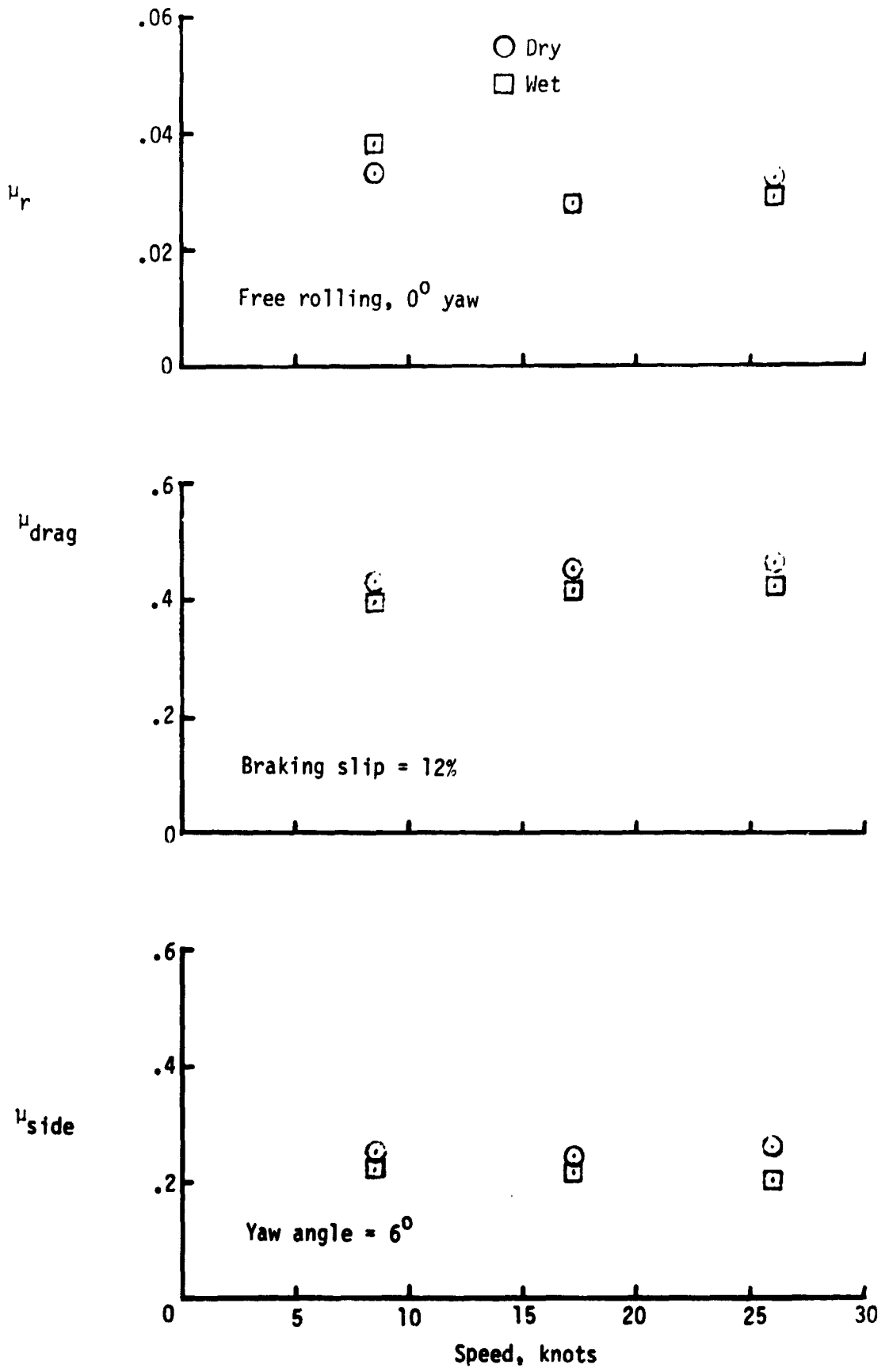


Figure 10. - Effect of gypsum surface wetness on tire friction coefficient variation with speed.

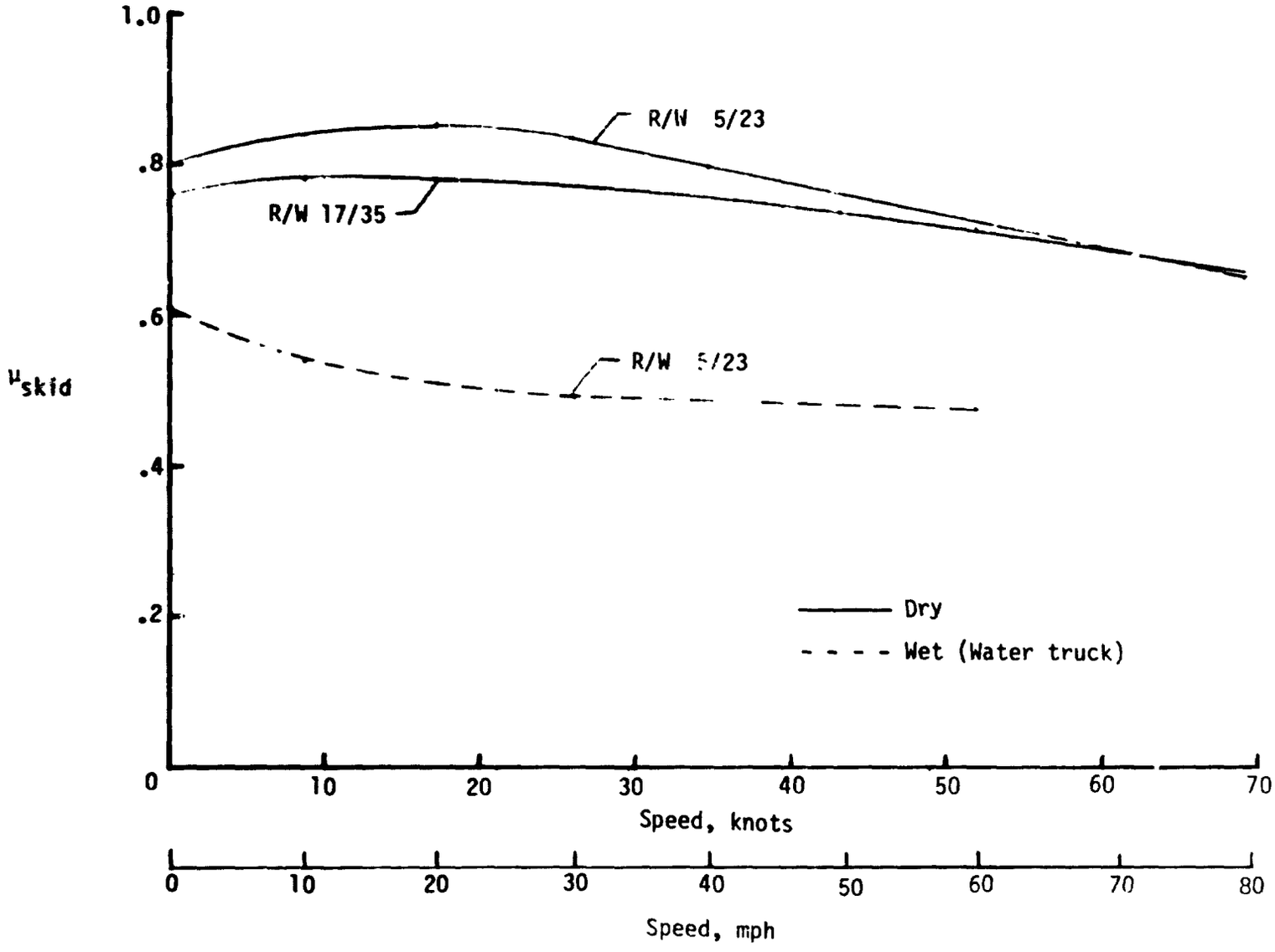


Figure 11. - Variation of diagonal-braked vehicle skidding (locked-wheel) friction coefficient with speed on gypsum surface runways. ASTM smooth test tires; p = 165 kPa (24 psi).


(a) 0% slip (free rolling)

**Figure 12** - Effect of tire braking slip on dry surface rutting at approximately 2 knot (1 m/s) speed.


(b) 45% slip

Figure 12.- Continued.

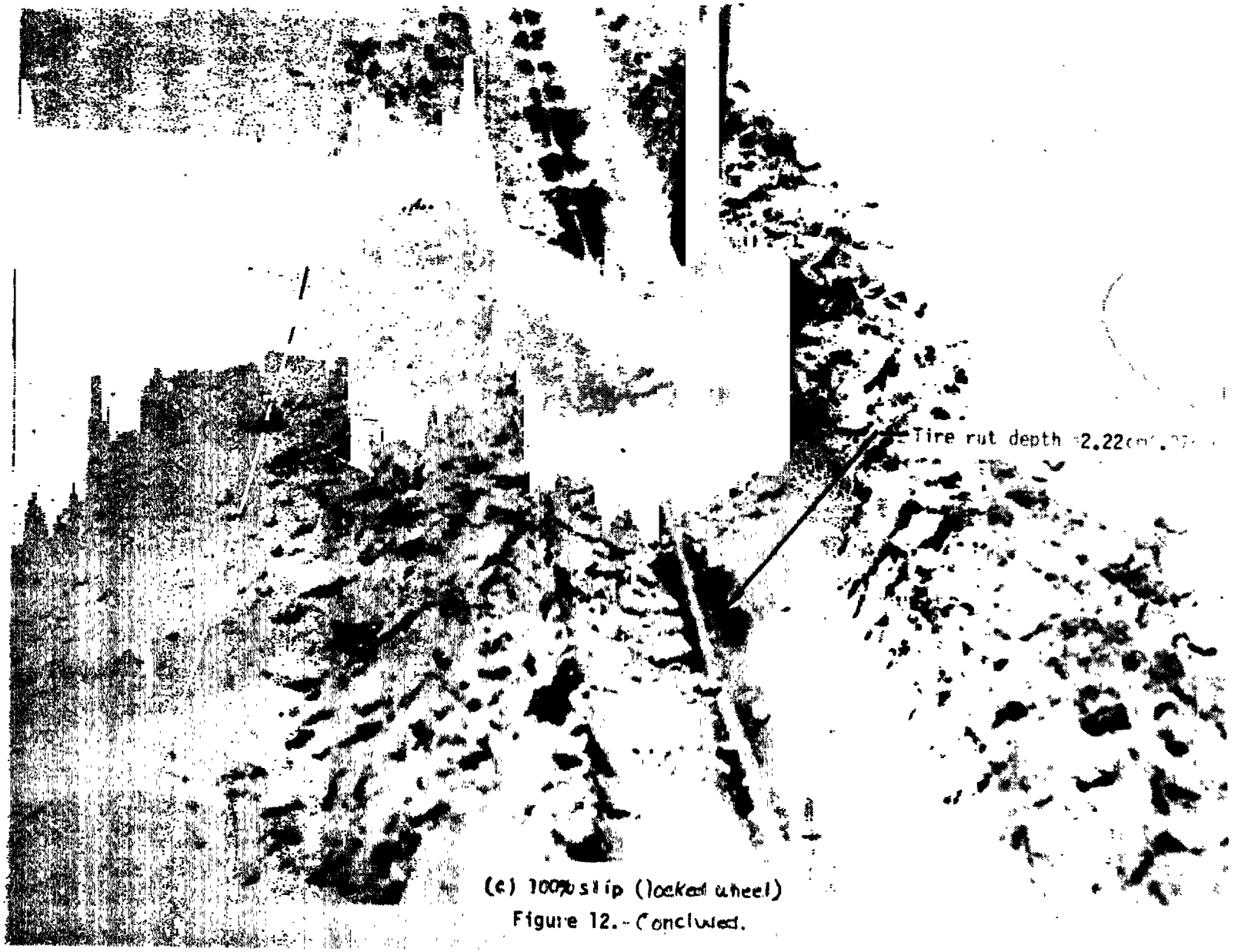


(c) 100% slip (locked wheel)

Figure 12.- Concluded.


Figure 13 – Effect of ground speed on dry surface rolling driving tire braking test at 45% slip.


(a) Yaw angle = 3°

Figure 14.- Effect of tire yaw angle on dry surface rutting at approximately 1 Knot ground speed.


(b) Speed = 21.7 knots

Figure 13.- Concluded.

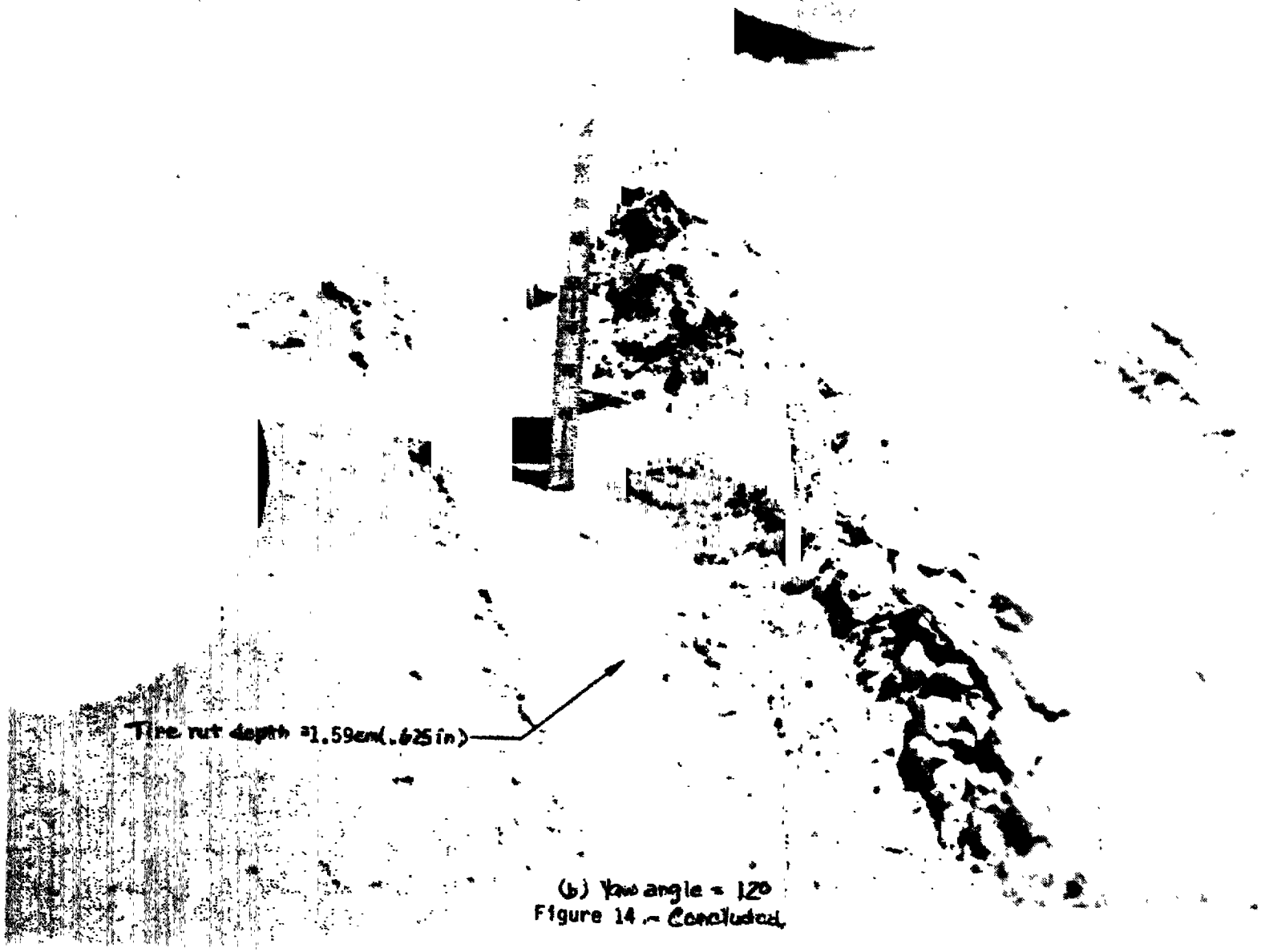


(b) Yaw angle = 12°

Figure 14.- Concluded.

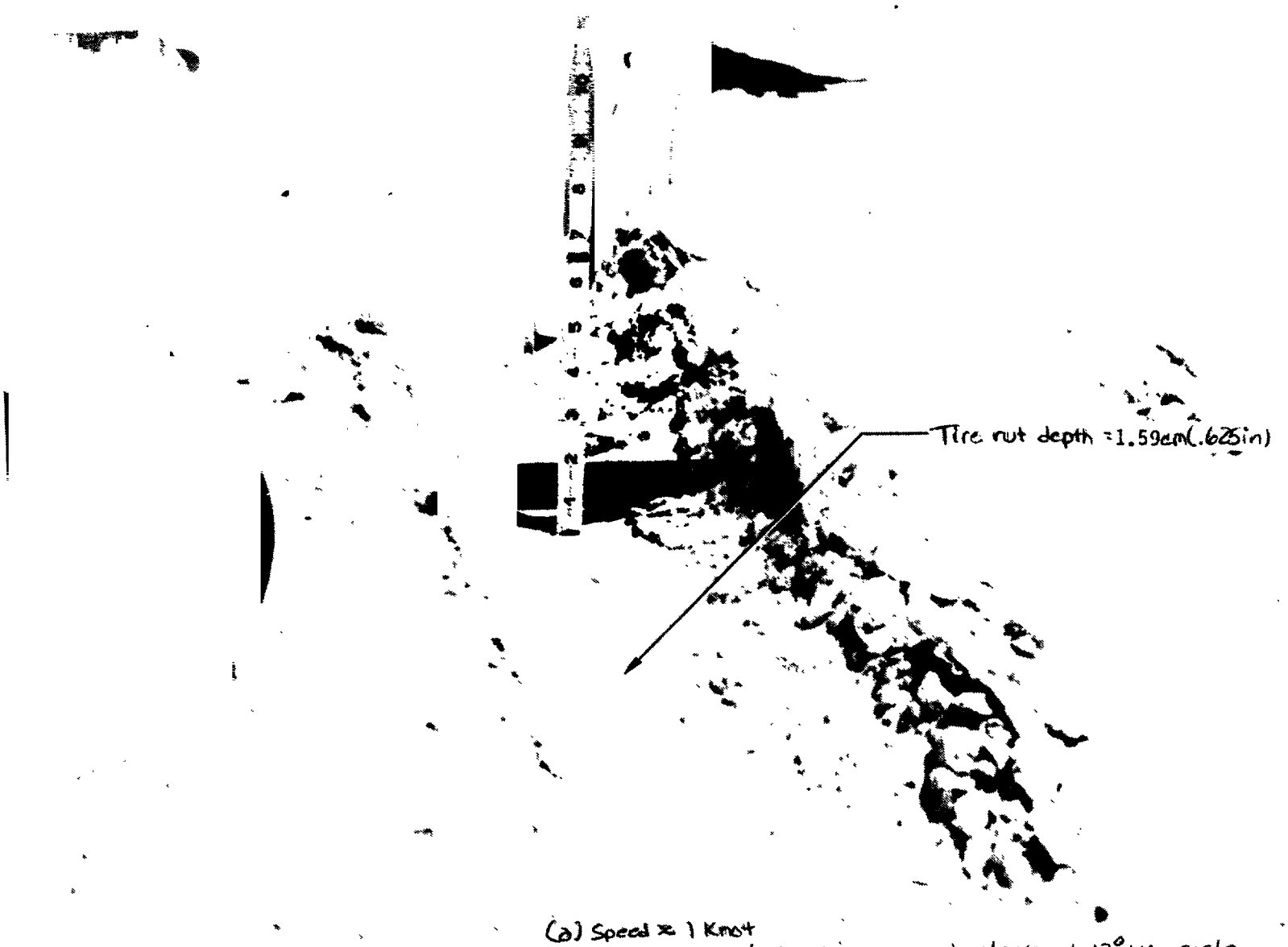


(a) Speed ≈ 1 Knot

Figure 15.– Effect of ground speed on dry surface rutting during tire cornering tests at 12° yaw angle.

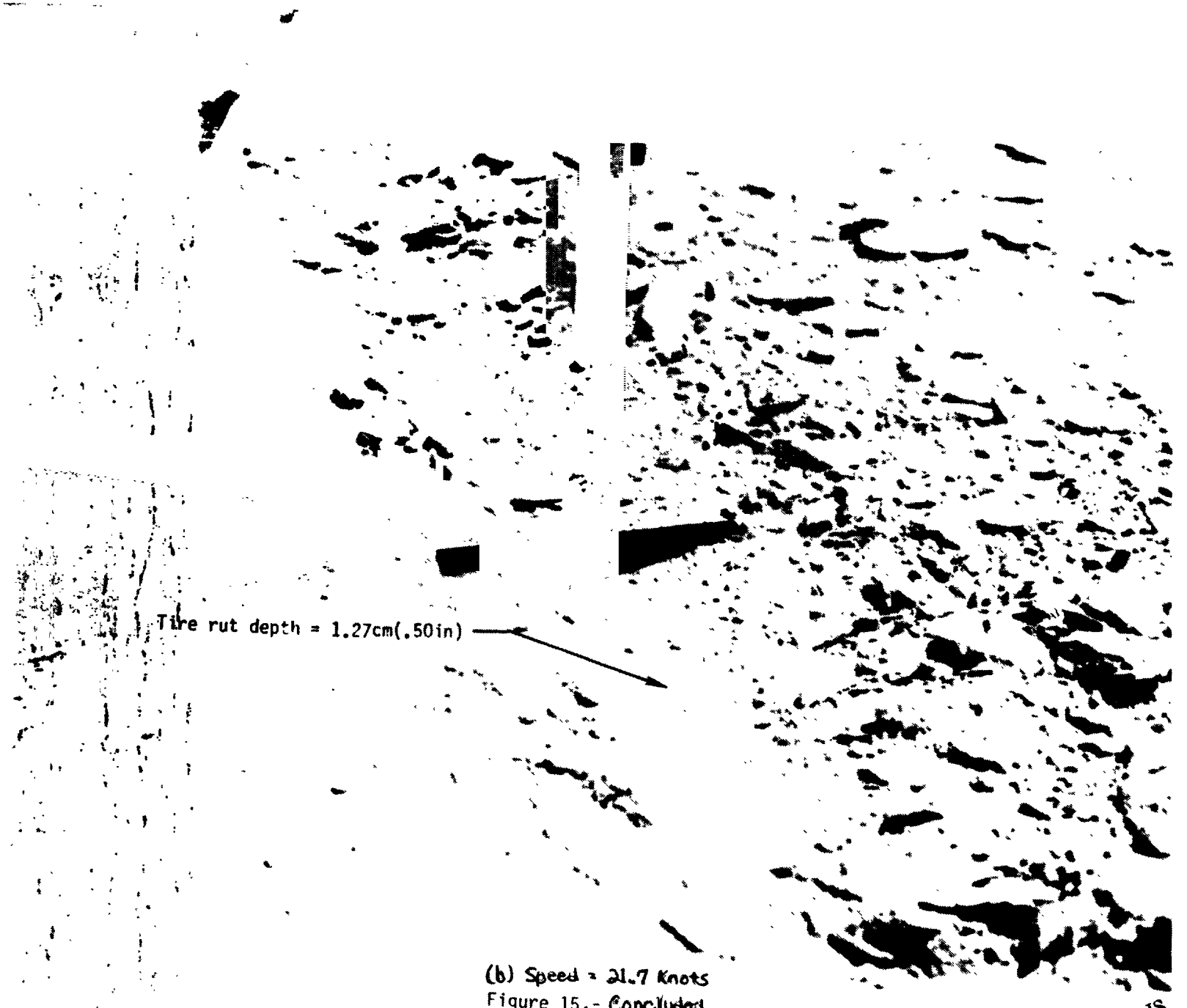


(b) Speed = 21.7 Knots

Figure 15.- Concluded.

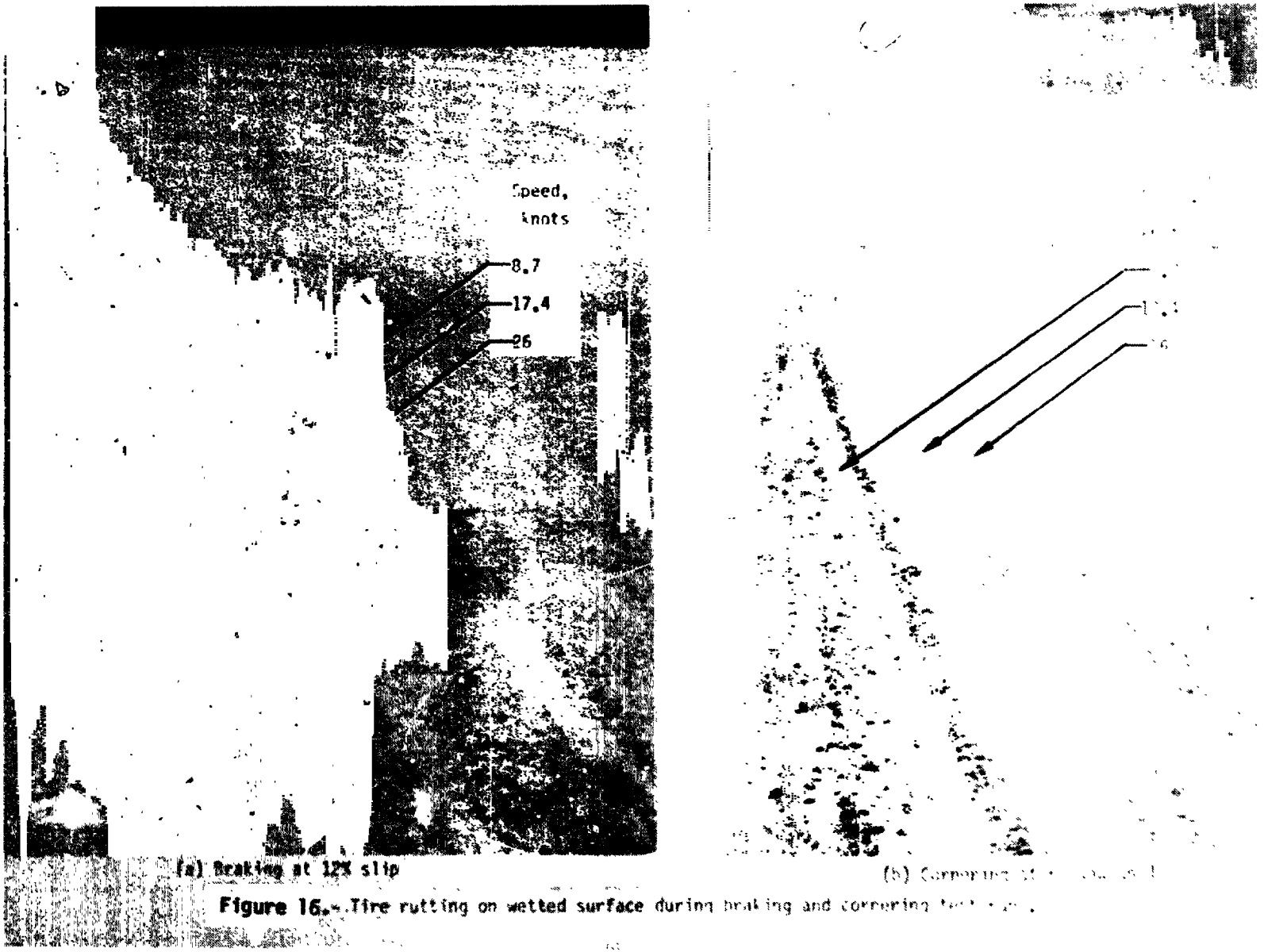


(a) Braking at 12% slip

(b) Cornering

**Figure 16.–** Tire rutting on wetted surface during braking and cornering tests.

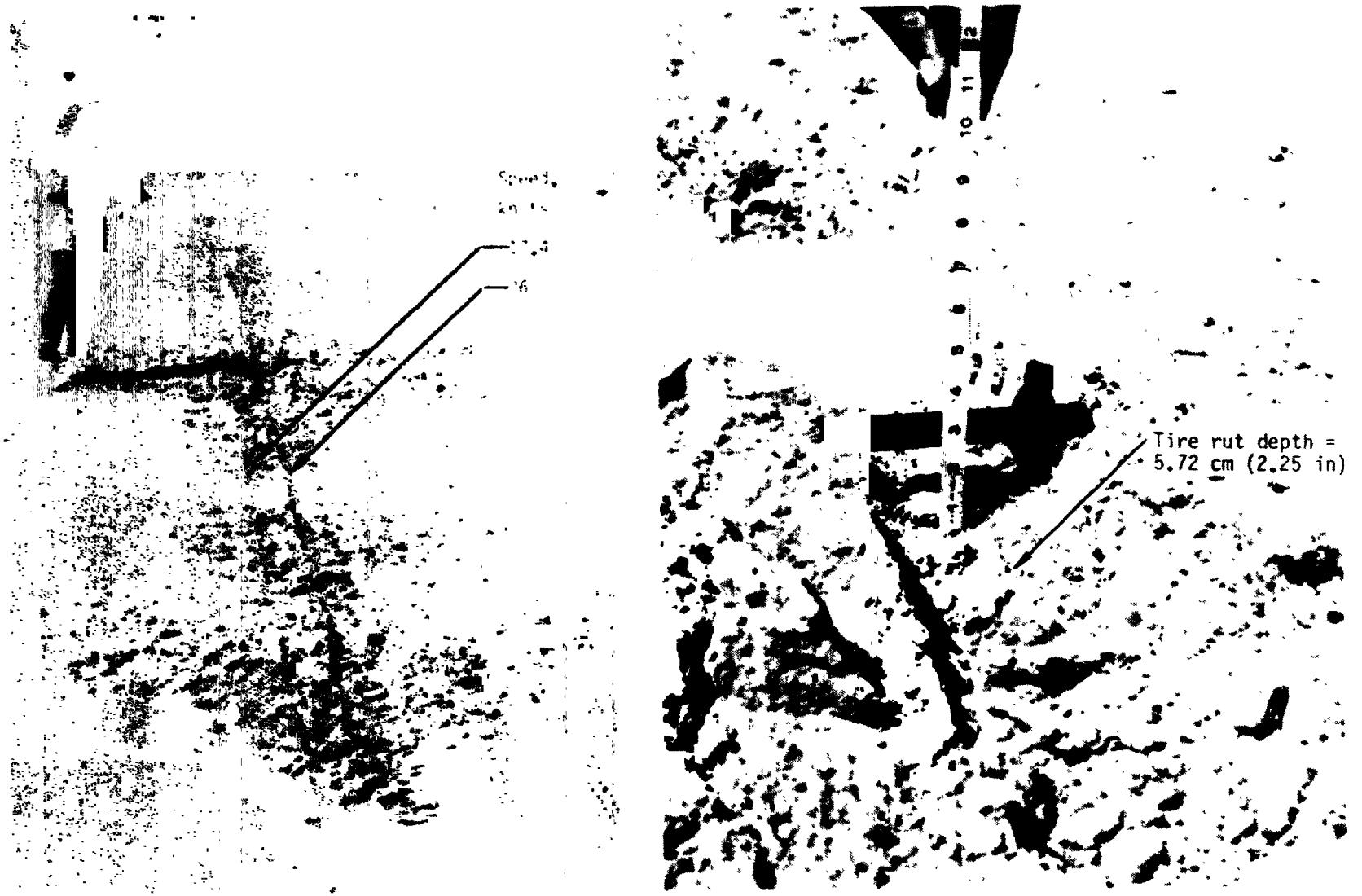


(a) Overall view

**Figure 17.-** Tire rutting on wetted silt surface [illegible]

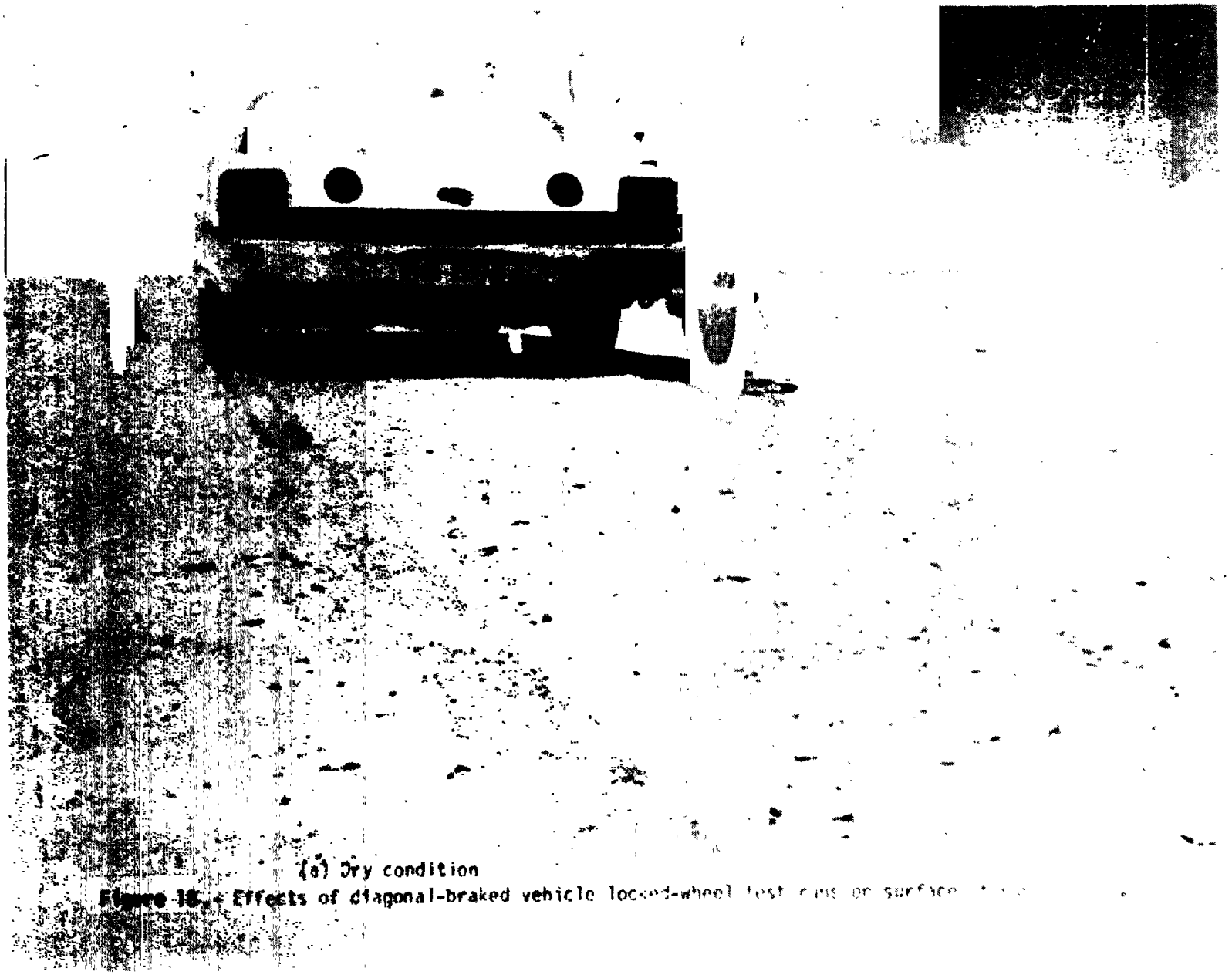

(a) Dry condition

Figure 18.- Effects of diagonal-braked vehicle locked-wheel test runs on surface

Figure 18.-

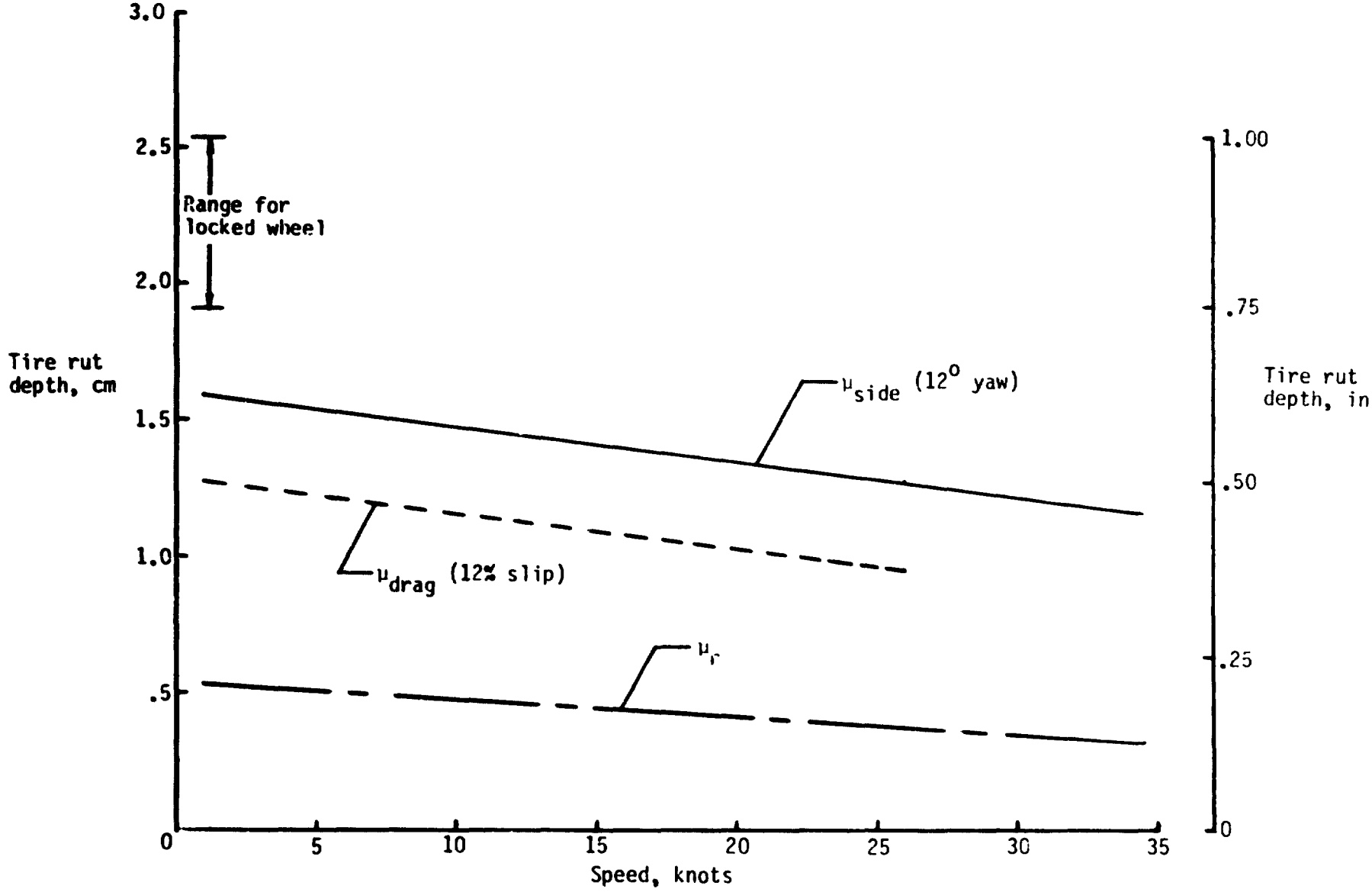


Figure 19. - Variation in average tire rut depth with speed and tire operating mode on dry gypsum surface runways. Instrumented tire test vehicle; 22 x 5.5 tire.

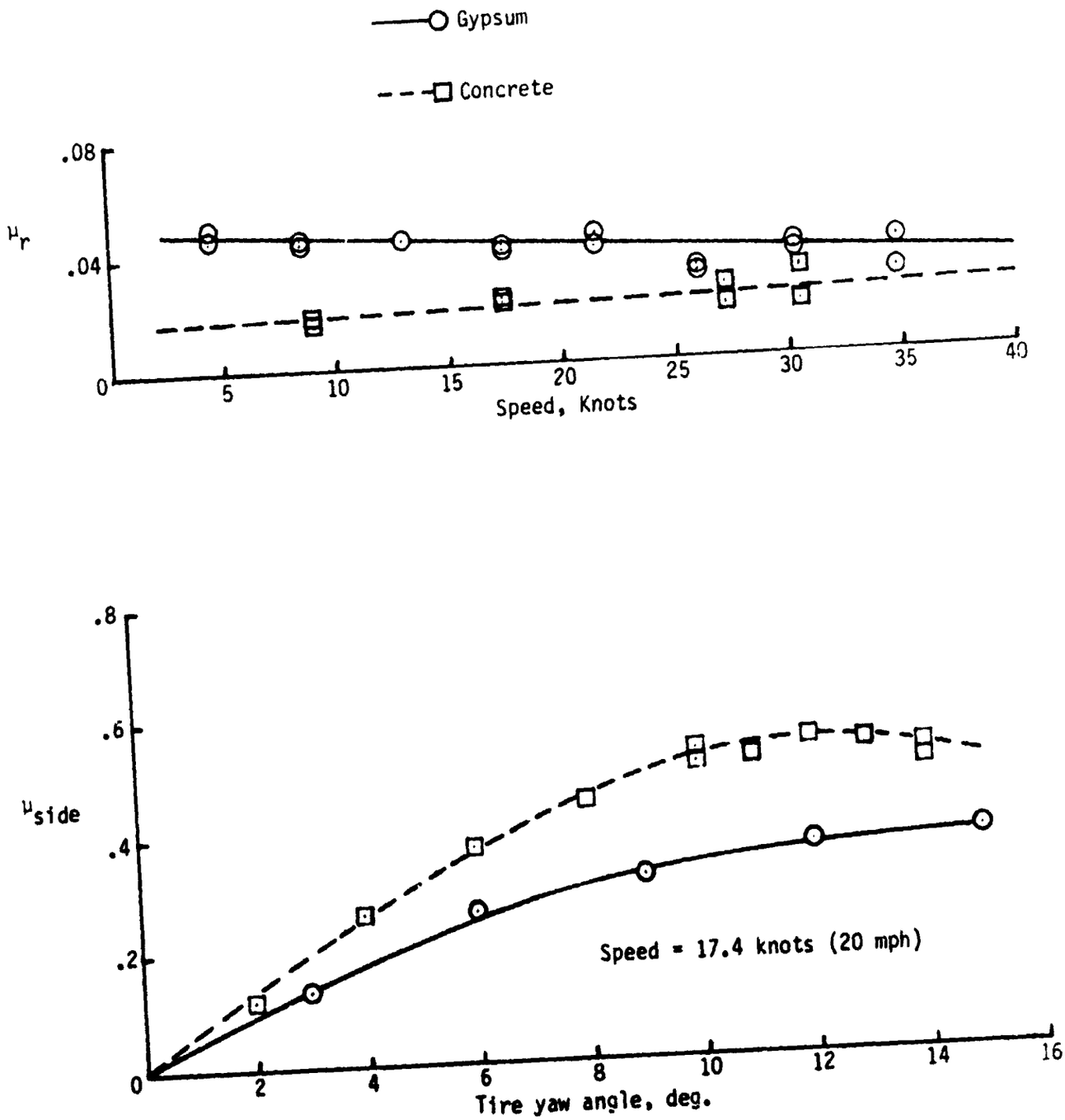


Figure 20.- Tire friction coefficients developed on dry gypsum and concrete surfaces. Instrumented tire test vehicle; 22 x 5.5 tire; p = 2172 kPa (315 lb/in$^2$).

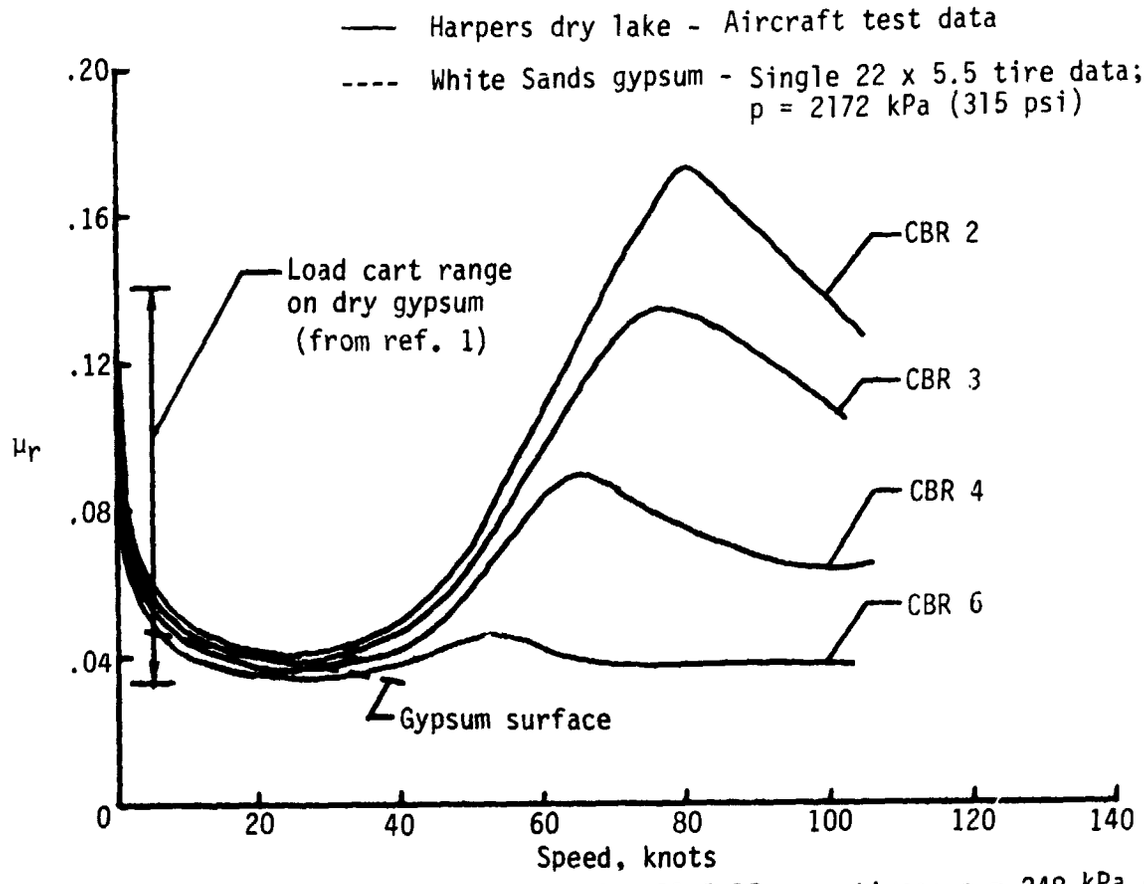


(a) B-707/KG135 prototype aircraft; 32 x 11.5-15 nose tires; p = 248 kPa (36 psi); 46 x 16 main tires; p = 207 kPa (30 psi).

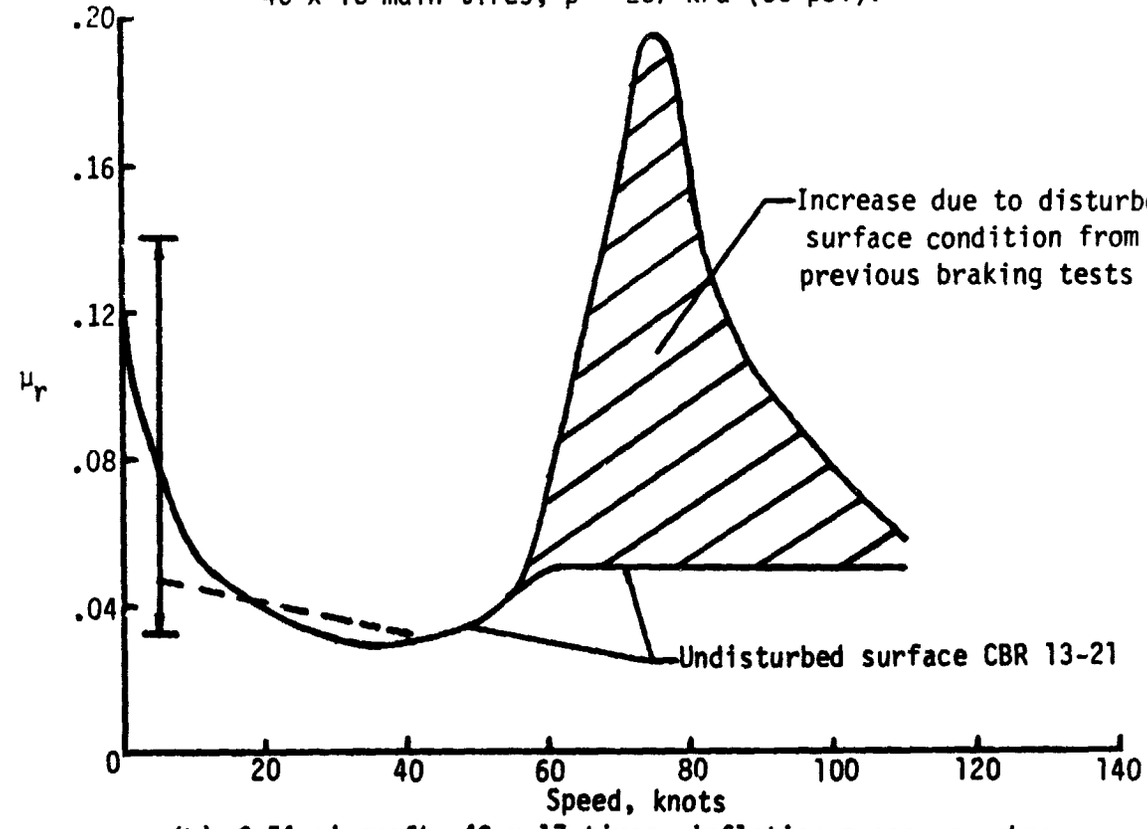


(b) C-5A aircraft; 49 x 17 tires; inflation pressure unknown.

Figure 21. - Comparison of free rolling friction coefficient variation with speed between Harpers dry lakebed aircraft tests and White Sands dry gypsum ground vehicle tests.

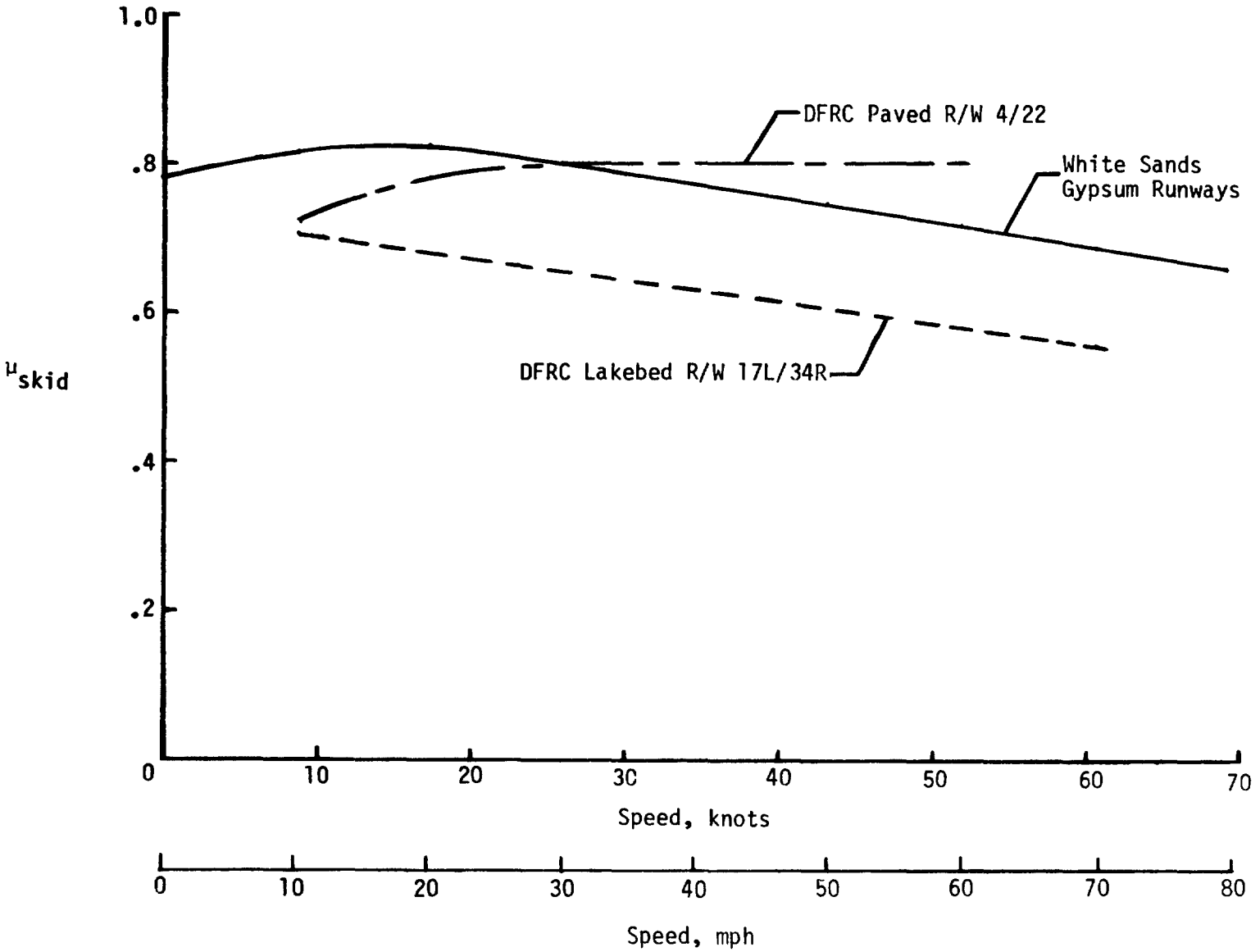


Figure 22.- Comparison of diagonal-braked vehicle skidding (locked-wheel) friction coefficients obtained on dry runway surfaces at DFRC and White Sands, N.M. ASTM smooth test tires; p = 165 kPa (24 psi).

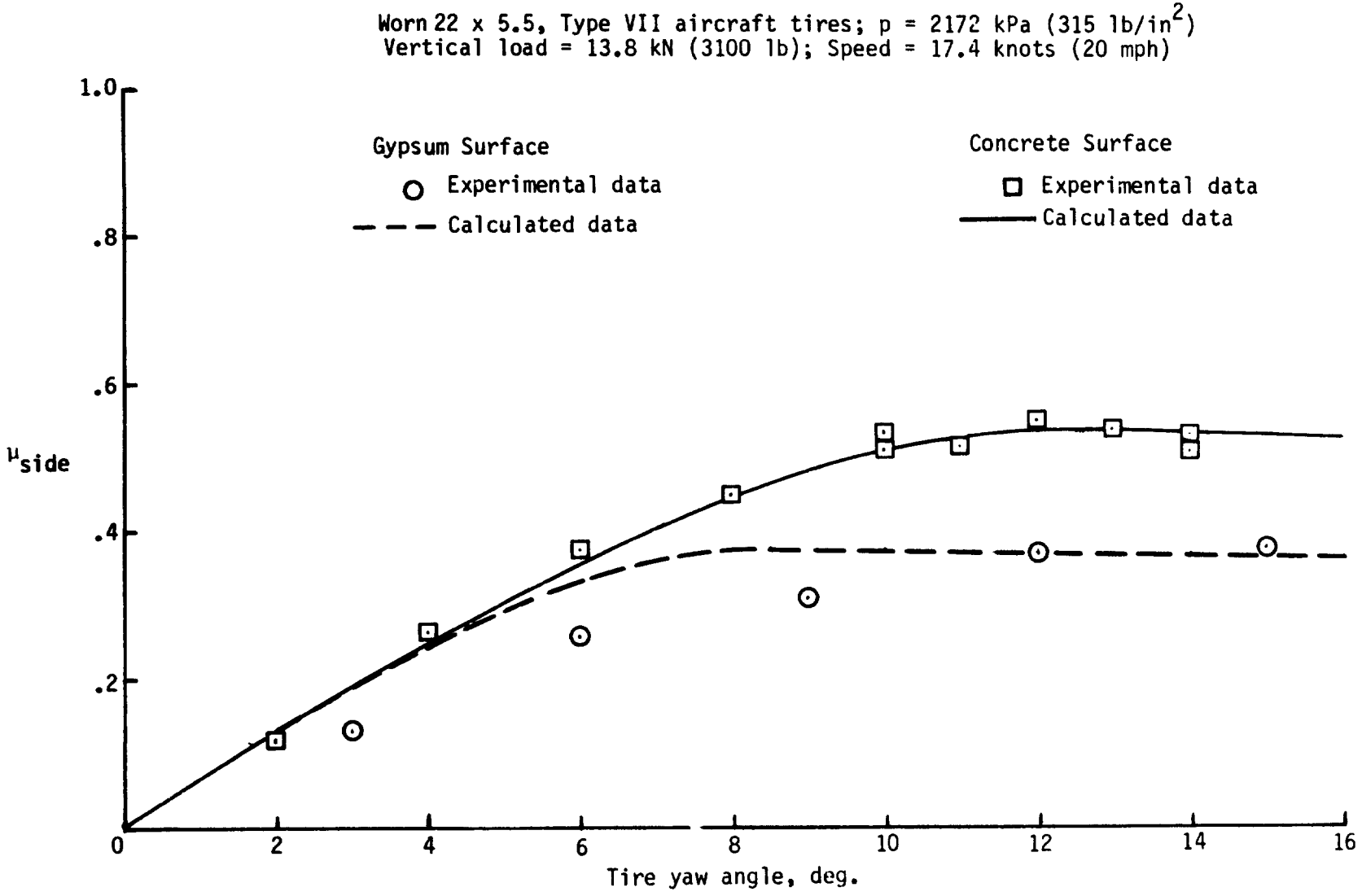


Figure 23.- Comparison of experimental and calculated tire cornering friction coefficient variation with yaw angle on both dry gypsum and concrete surfaces.

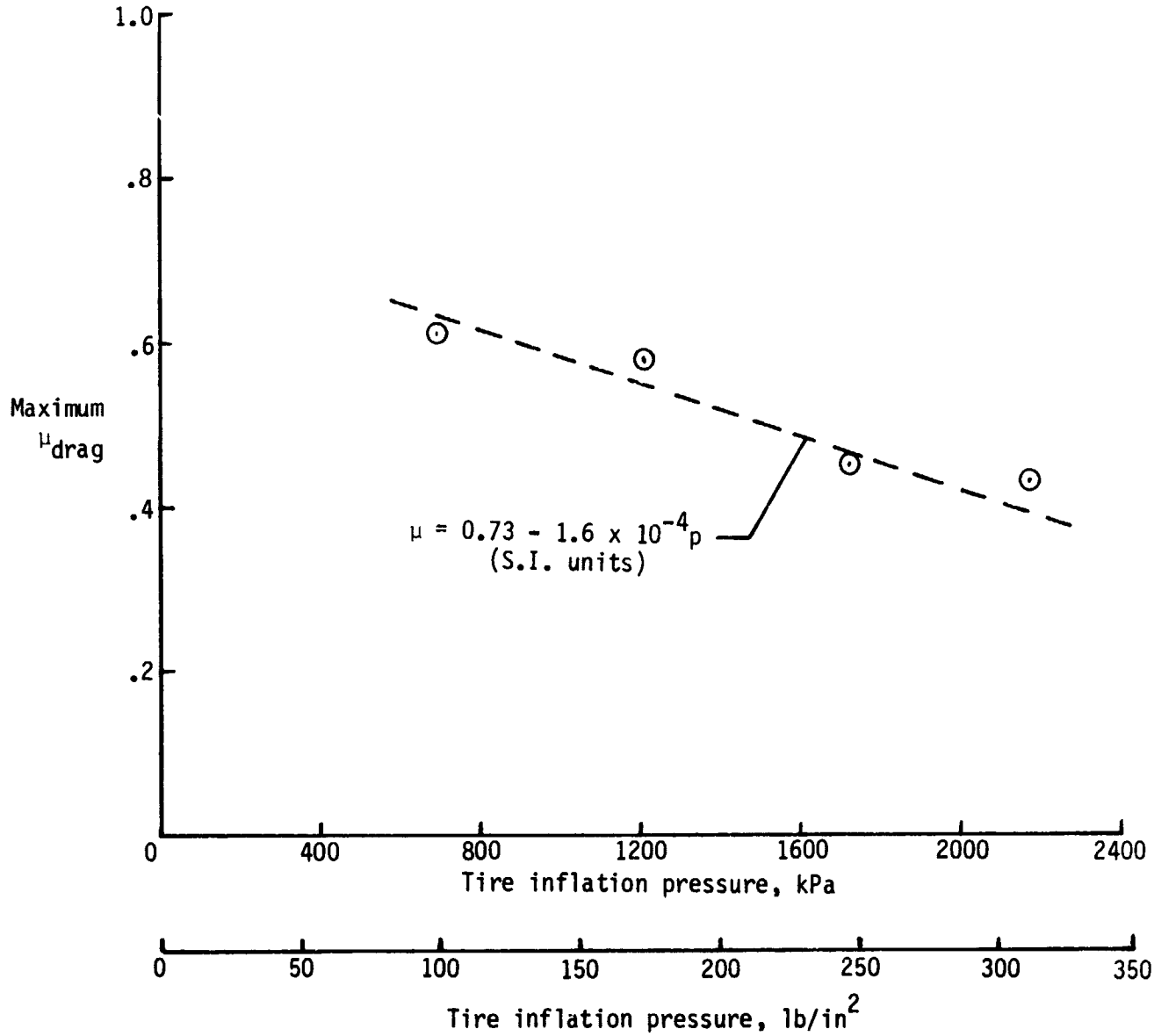


Figure 24.- Variation of drag friction coefficient with inflation pressure on dry gypsum at a braking slip of 12 percent.

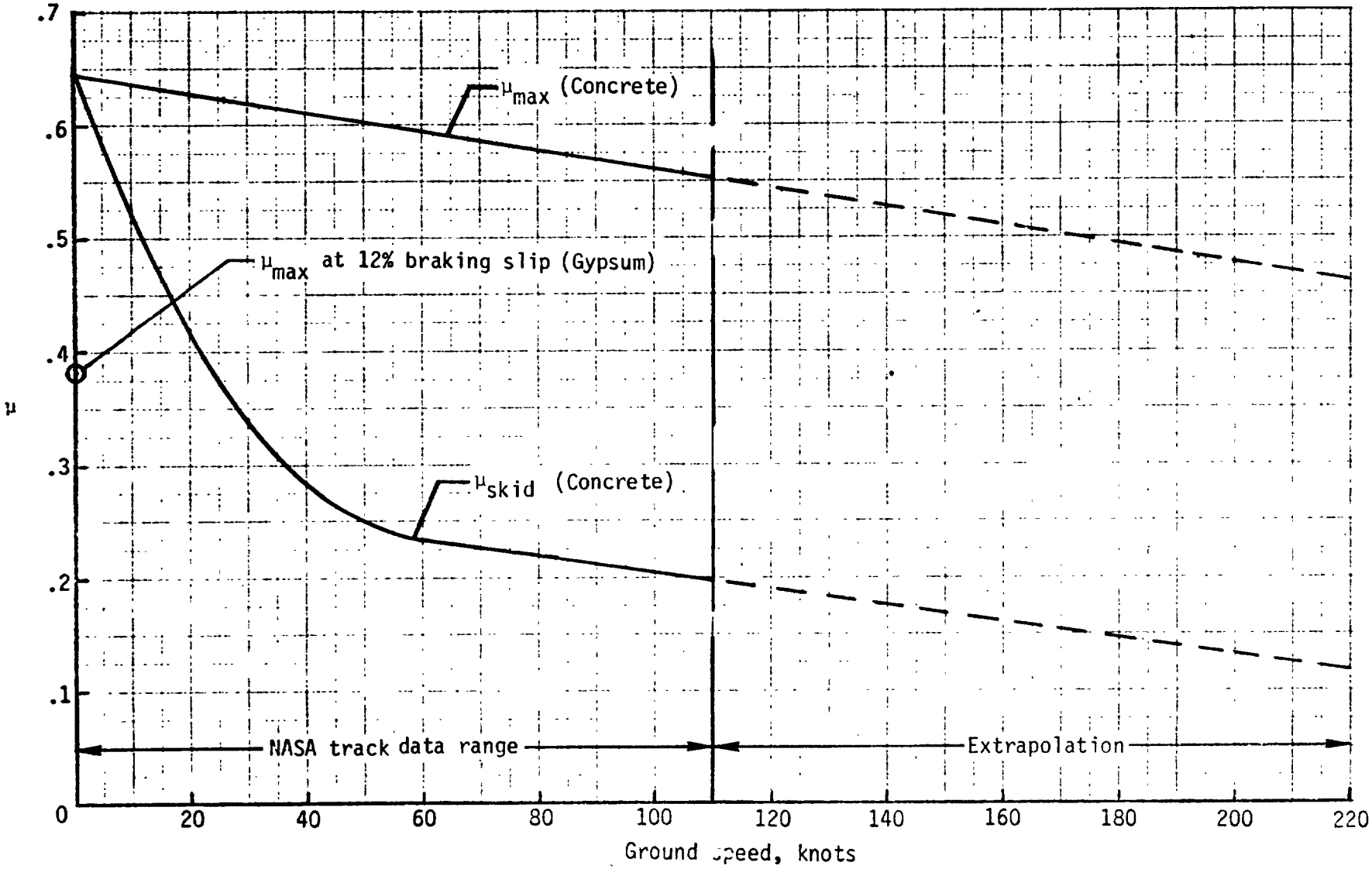


(a) Shuttle Orbiter light weight main gear tire.

Figure 25.- Estimated Shuttle Orbiter main gear tire braking friction coefficient on dry concrete and gypsum surface runways.

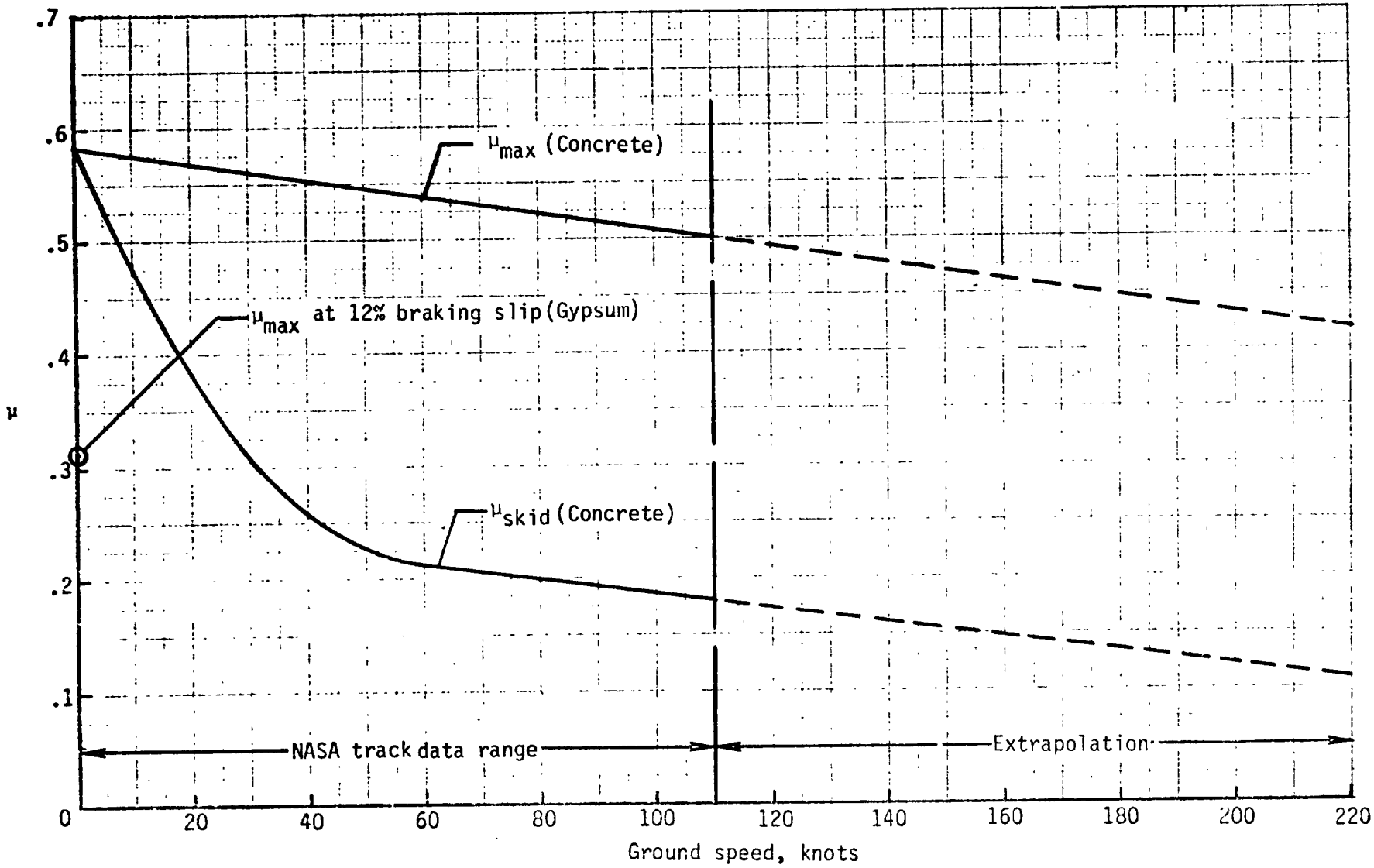


(b) Shuttle Orbiter heavy weight main gear tire.

Figure 25.- Concluded.

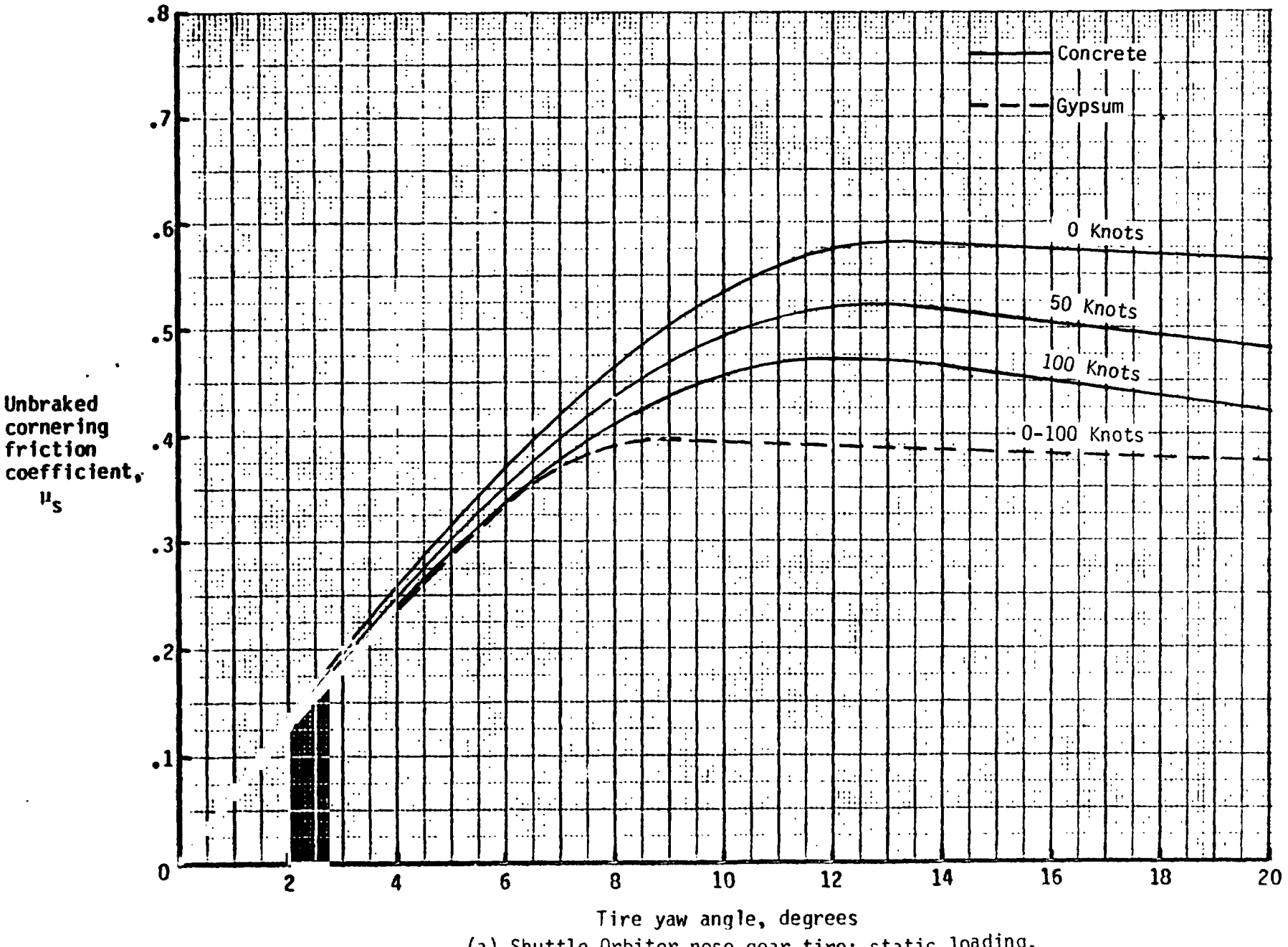


(a) Shuttle Orbiter nose gear tire; static loading.

Figure 26.- Estimated unbraked cornering friction coefficient variation with yaw angle and ground speed for Shuttle Orbiter tires on dry concrete and gypsum surface runways. Static loading case.

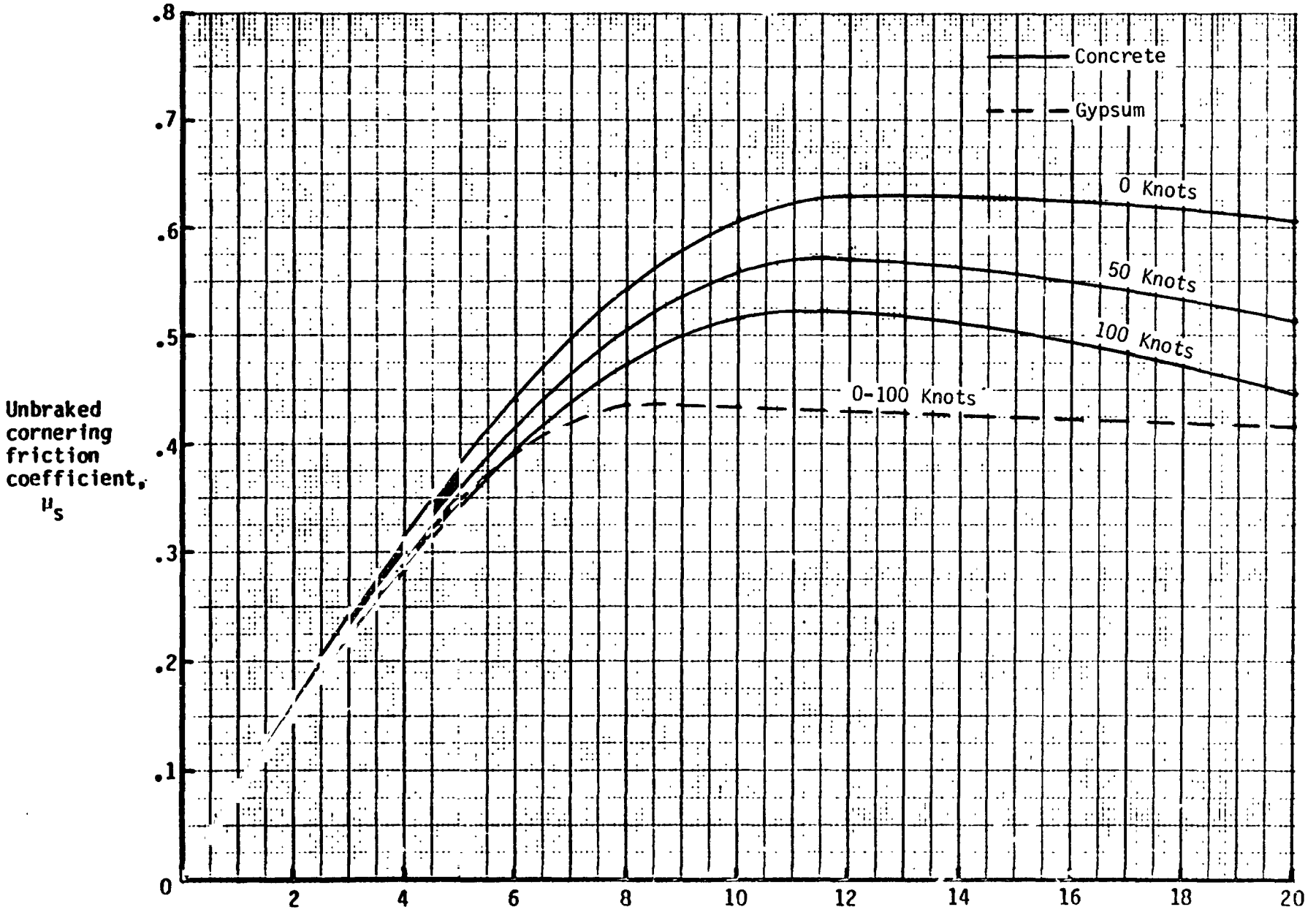


(b) Shuttle Orbiter light-weight main gear tire; static loading.

Figure 26.- Continued.

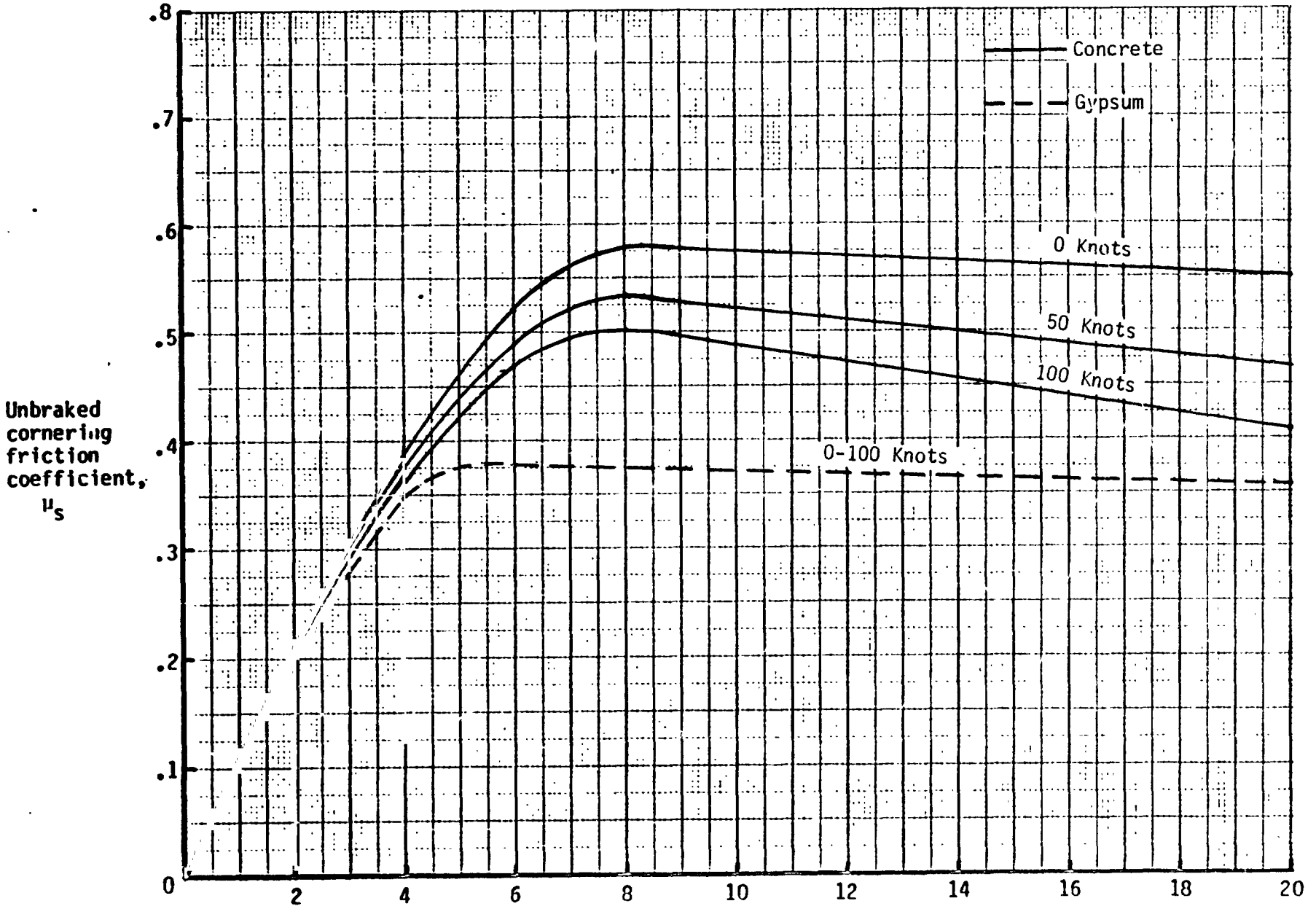


(c) Shuttle Orbiter heavy-weight main gear tire; static loading.

Figure 26.- Concluded.

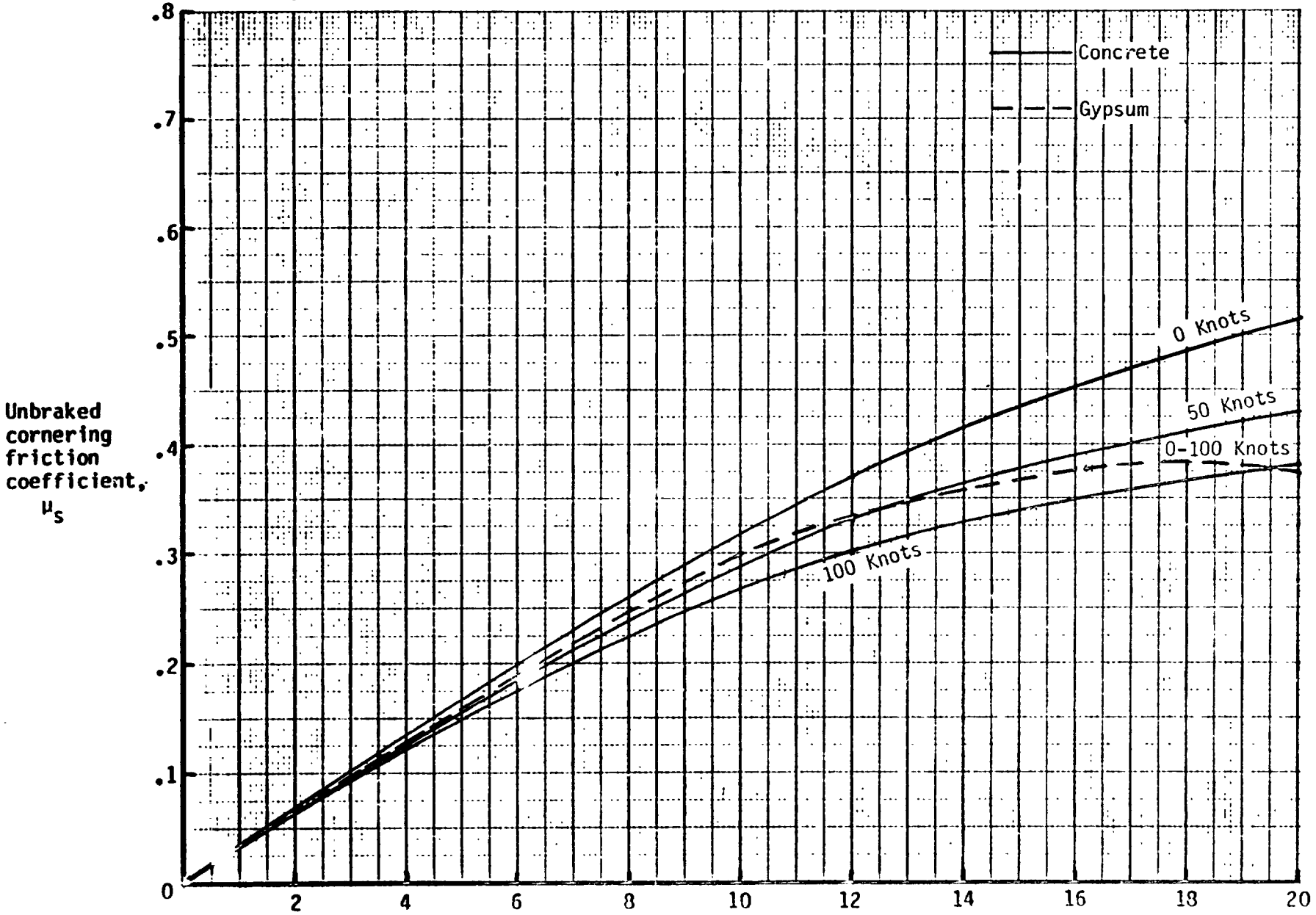


(a) Shuttle Orbiter nose gear tire; dynamic loading.

Figure 27.- Estimated unbraked cornering friction coefficient variation with yaw angle and ground speed for Shuttle Orbiter tires on dry concrete and gypsum surface runways. Dynamic loading case.

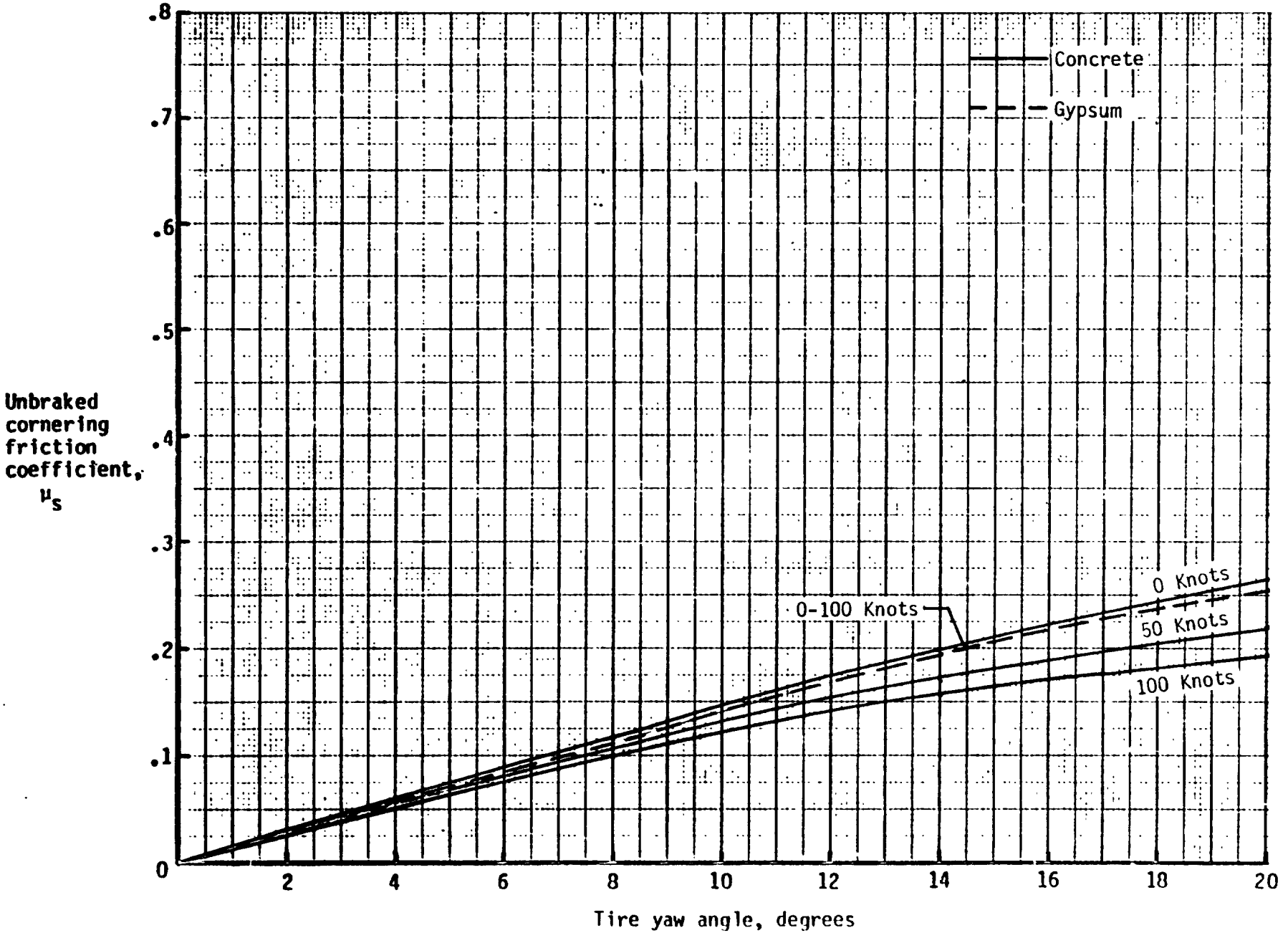


(b) Shuttle Orbiter light-weight main gear tire; dynamic loading.

Figure 27.- Continued.

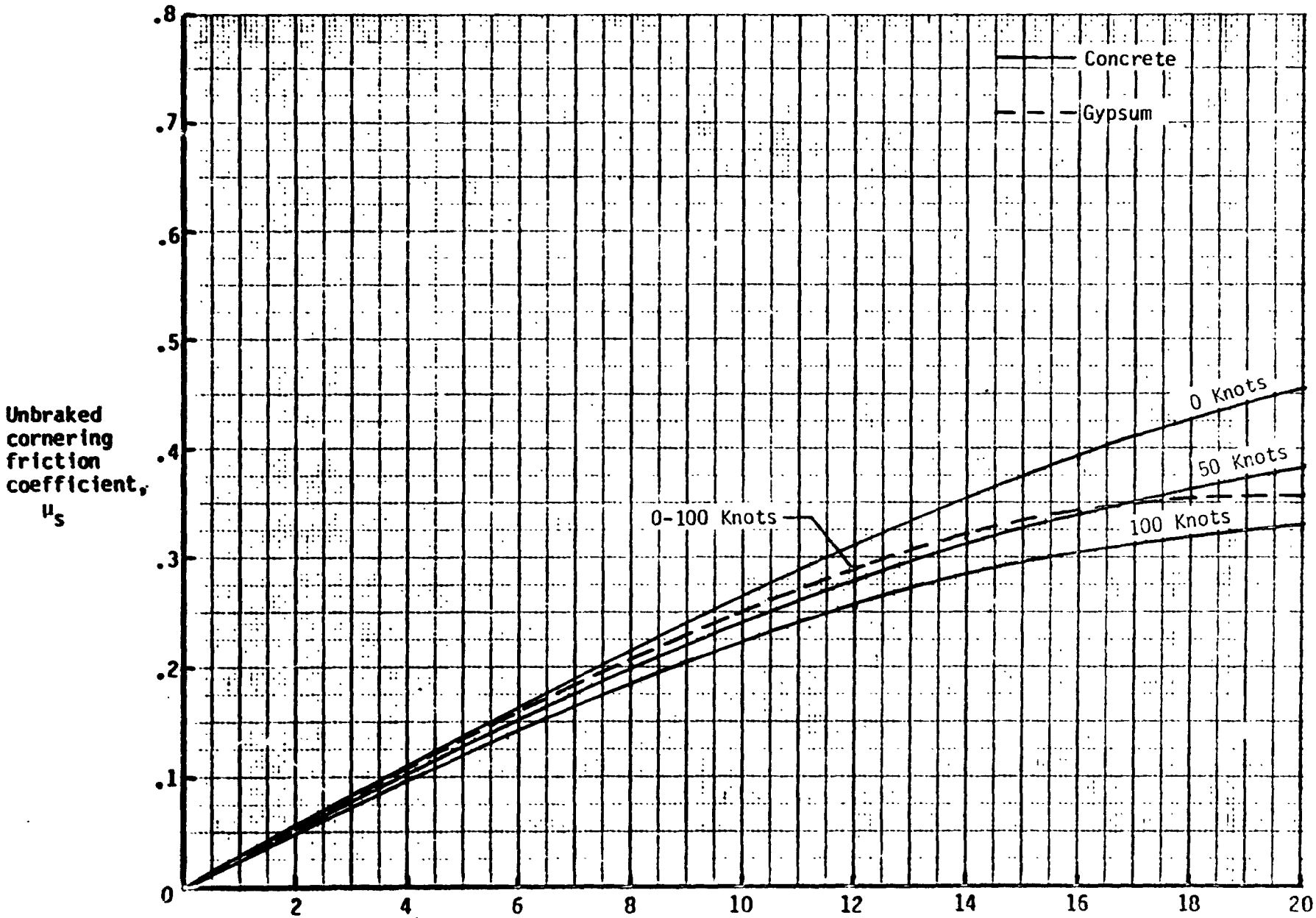


(c) Shuttle Orbiter heavy-weight main gear tire; dynamic loading.

Figure 27.- Concluded.

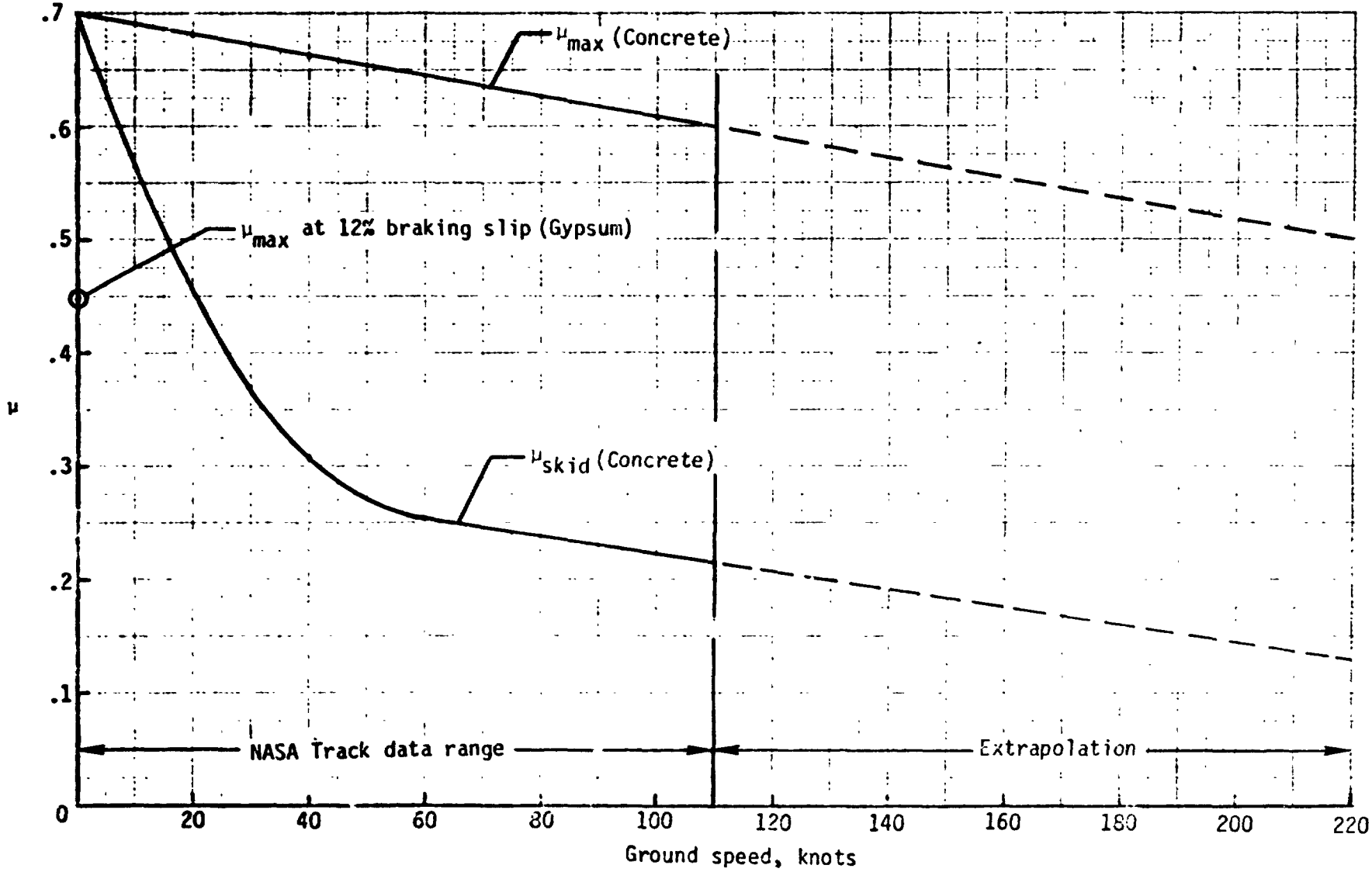


Figure 28.- Estimated B-747-100 aircraft main gear tire braking friction coefficient on dry concrete and gypsum surface runways.


(a) B-747 aircraft nose gear tire.

Figure 29.- Estimated unbraked cornering friction coefficient variation with yaw angle and ground speed for B-747-100 aircraft tires on dry concrete and gypsum surface runways.

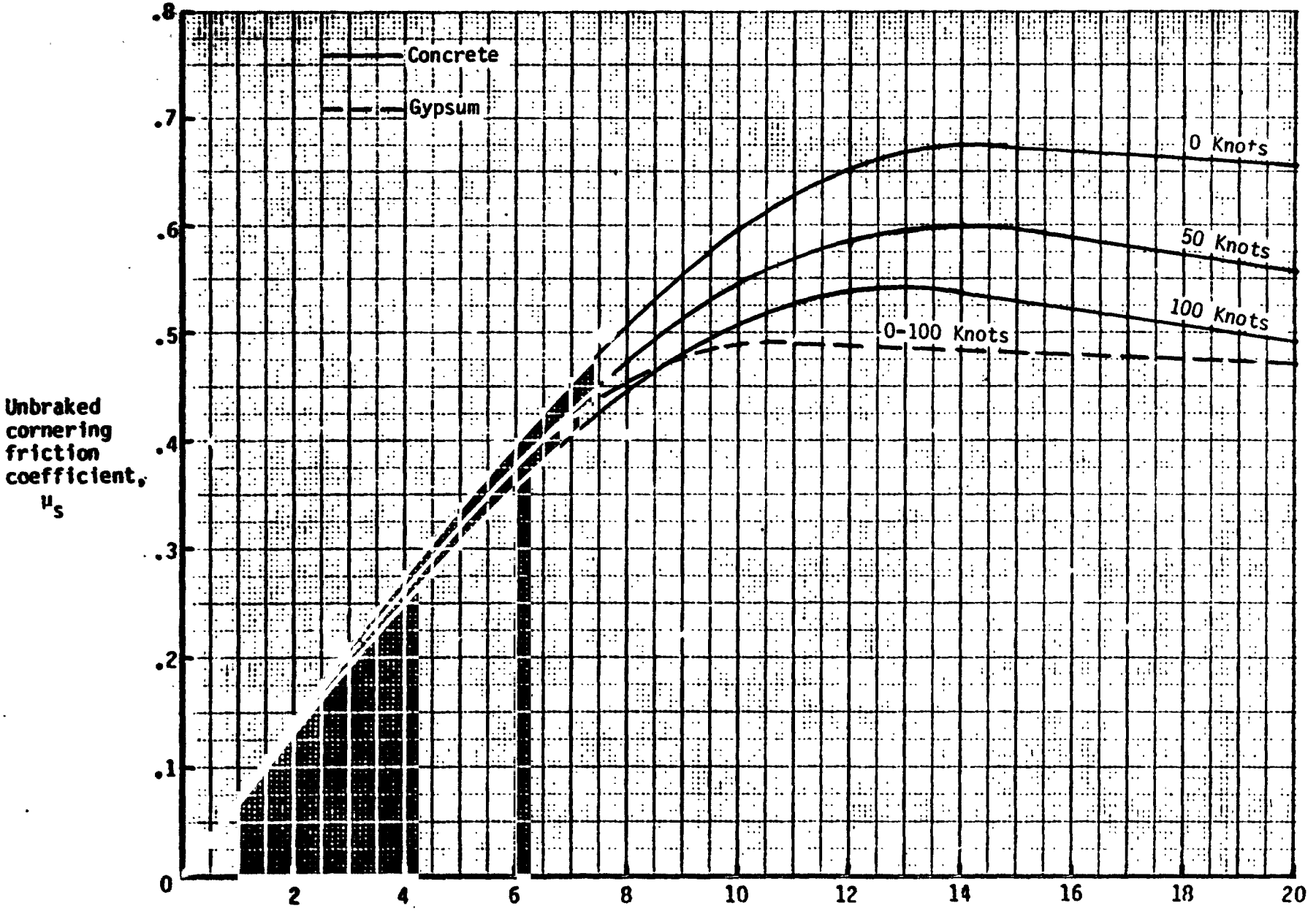


(b) B-747 aircraft main gear tire.

Figure 29.- Concluded.

## APPENDIX

This appendix presents some additional data analysis to provide an estimate of the influence of tire surface rutting on the braking or drag force friction coefficient values obtained using both the instrumented tire test vehicle at Northrup Strip and several different aircraft flight tests conducted prior to ALT at Dryden Flight Center. If it can be assumed that the characteristic dry friction coefficient on gypsum, estimated at 0.38, is correct for the 22 x 5.5 size tire inflated to 2172 kPa (315 lb/in.$^2$) and that the effect of tire surface rutting on the developed side force is negligible, then the effect of rutting on the developed drag force friction coefficient can be estimated.

Figure A1(a) was prepared from the faired data of figure 6 to provide an estimate of the effect of tire surface rutting on the measured levels of $\mu_{drag}$ at 12- and 45-percent braking slip. The difference between the faired drag friction coefficient data and the characteristic dry friction coefficient $\mu_{cd}$ on gypsum is assumed to be attributed to rutting and that difference, labeled $\mu_{rut}$, is also presented in the figure for the two braking slip values. It is apparent from this figure that braking slip is a dominating factor in developing tire surface rutting. Figure A1(b) further illustrates the effects of braking slip on the buildup of $\mu_{rut}$. The faired $\mu_{drag}$ curve was obtained from the data of figure 7 at speeds of 8.7, 17.4, and 26 knots (10, 20, and 30 mph) and the difference between the experimental $\mu_{drag}$ and the $\mu_{cd}$ is again assumed to correspond to $\mu_{rut}$. The data shown in figure A1 was obtained at relatively low speeds and with a tire pressure of 2172 kPa (315 lb/in$^2$), and operations at other inflation pressures and higher speeds would probably result in different $\mu_{rut}$ values. Insufficient data is currently available to obtain an accurate assessment of all the factors influencing the magnitude of $\mu_{rut}$ at White Sands, but some additional data obtained from previous aircraft braking tests at Dryden, which were conducted at different tire inflation pressures and through a greater speed range, is presented.

Figure A2 shows comparative data indicating the variation in aircraft braking capability measured during tests on both Harpers and Rodgers dry lakebed runways as well as the concrete runway 22. The three aircraft used in these tests, a KC-135, a C-5, and a RF-4C, had antiskid brake systems and the pilots used three types of brake application: light, moderate (medium), and maximum (heavy) braking. Figure A2(a) shows comparative cockpit vertical, transverse, and longitudinal acceleration time histories obtained during KC-135 aircraft landings on runway 17C at Rodgers dry lakebed and the concrete runway 22. The longitudinal deceleration levels obtained during the light, medium and heavy braking segments of the KC-135 aircraft landing rollout are nearly equal on both runways. Similar braking performance was obtained during the C-5A and RF-4C aircraft tests indicated by the variation in aircraft effective braking friction coefficient with speed shown in figures A2(b) and (c). The C-5A aircraft braking performance on the Harpers dry lakebed runway (see fig. A2(b)) was higher during maximum antiskid braking compared to that obtained during moderate antiskid braking. Some of this difference may be due to greater tire surface

rutting during maximum antiskid braking but measurements of rut depth were not recorded. The RF-4C aircraft braking performance on the concrete runway 22 and the lakebed runway 17C is similar (see fig. A2(c)), but significantly higher effective braking friction coefficient values were obtained on the lakebed runway 15. Although CBR values on this runway are not available, the approach end of runway 15, near the lakebed shoreline, is known to be considerably softer than the approach end of 17C which is located near the lakebed center. The difference in RF-4C aircraft braking capability between runway 15 and the other two runways might be due to greater tire surface rutting during braking on this softer runway surface and hence, higher drag forces. Unfortunately, measurements of aircraft tire surface rutting after these aircraft braking tests on the different lakebed runways were not recorded.

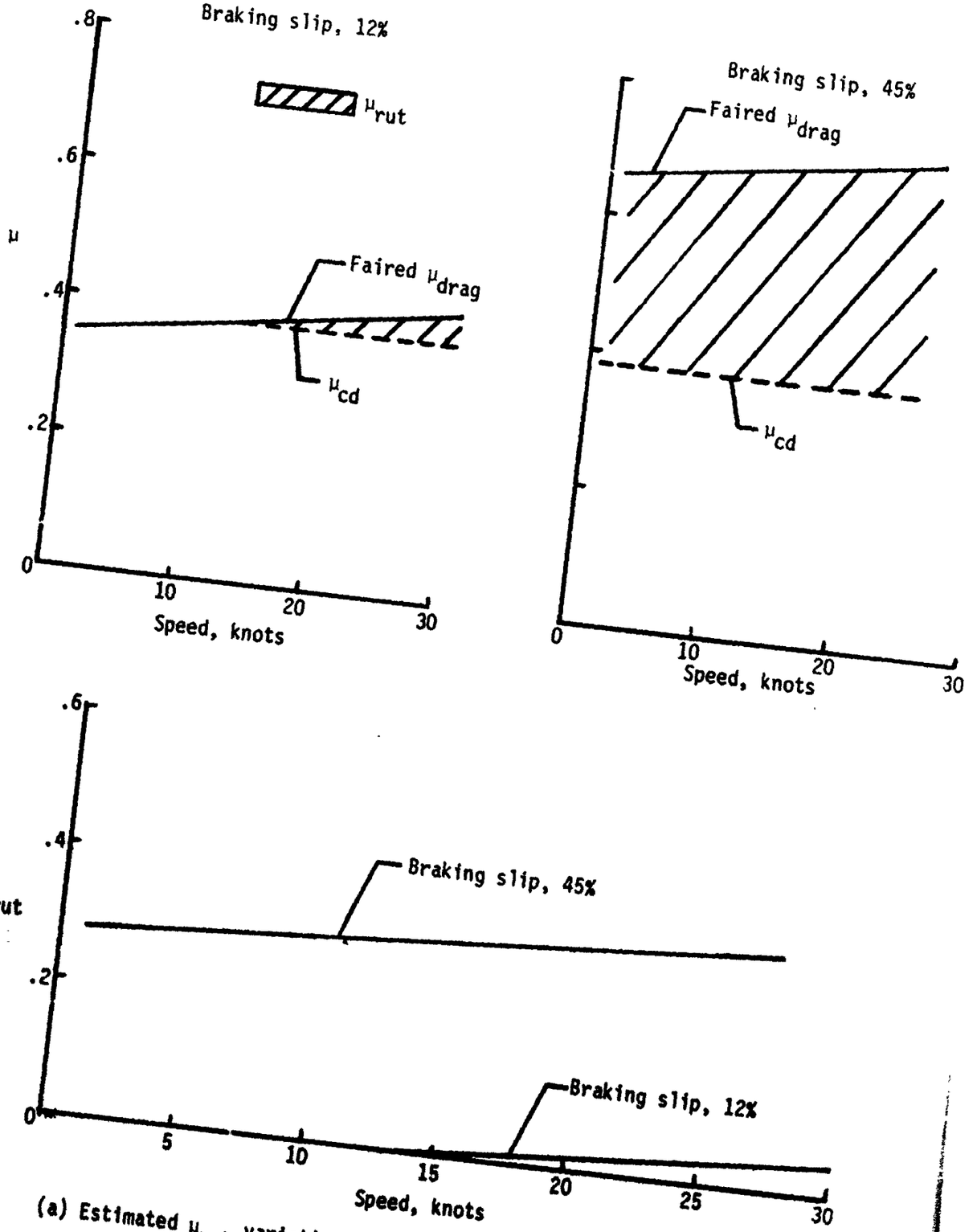


(a) Estimated $\mu_{rut}$ variation with speed at two braking slip values.

Figure A1. - Determination of 22 x 5.5 tire braking friction coefficient component due to surface rutting at White Sands. Inflation pressure, 2172 kPa (315 lb/in$^2$)

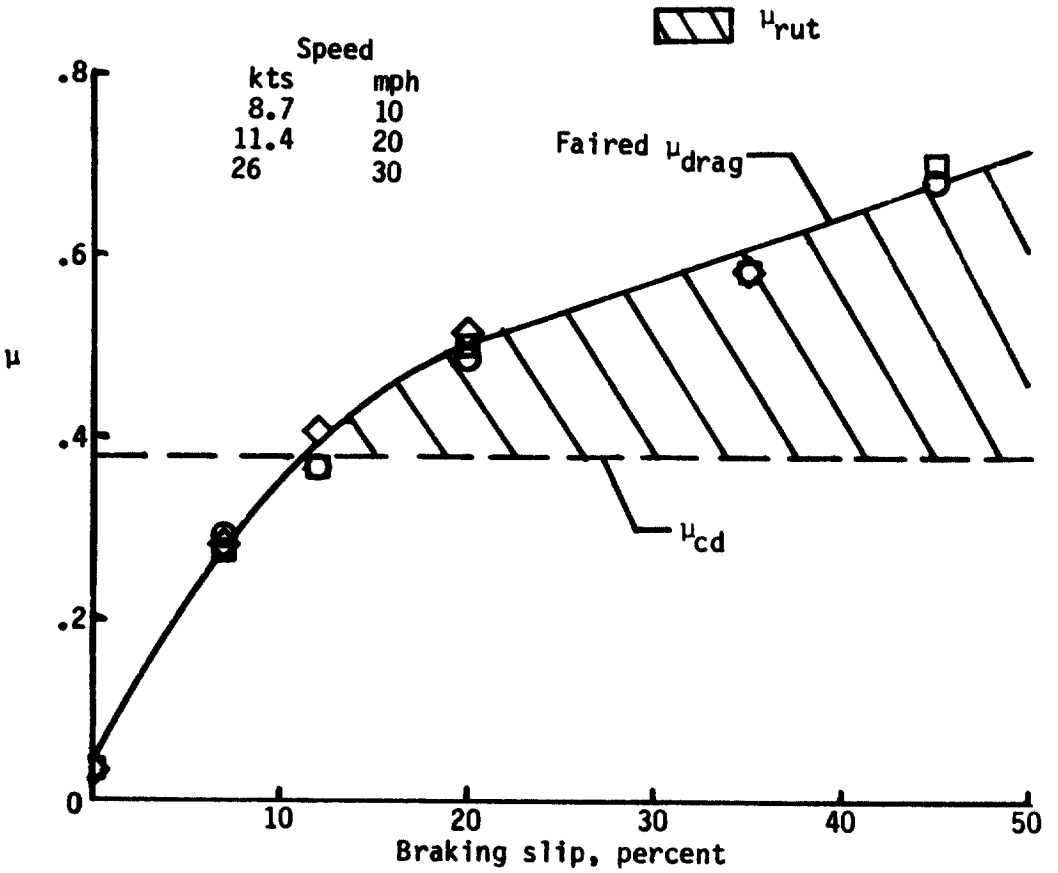


(b) Estimated $\mu_{rut}$ variation with braking slip.

Figure A1. - Concluded.

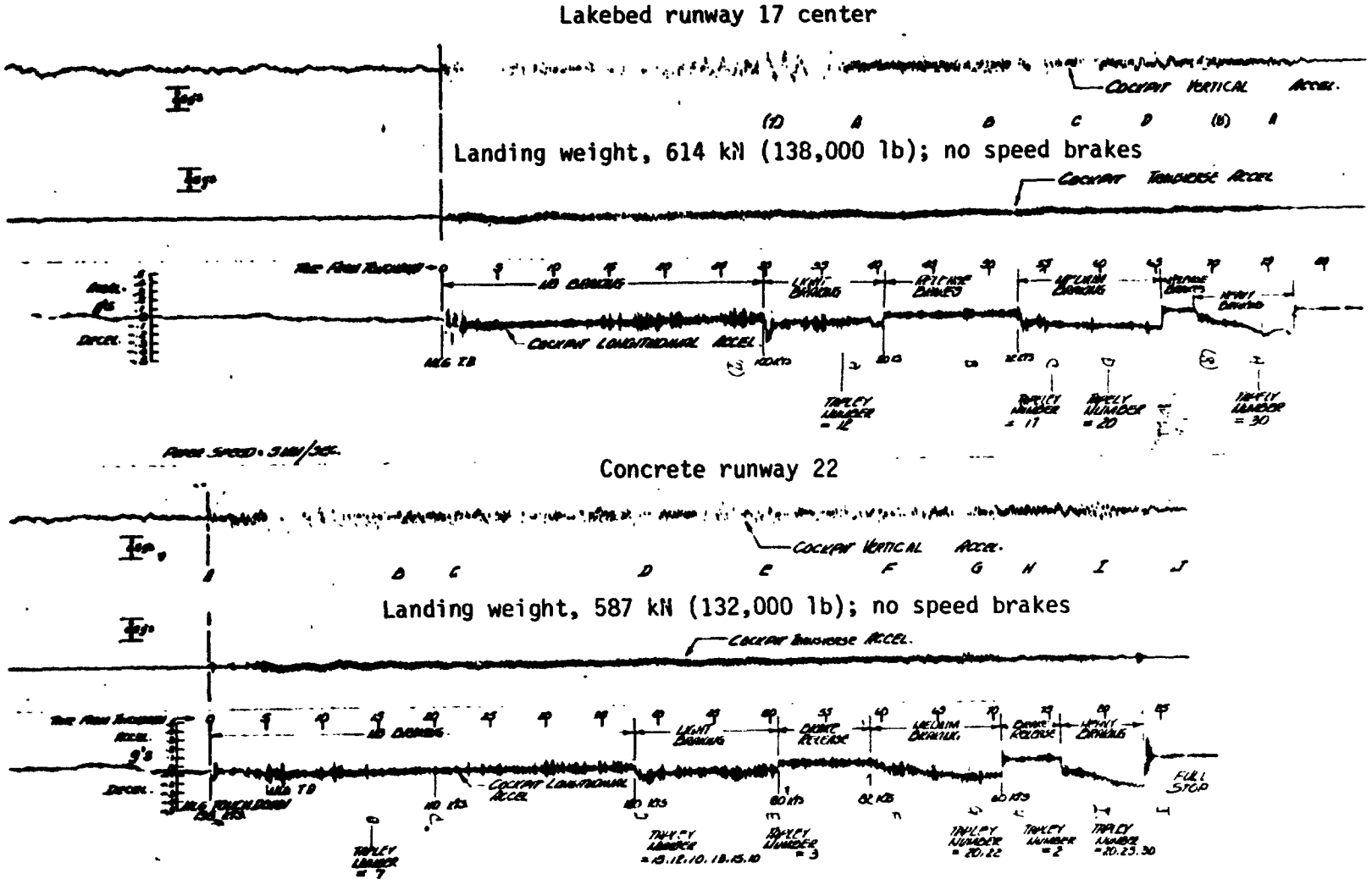


(a) KC-135 aircraft landing acceleration time histories; main tire pressure, 1069 kPa (155 psi)

ORIGINAL PAGE IS
OF POOR QUALITY

Figure A2. - Braking performance data obtained from three different aircraft tests on concrete and lakebed runway surfaces at Edwards AFB.

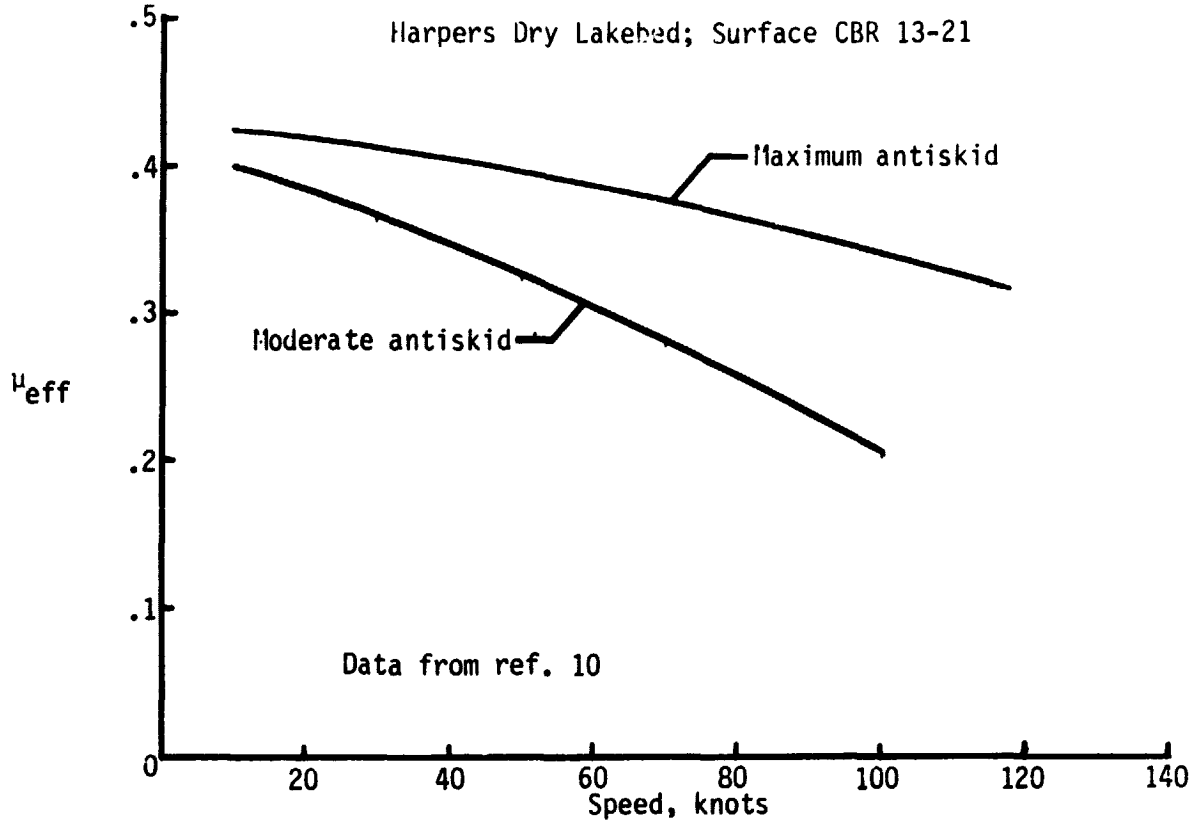


(b) C-5A Aircraft; 49 x 17 tires; estimated main tire pres., 689-1172 kPa (100-170 psi)

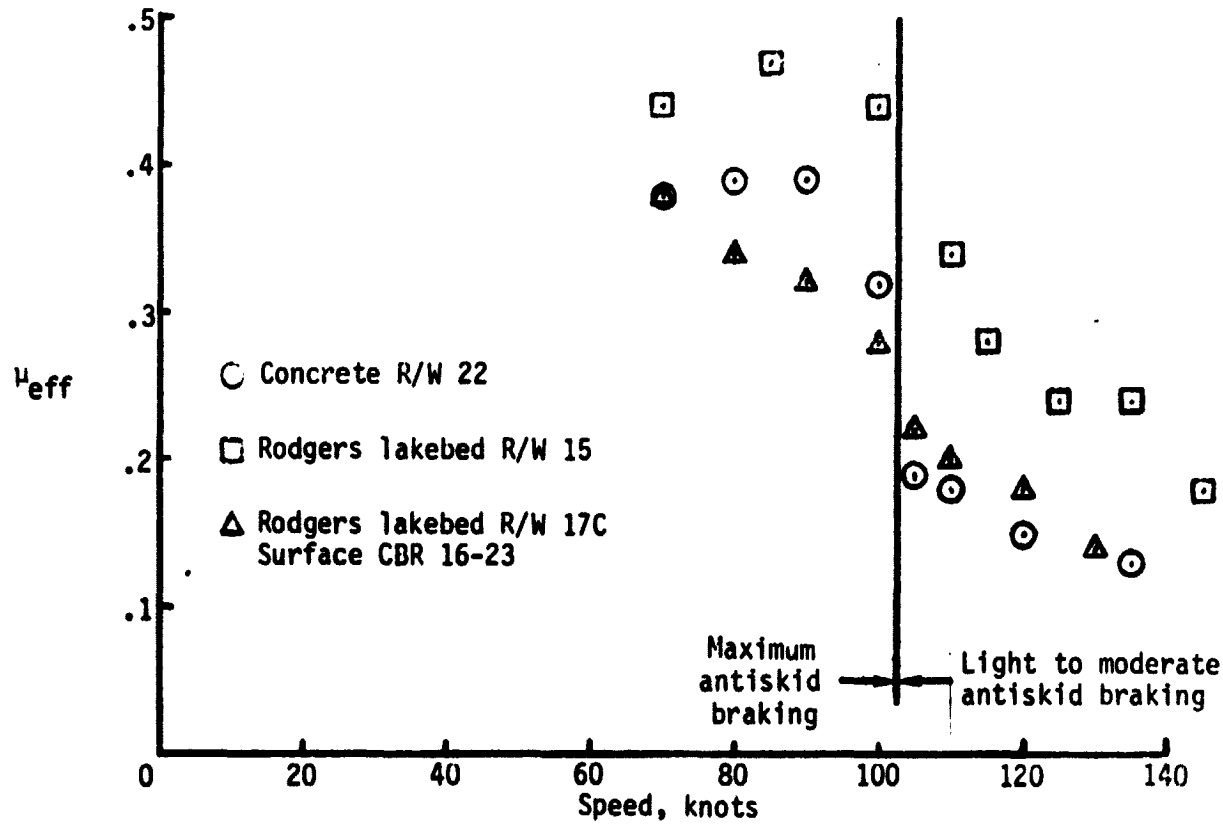


(c) RF-4C aircraft; 30 x 11.50-14.5 main tires; Infl. pressure = 1827 kPa (265 psi)

Figure .. - Concluded.

| 1. Report No. | 2. Government Accession No. | 3. Recipient's Catalog No. |
|---|---|---|
| NASA TM-81811 | | |

| 4. Title and Subtitle | 5. Report Date |
|---|---|
| Friction Evaluation of Unpaved, Gypsum-Surface Runways at Northrup Strip, White Sands Missile Range, in Support of Space Shuttle Orbiter Landing and Retrieval Operations | June 1980 |
| | 6. Performing Organization Code |

| 7. Author(s) | 8. Performing Organization Report No. |
|---|---|
| Thomas J. Yager and Walter B. Horne | |
| | 10. Work Unit No. |

| 9. Performing Organization Name and Address | 11. Contract or Grant No. |
|---|---|
| NASA Langley Research Center<br>Hampton, VA 23665 | |
| | 13. Type of Report and Period Covered |
| 12. Sponsoring Agency Name and Address | Technical Memorandum |
| National Aeronautics and Space Administration<br>Washington, DC 20546 | 14. Sponsoring Agency Code |

15. Supplementary Notes

16. Abstract

Friction measurement results obtained on the gypsum surface runways at Northrup Strip, White Sands Missile Range, N.M. using an instrumented tire test vehicle and a diagonal-braked vehicle, are presented. These runways were prepared to serve as backup landing and retrieval sites to the primary sites located at Dryden Flight Research Center for Shuttle Orbiter during initial test flights. Similar friction data obtained on paved and other unpaved surfaces is shown for comparison and to indicate that the friction capability measured on the dry gypsum surface runways is sufficient for operations with the Shuttle Orbiter and the B-747 aircraft. Based on these ground vehicle friction measurements, estimates of Shuttle Orbiter and B-747 aircraft tire friction performance are presented and discussed. General observations concerning the gypsum surface characteristics are also included and several recommendations are made for improving and maintaining adequate surface friction capabilities prior to the first Shuttle Orbiter landing.

| 17. Key Words (Suggested by Author(s)) | 18. Distribution Statement |
|---|---|
| Gypsum surface runway<br>Shuttle Orbiter<br>Tire friction | Unclassified - Unlimited<br>Subject Category 14 |

| 19. Security Classif. (of this report) | 20. Security Classif. (of this page) | 21. No. of Pages | 22. Price* |
|---|---|---|---|
| Unclassified | Unclassified | 75 | $5.25 |

* For sale by the National Technical Information Service, Springfield, Virginia 22161